

High-precision measurement of the W boson mass with the CDF II detector



Chris Hays, Oxford University

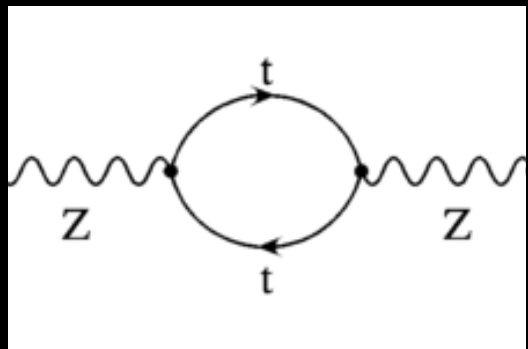
QCD@Work
29 June, 2022



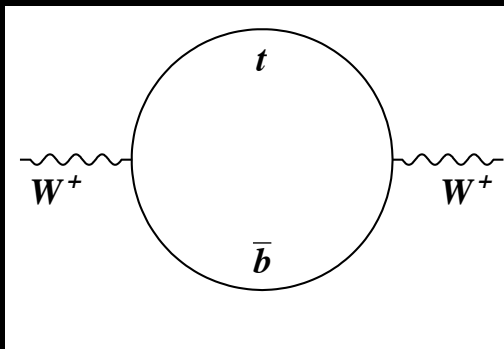
Electroweak boson masses

Gauge boson masses

$$m_Z = \frac{v}{2} \sqrt{g^2 + g'^2}$$

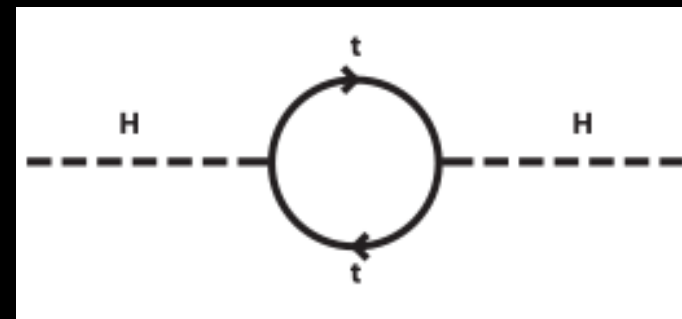


$$m_W = \frac{v}{2} g$$



Higgs boson mass

$$m_H = v \sqrt{2\lambda}$$



$$m_W^2 = \frac{\hbar^3}{c} \frac{\pi \alpha_{EM}}{\sqrt{2} G_F (1 - m_W^2/m_Z^2)(1 - \Delta r)}$$

$$\Delta r_{tb} = \frac{c}{\hbar^3} \frac{-3G_F m_W^2}{8\sqrt{2}\pi^2(m_Z^2 - m_W^2)} \times \\ \left[m_t^2 + m_b^2 - \frac{2m_t^2 m_b^2}{m_t^2 - m_b^2} \ln(m_t^2/m_b^2) \right]$$

SM calculation of W boson mass yields
 81358 ± 4 MeV

Naively integrating to a cutoff scale Λ :

$$\Delta m_H = \frac{3g^2 m_t^2}{16\pi^2 m_W^2} \Lambda^2$$

If there is no new physics up to scale Λ then we have ‘fine-tuning’ to cancel the quantum corrections

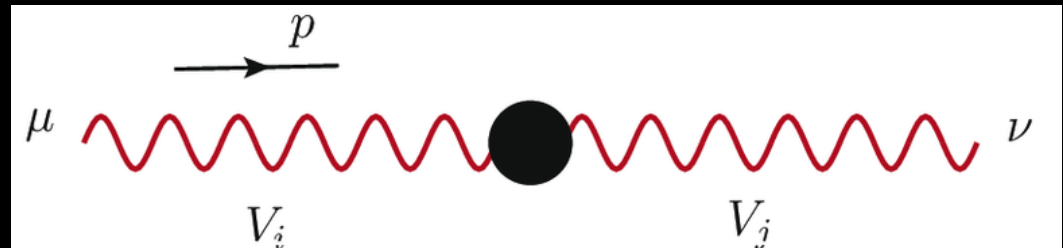
1% fine tuning: $\Lambda = 6.6$ TeV

Motivates TeV-scale new physics

W boson mass

More generally the SM effective field theory parameterizes high-scale effects

$$\mathcal{L}_{SMEFT} = \mathcal{L}_{SM} + \mathcal{L}^{(5)} + \mathcal{L}^{(6)} + \mathcal{L}^{(7)} + \dots, \quad \mathcal{L}^{(d)} = \sum_{i=1}^{n_d} \frac{C_i^{(d)}}{\Lambda^{d-4}} Q_i^{(d)} \quad \text{for } d > 4.$$



$$\frac{\delta m_W}{m_W} = (0.34c_{HD} + 0.72c_{HWB} + 0.37c_{Hl3} - 0.19c_{ll1}) \frac{v^2}{\Lambda^2}$$

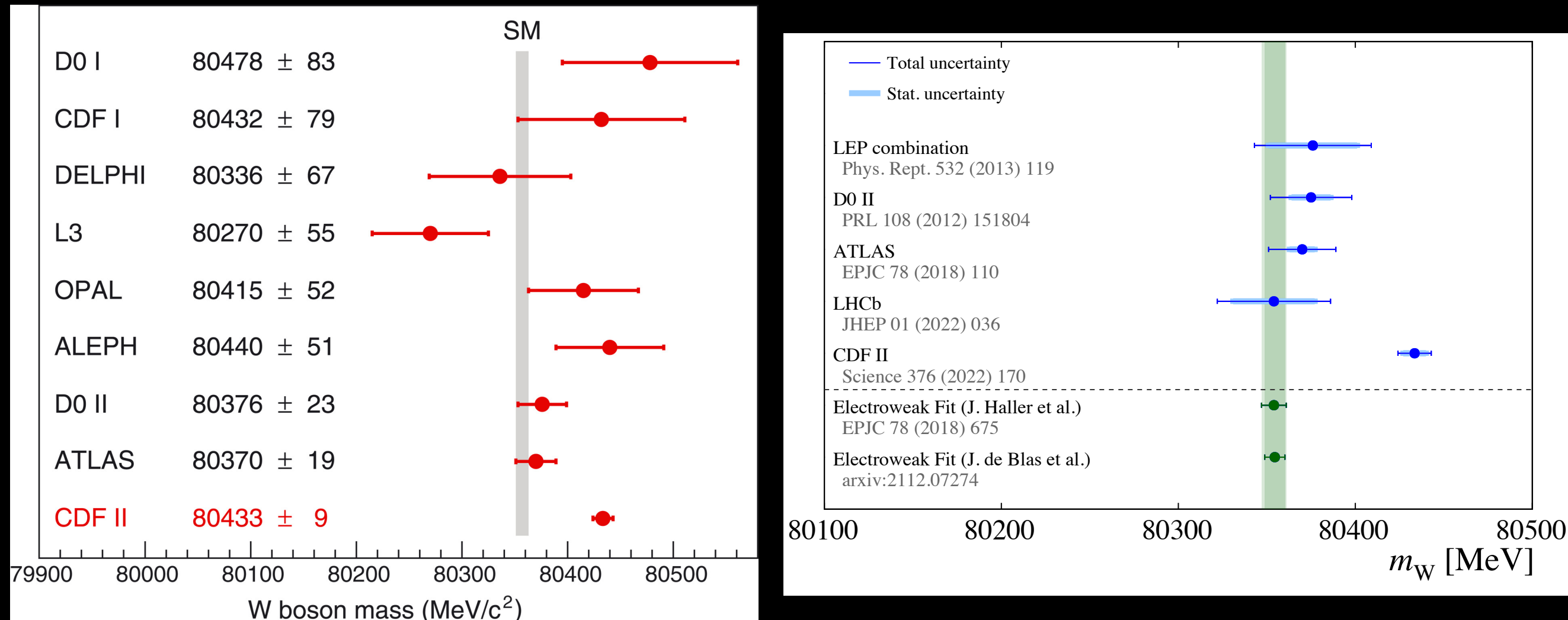
For $\delta m_W/m_W = 0.1\%$ and $c_{HD}=1$, $\Lambda = 4.5$ TeV
e.g. Z' boson

I. Brivio and M. Trott,
Phys. Rep. 793 (2019) 1

For $\delta m_W/m_W = 0.1\%$ and $c_{HWB}=1$, $\Lambda = 6.6$ TeV
e.g. compositeness

Smaller $c_i \rightarrow$ smaller Λ

W boson mass measurements

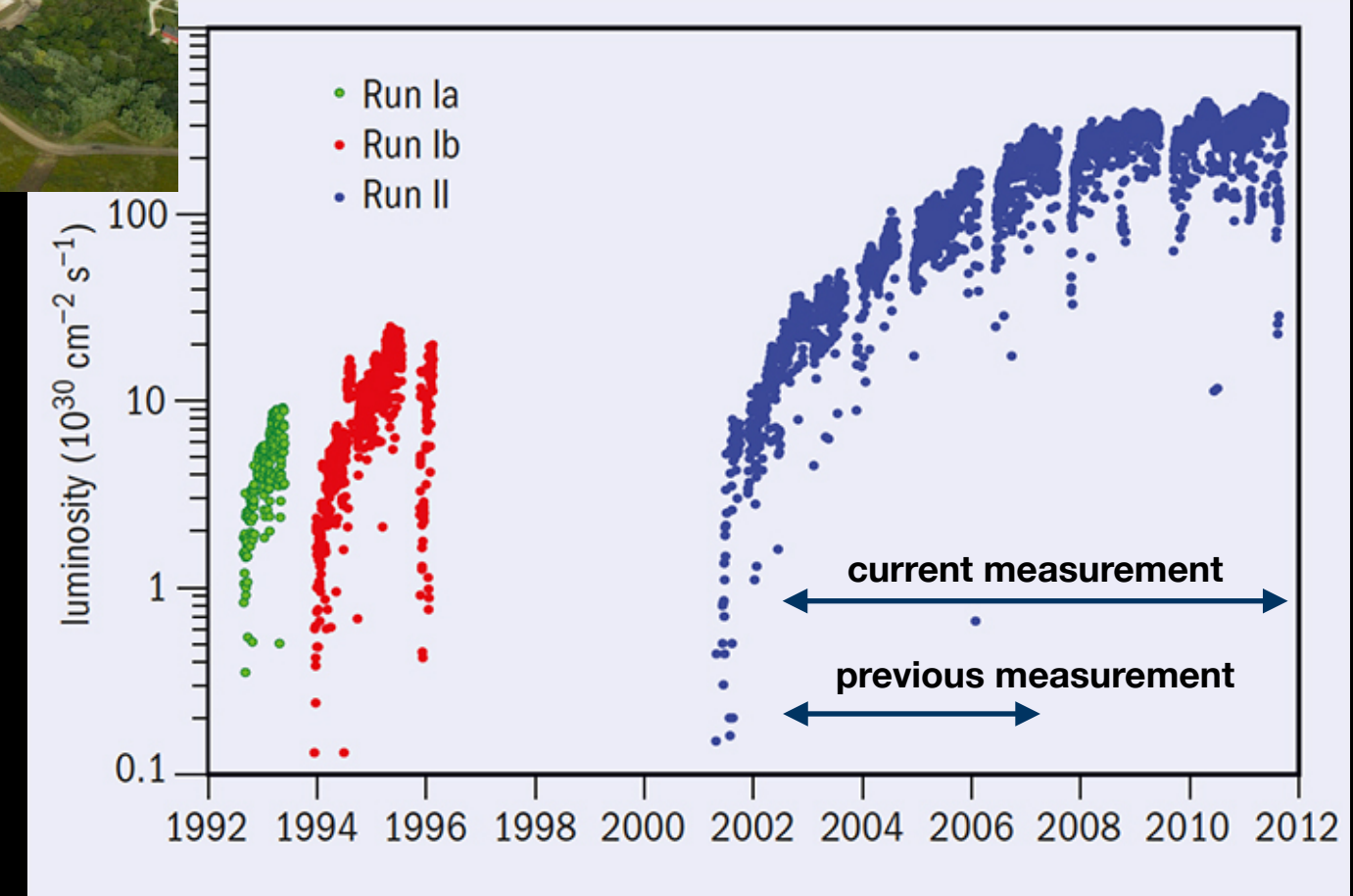


CDF II measurement of the W boson mass

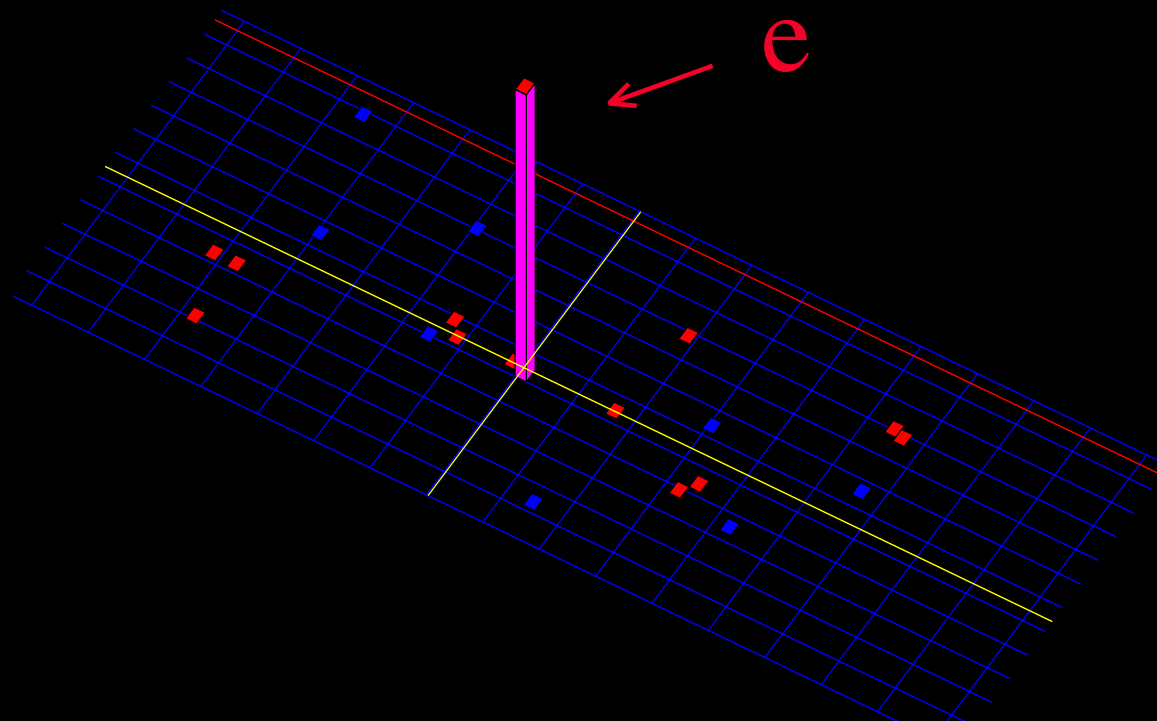


$\sqrt{s} = 1.96$ TeV proton-antiproton collisions from the Fermilab Tevatron

Measurement uses complete
Tevatron Run II data set



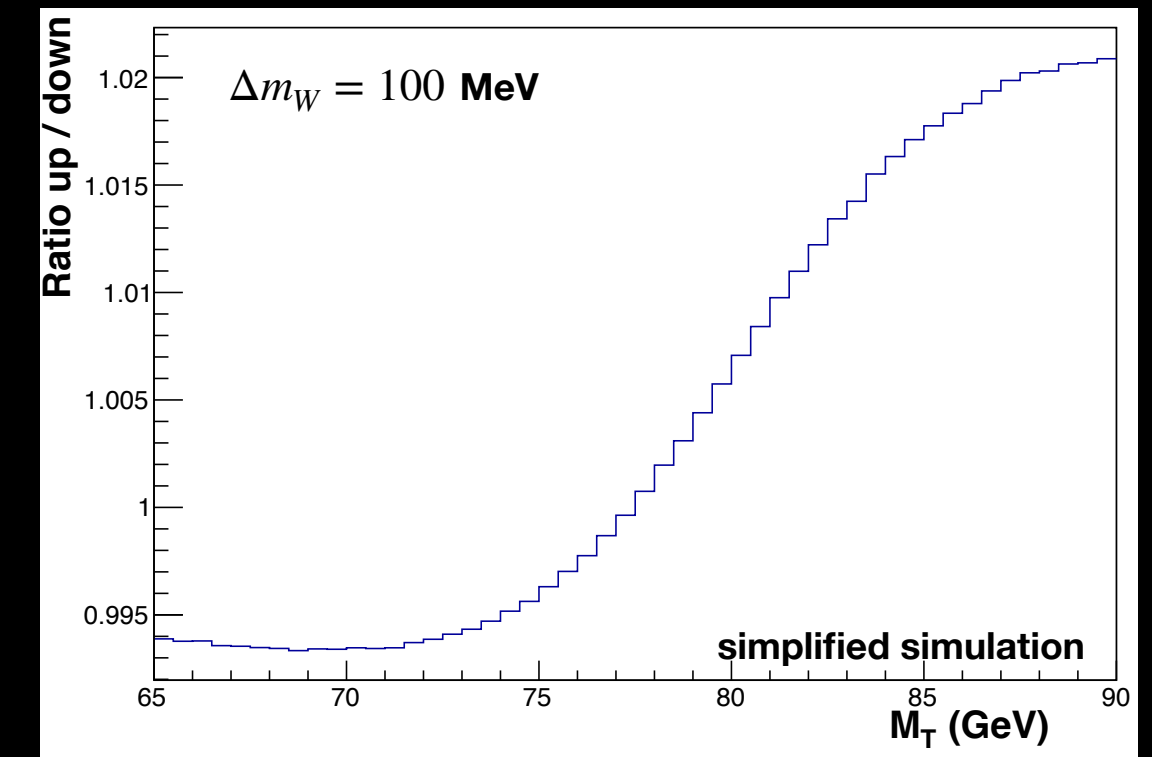
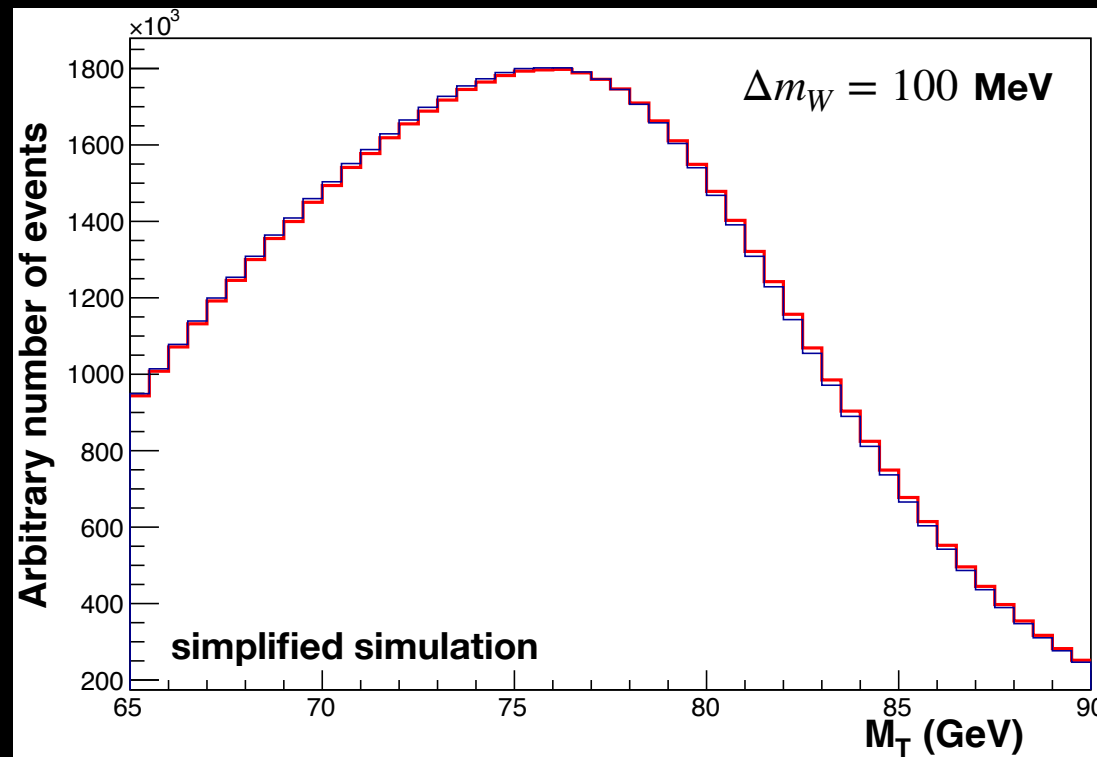
CDF II measurement of the W boson mass



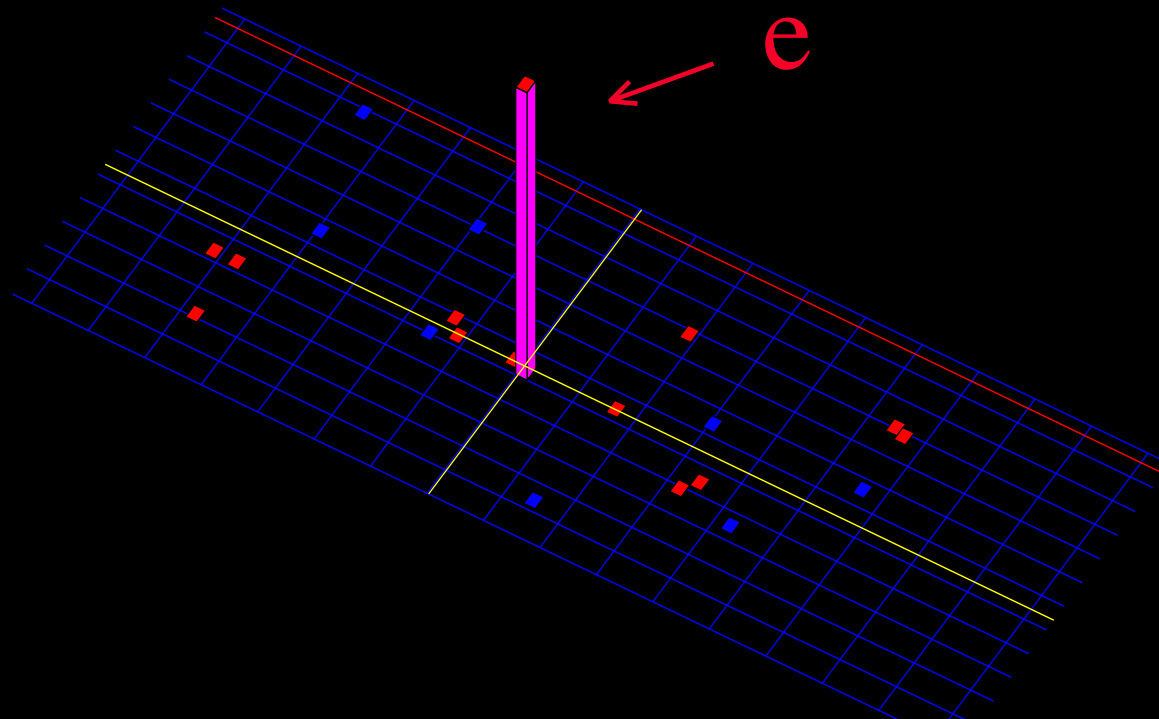
W bosons identified in their decays to $e\nu$ and $\mu\nu$

Mass measured by fitting template distributions
of transverse momentum and mass

$$m_T = \sqrt{2p_T^l p_T (1 - \cos \Delta\phi)}$$



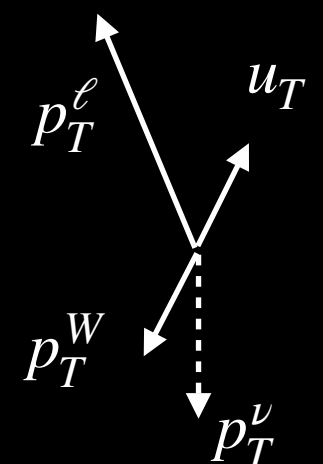
Calibrations



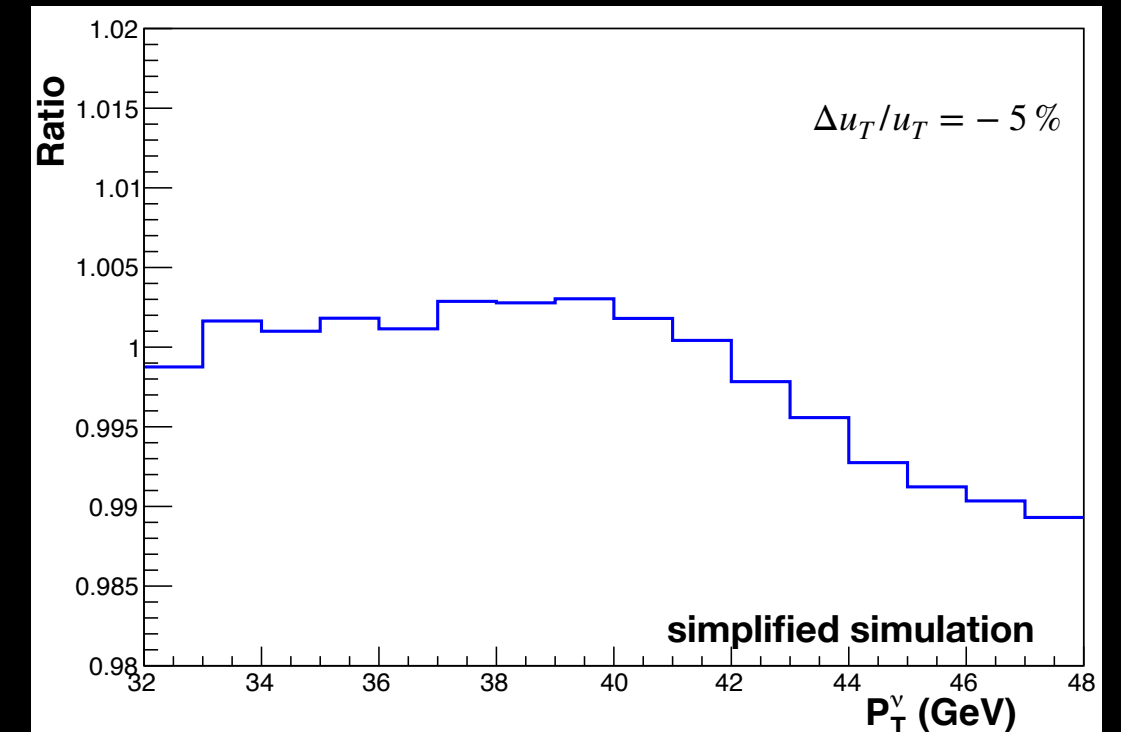
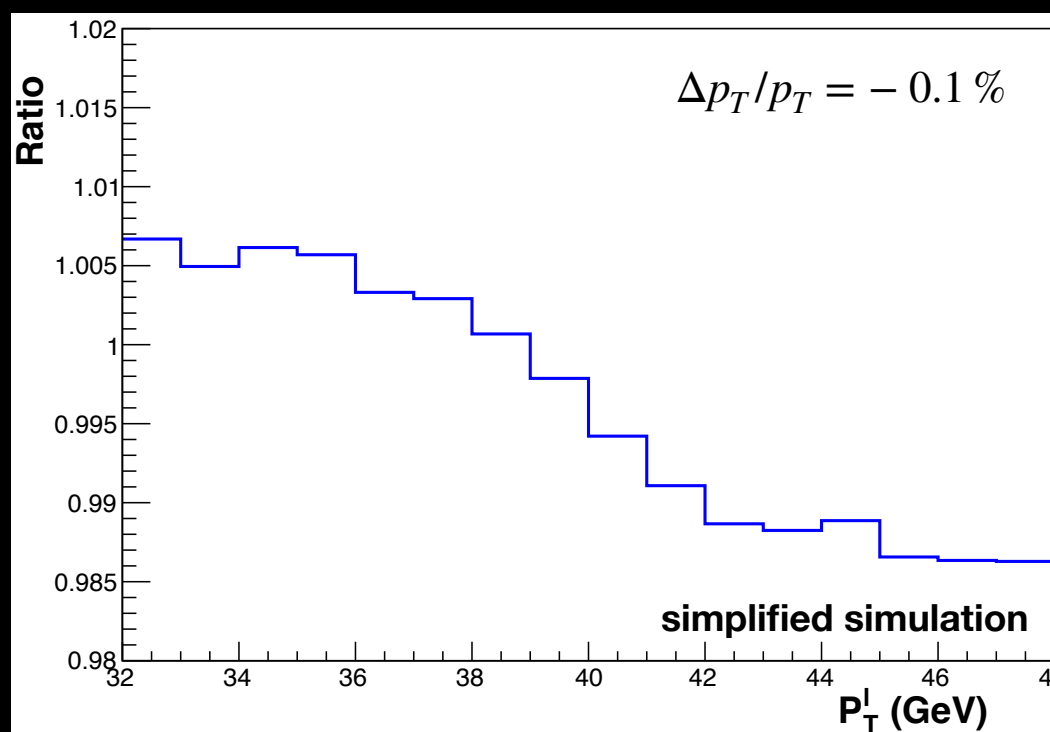
Charged lepton scale

Measurement requires precise calibrations
and momentum scale and resolution

$$\vec{p}_T = -(\vec{p}_T^l + \vec{u}_T)$$



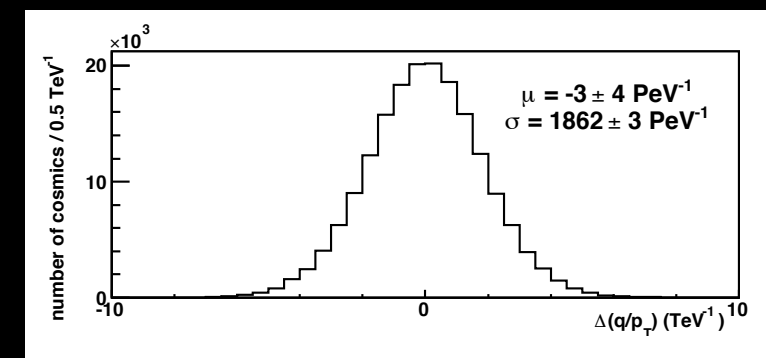
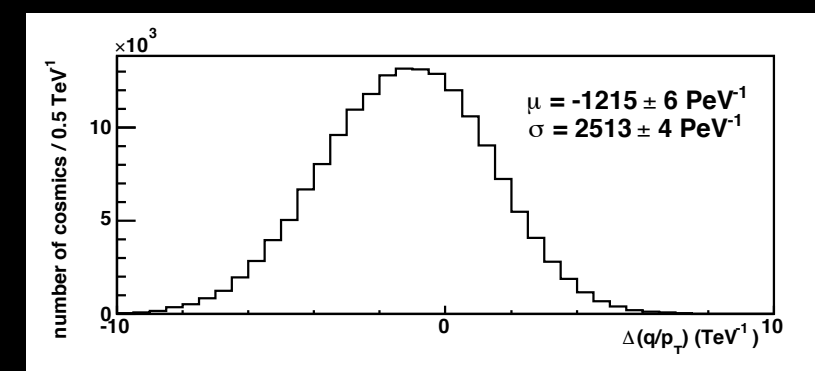
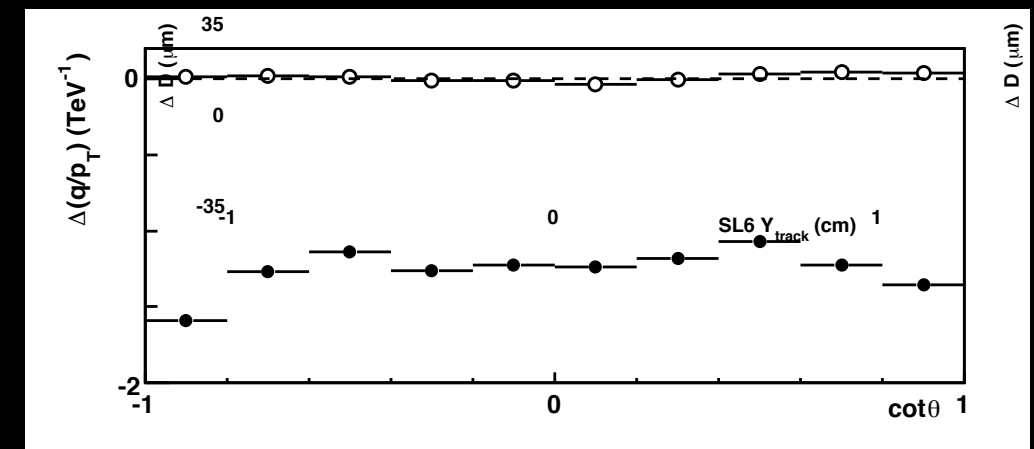
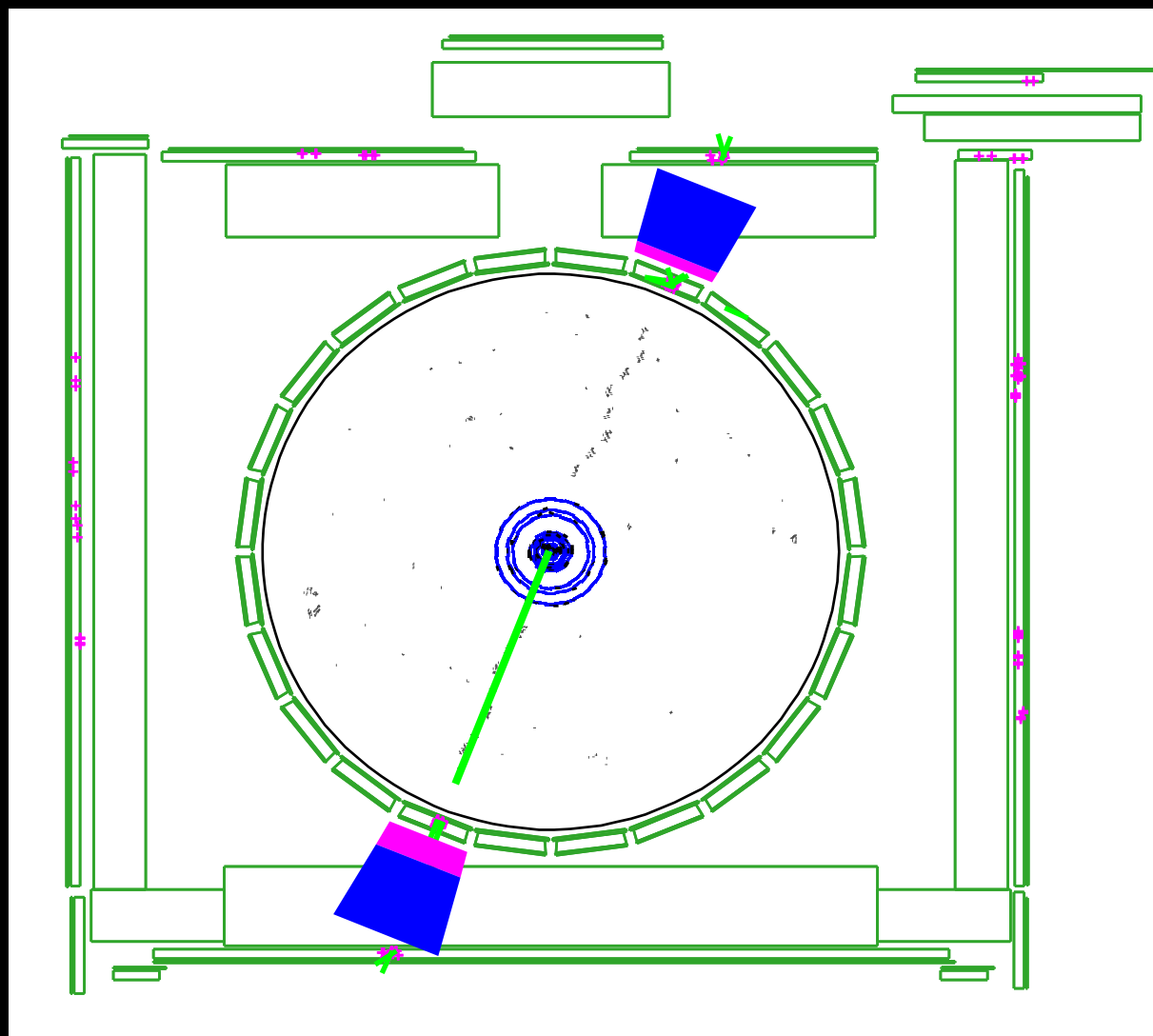
Recoil scale



Muon momentum calibration

First step is to align the drift chamber (the “central outer tracker” or COT)

Two degrees of freedom (shift & rotation) for each of 2520 cells made up of twelve sense wires constrained using hit residuals from cosmic-ray tracks



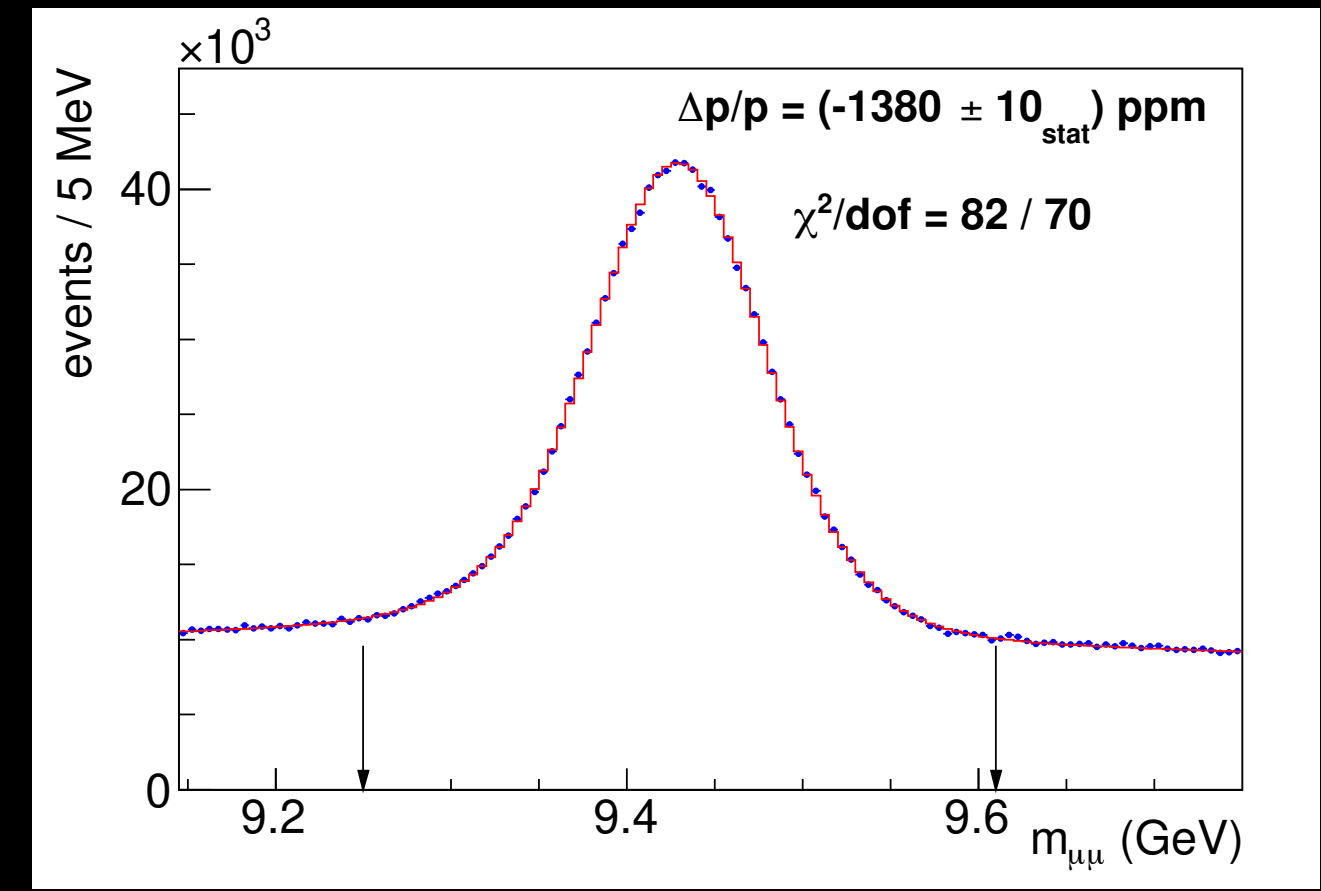
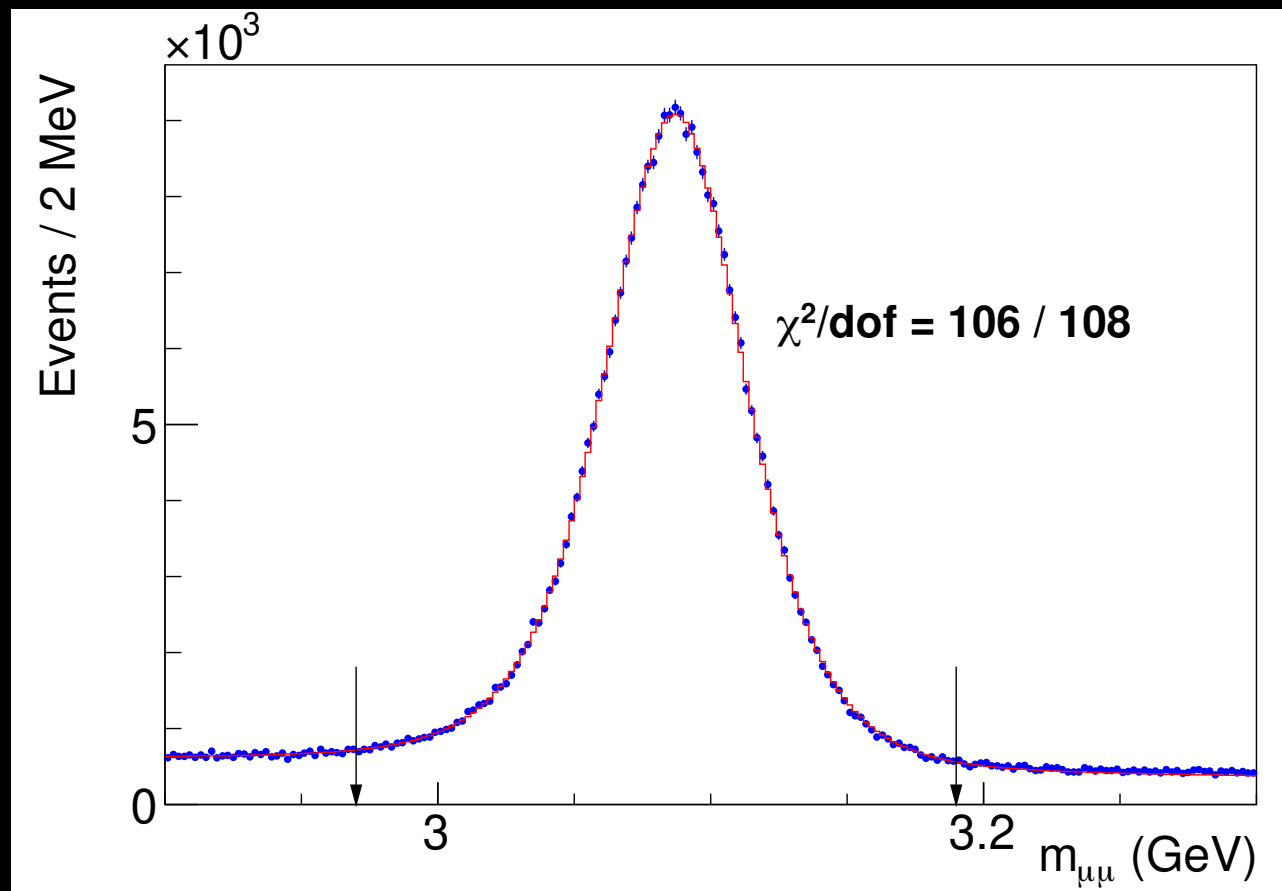
Muon momentum calibration

Second step is to calibrate the momentum scale using J/ψ and Υ decays to muons

Simulation:

Adjust kinematics to match the data

Model resonance shape using hit-level simulation and NLO form factor for QED radiation

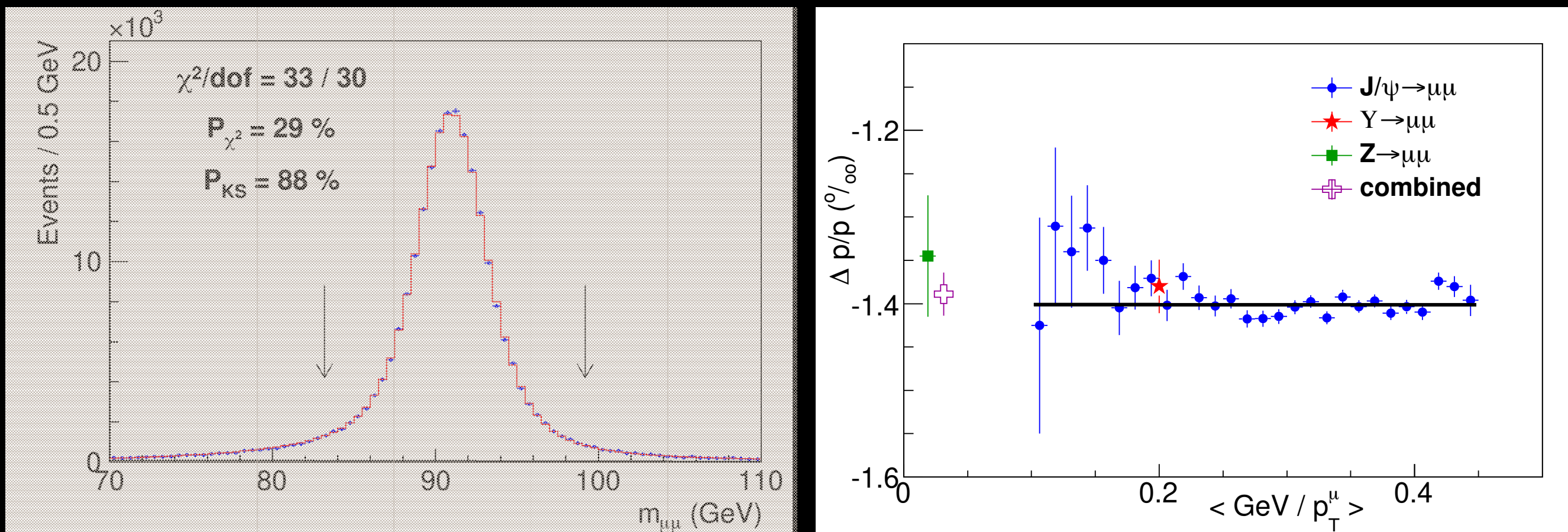


Muon momentum calibration

Final step is to measure the Z boson mass

$$M_Z = 91\ 192.0 \pm 6.4_{stat} \pm 4.0_{sys} \text{ MeV}$$

Result blinded with [-50,50] MeV offset until previous steps were complete
Combine all measurements into a final charged-track momentum scale



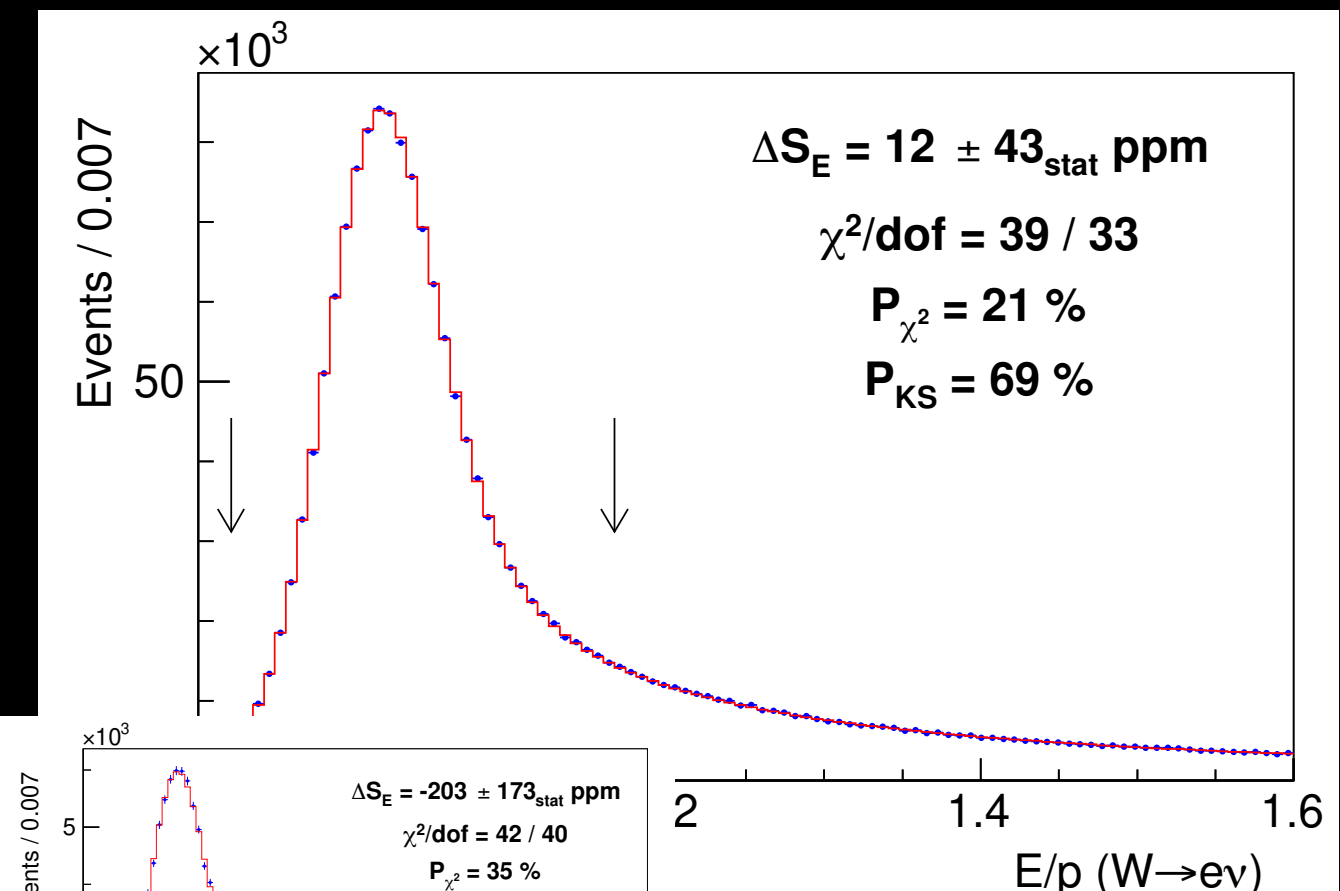
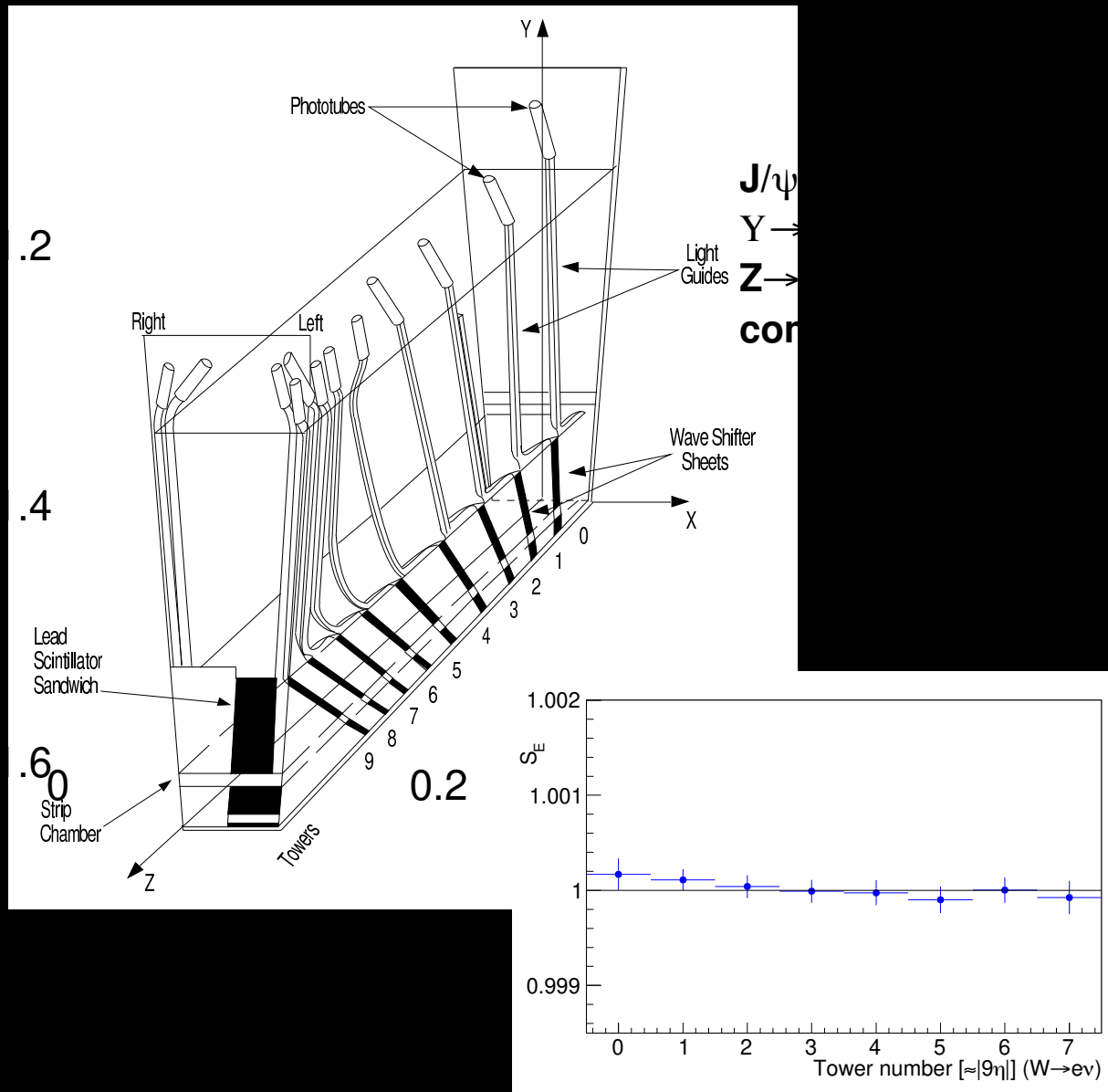
Electron momentum calibration

First step is to transfer the track calibration to the calorimeter (E/p) using W & Z decays

Data corrections:

Use mean E/p to remove time dependence & response variations in tower

Fit ratio of calorimeter energy to track momentum to correct each tower in η



Electron momentum calibration

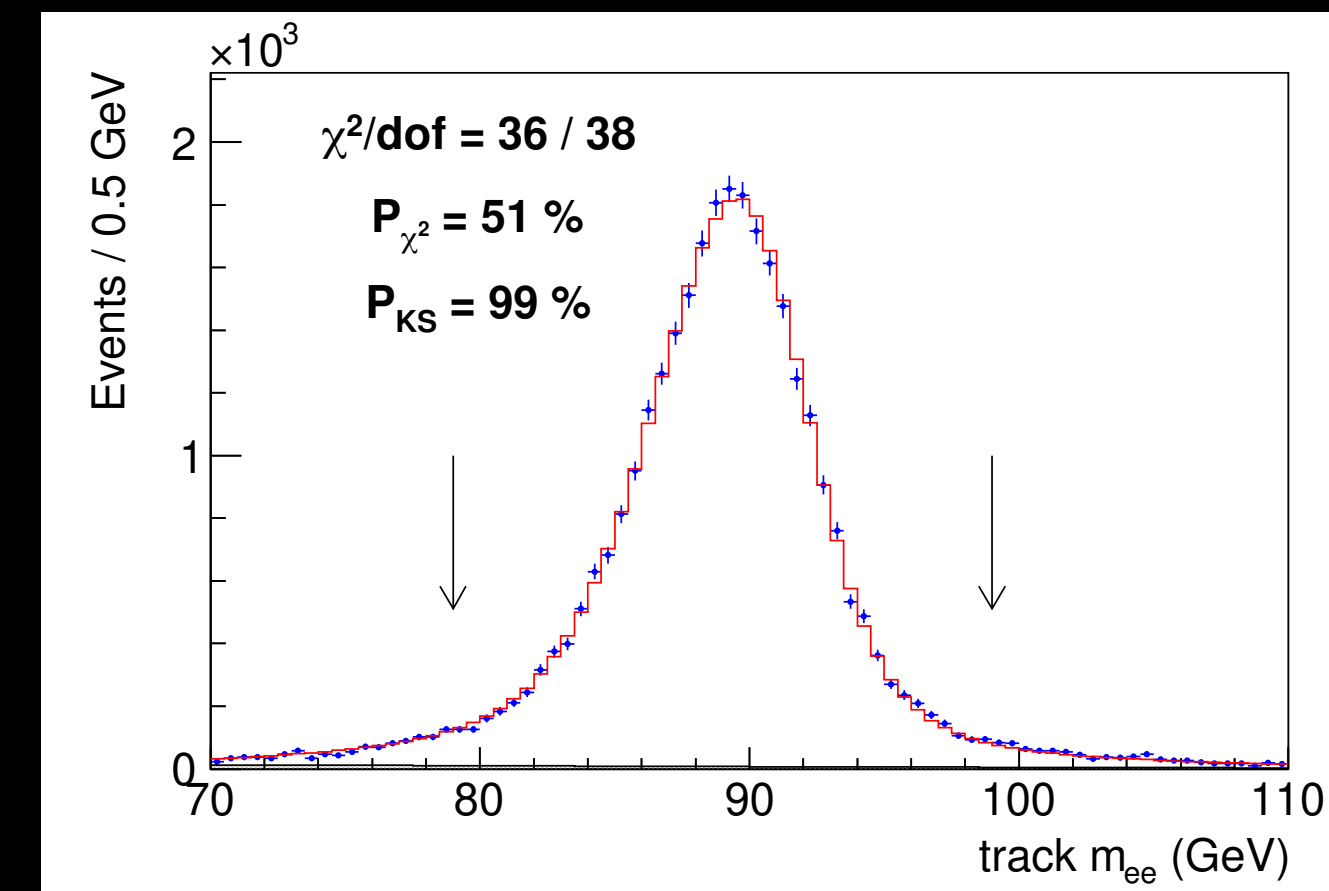
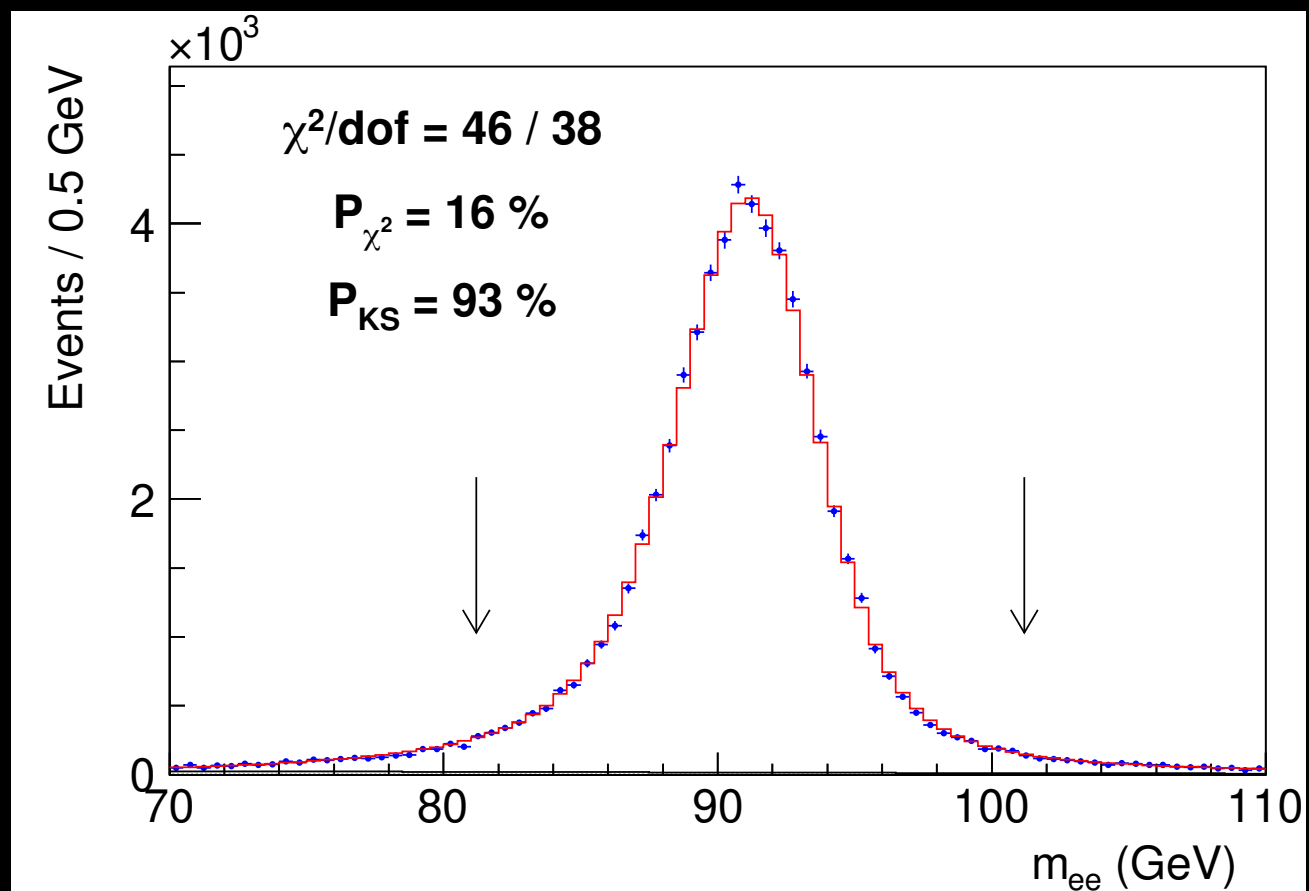
Second step is the measurement of the Z boson mass

$$M_Z = 91\ 194.3 \pm 13.8_{stat} \pm 7.6_{sys} \text{ MeV}$$

As a consistency check measure mass using only track information

e.g. $M_Z = 91\ 215.2 \pm 22.4 \text{ MeV}$ for non-radiative electrons ($E/p < 1.1$)

Same blinding as for muon channel

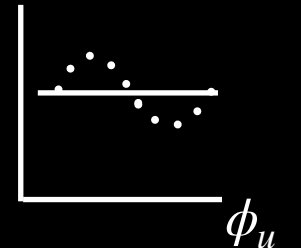


Recoil momentum calibration

First step is the alignment of the calorimeters

Misalignments relative to the beam axis cause a modulation in the recoil direction

Alignment performed separately for each run period using minimum-bias data

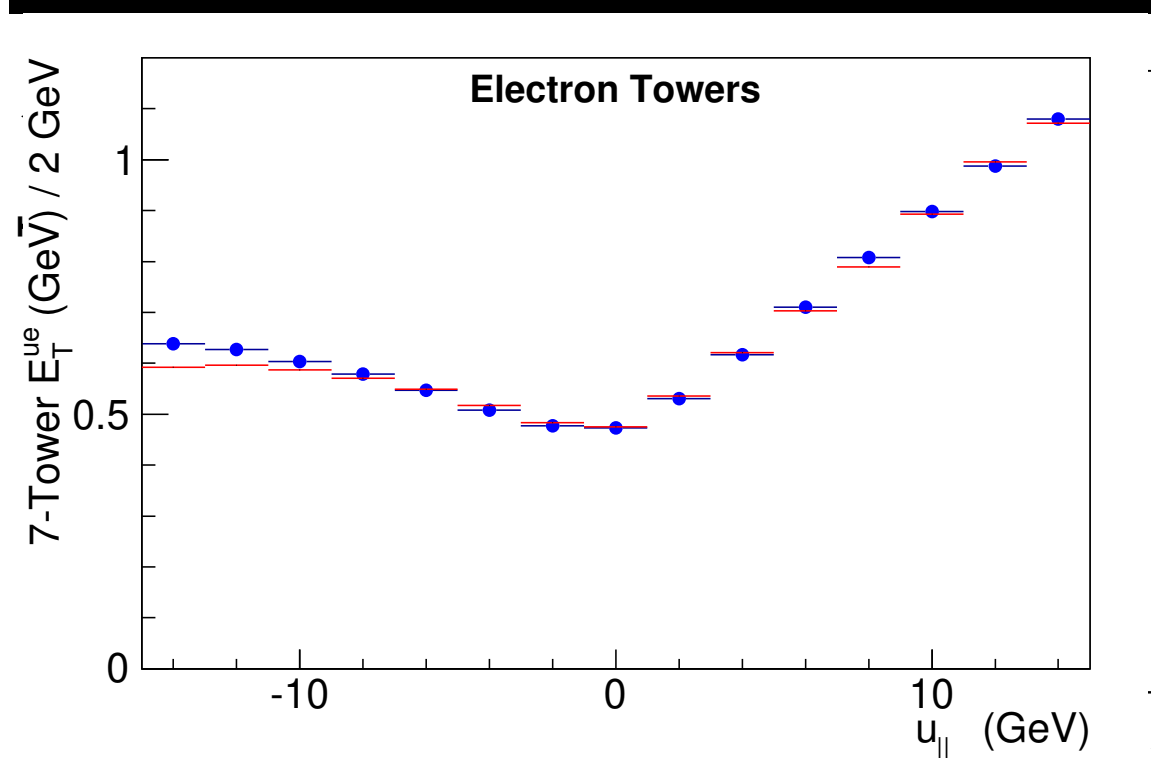
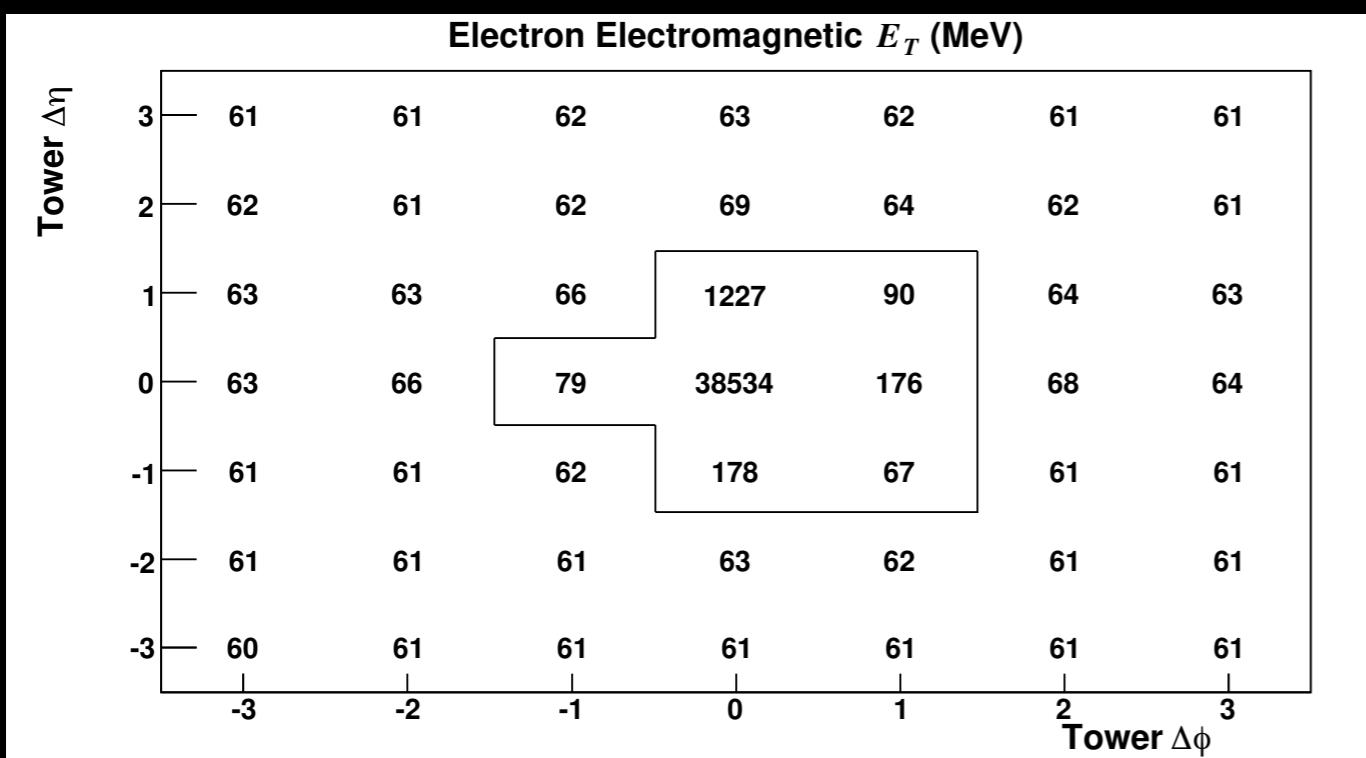


Second step is the reconstruction of the recoil

Remove towers traversed by identified leptons

Remove corresponding recoil energy in simulation using towers rotated by 90°

validate using towers rotated by 180°

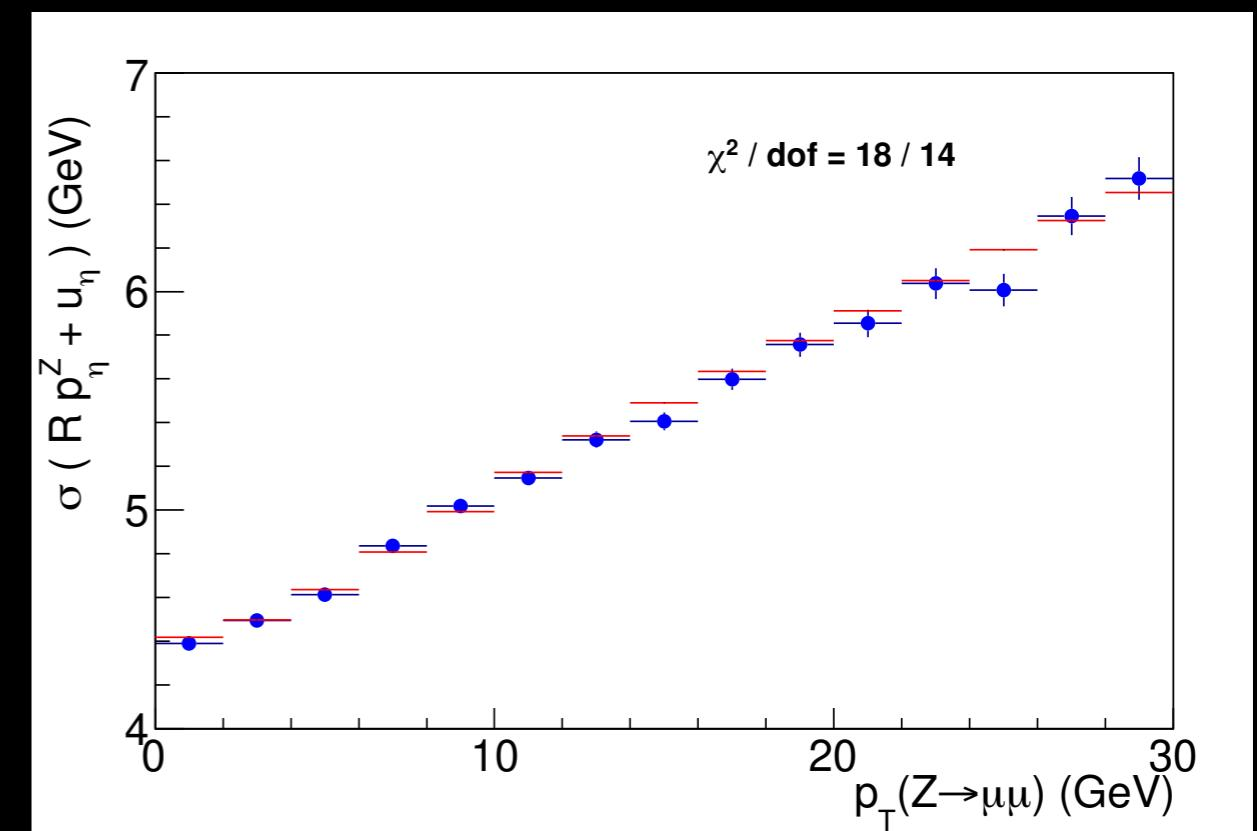
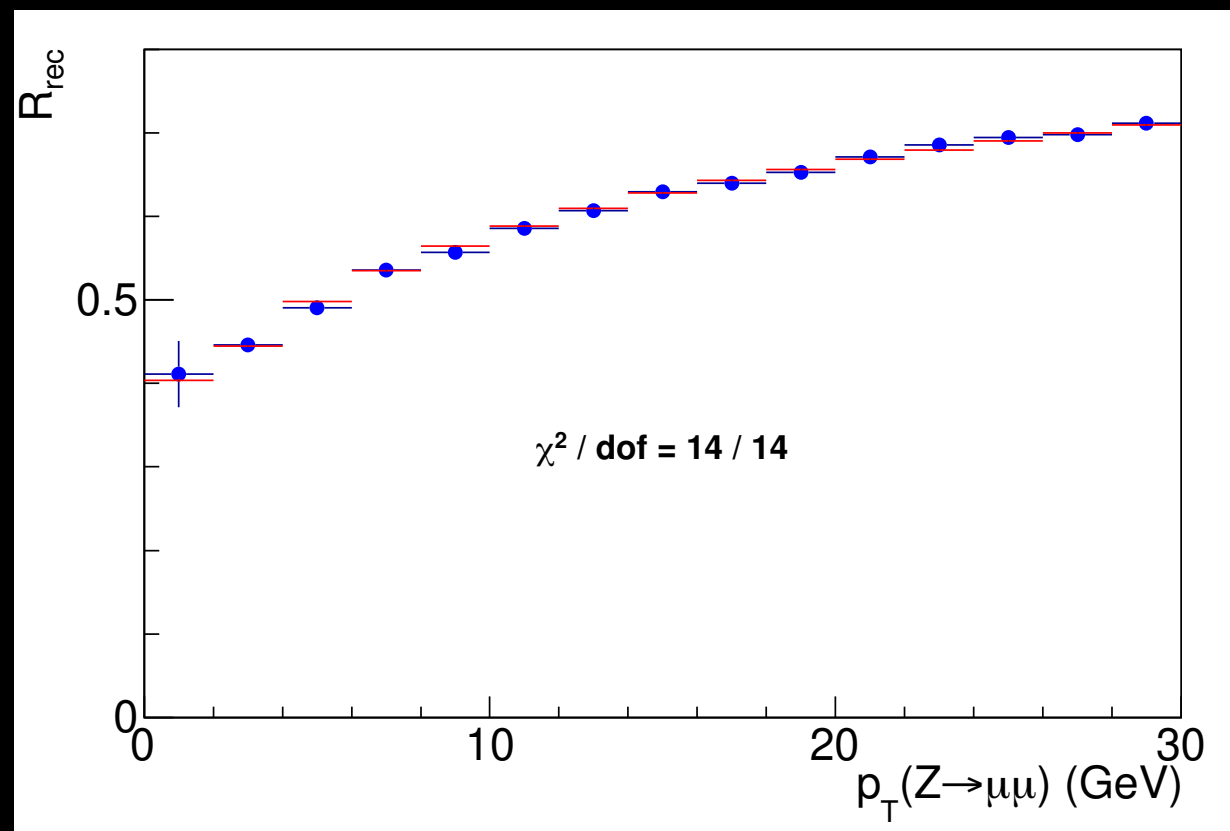
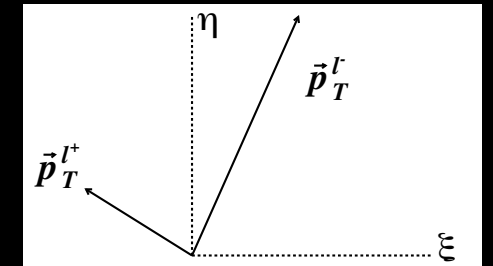


Recoil momentum calibration

Third step is the calibration of the recoil response

Balance recoil against direction of p_{T^Z}

Check calibration using ratio of recoil magnitude to p_{T^Z} along direction of p_{T^Z} (R_{rec})

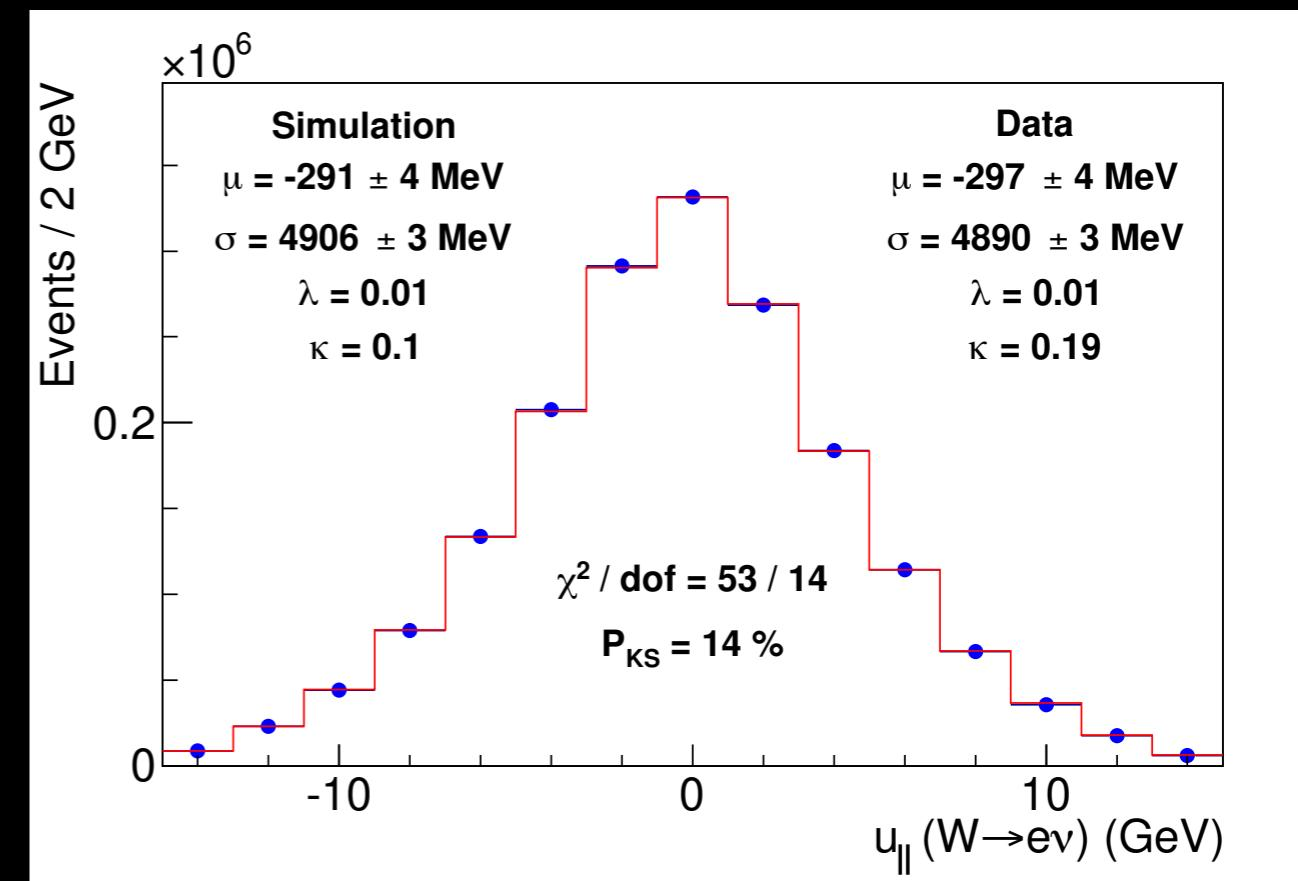
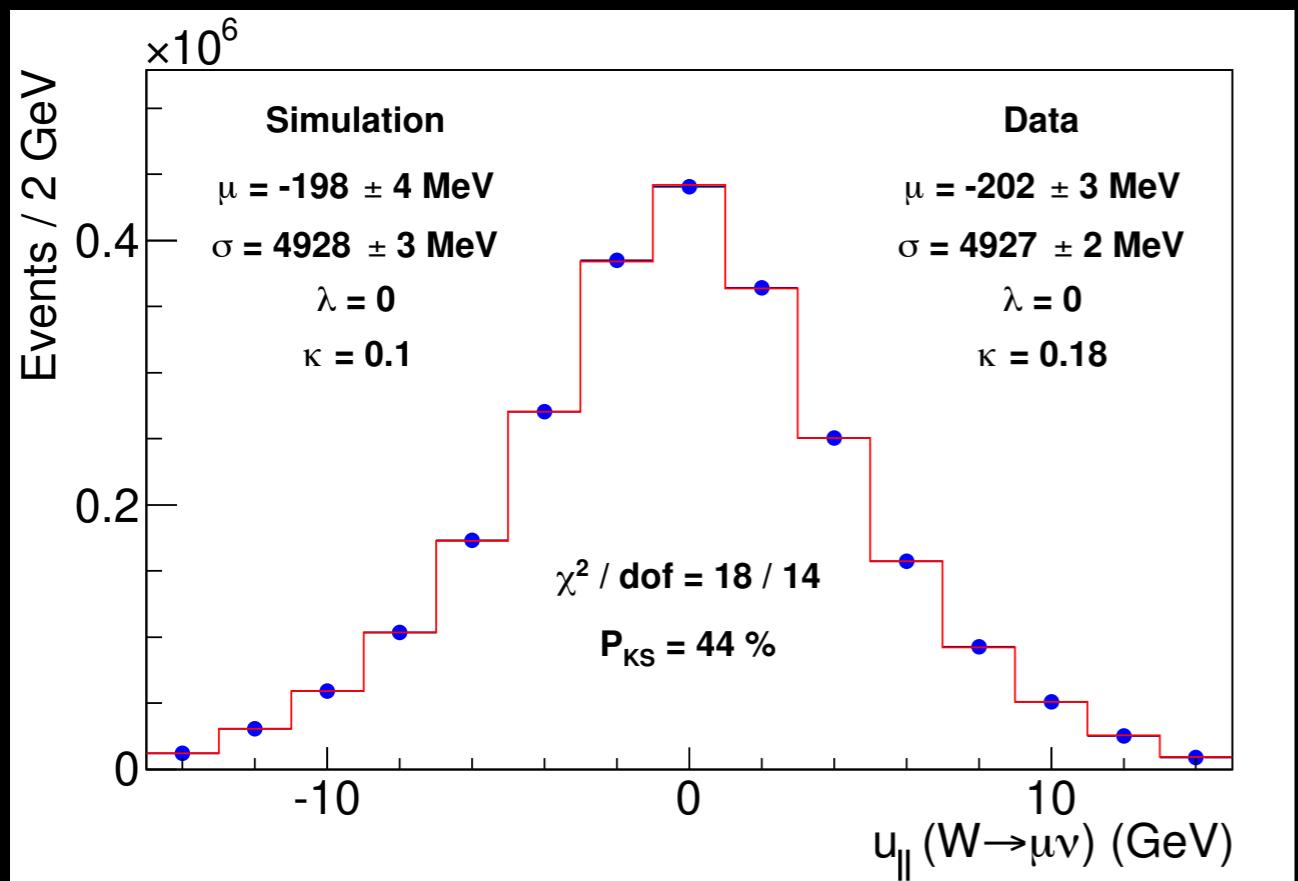
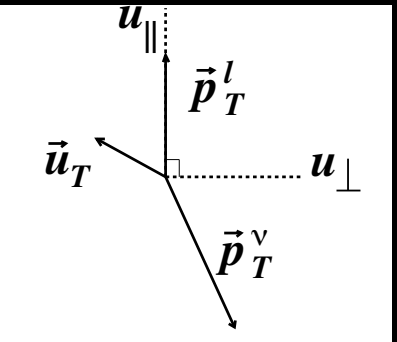


Recoil momentum validation

W boson recoil distributions validate the model

Most important is the recoil projected along the charged-lepton's momentum ($u_{||}$)

$$m_T \approx 2p_T \sqrt{1 + u_{||}/p_T} \approx 2p_T + u_{||}$$



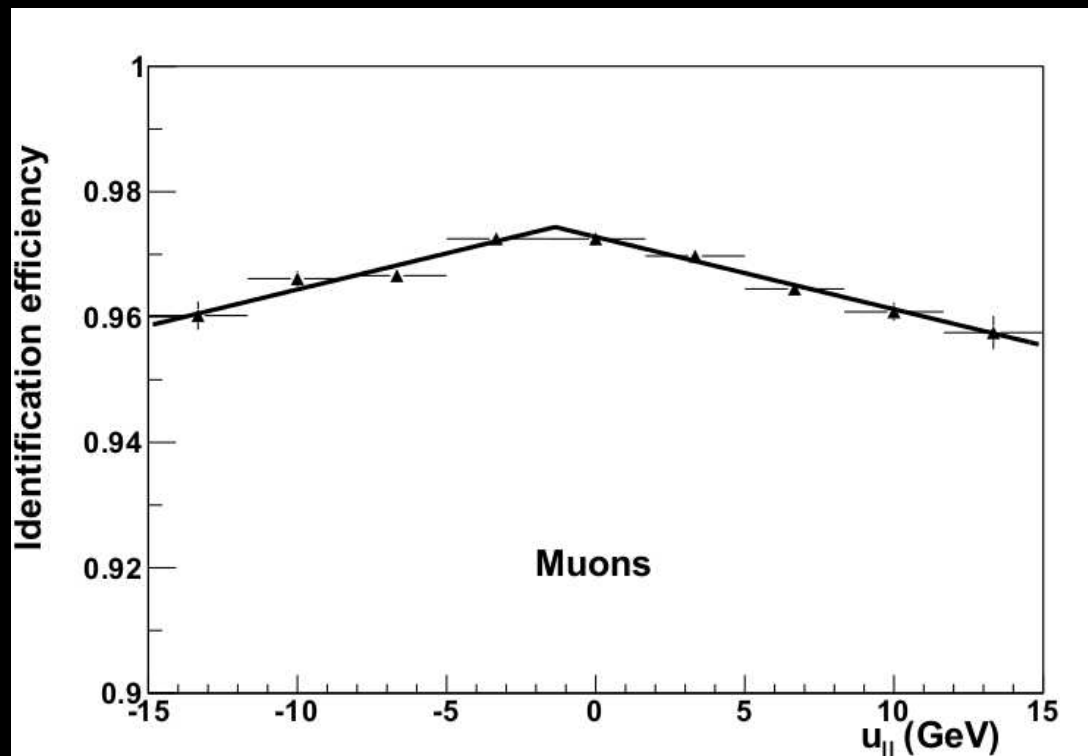
W boson candidates

W boson event selection

Triggers with low momentum thresholds (18 GeV) and very loose lepton id

Offline id also loose, efficiencies vary by 2% as hadronic recoil direction changes

No lepton isolation requirement in trigger or offline selection

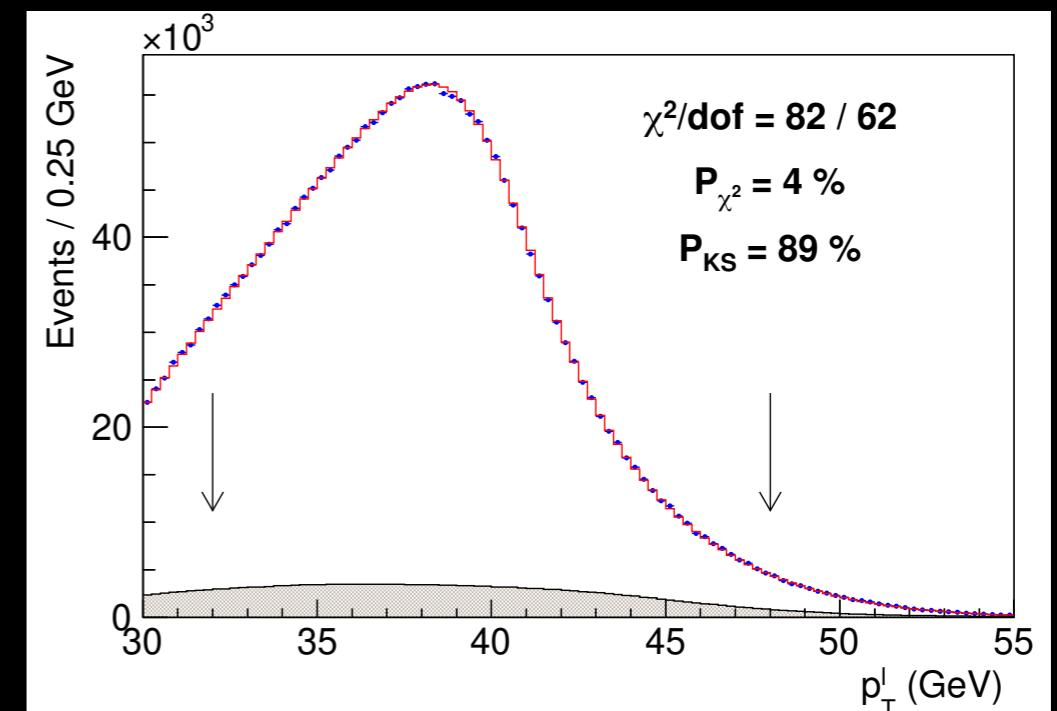


2.4 M $W \rightarrow \mu\nu$ candidates

1.8 M $W \rightarrow e\nu$ candidates

Background suppressed by stringent
hadronic recoil requirement

$$u_T < 15 \text{ GeV}$$



Other kinematic requirements

Lepton and missing p_T in the range 30-55 GeV
Transverse mass in the range 60-100 GeV

W boson production

Transverse mass insensitive to p_T^W to first order

O(1 MeV) change in m_W for each % change in p_T^W from 0-30 GeV

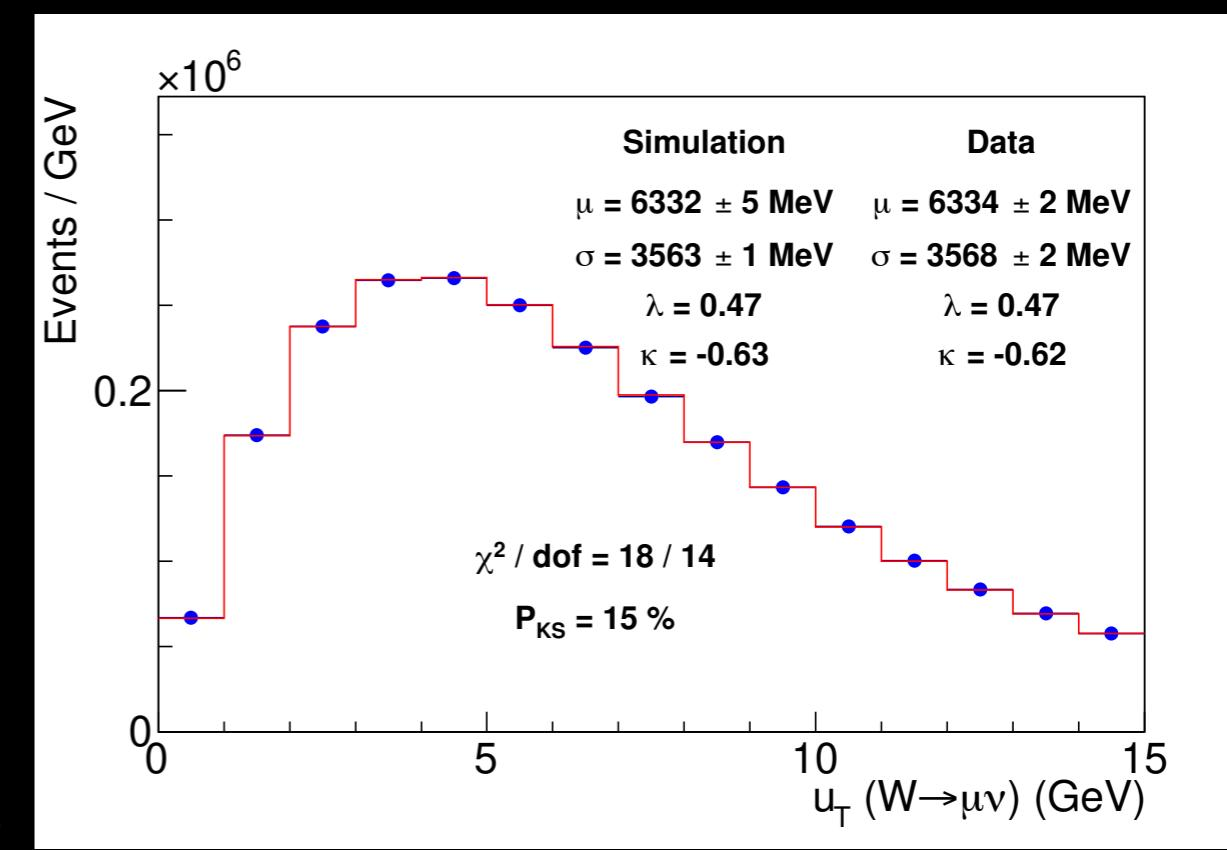
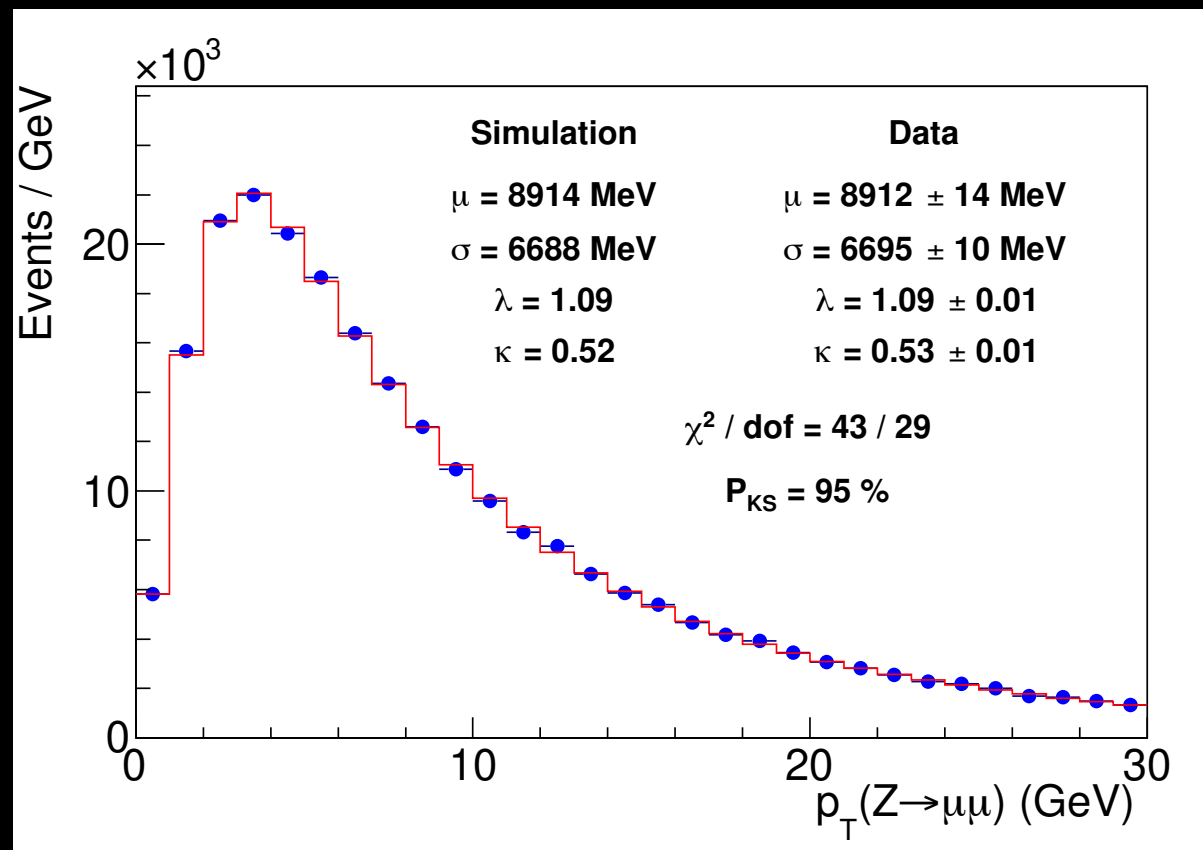
Lepton p_T distributions more sensitive to p_T^W

Generate events with Resbos: non-perturbative parameters & NNLL resummation

Z boson p_T used to constrain one non-perturbative parameter and the perturbative coupling

Parameterized Resbos model describes observed W boson recoil

uncertainty estimated using DYQT and constrained with data



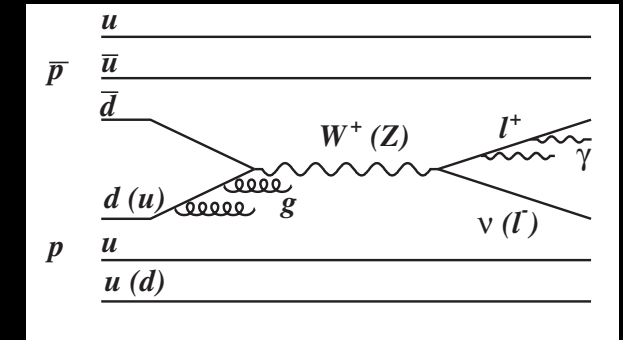
W boson production and decay

Parton distributions impact the measurement through lepton acceptance

Restriction in η reduces the fraction of low- p_T leptons

Small correction applied to update to NNPDF3.1 NNLO PDF

The set with the most W charge asymmetry measurements at the time



Uncertainty determined using a principal component analysis on the replica set

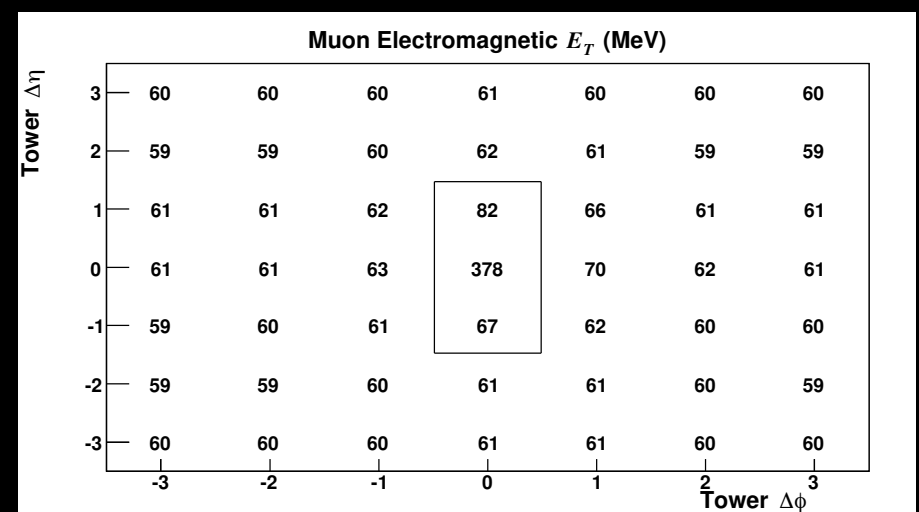
Measurement sensitive to ~ 15 eigenvectors

Leading 25 eigenvectors used to estimate uncertainty (3.9 MeV)

Three general NNLO PDF sets (NNPDF3.1, CT18, and MMHT14) have a range of ± 2.1 MeV from mean

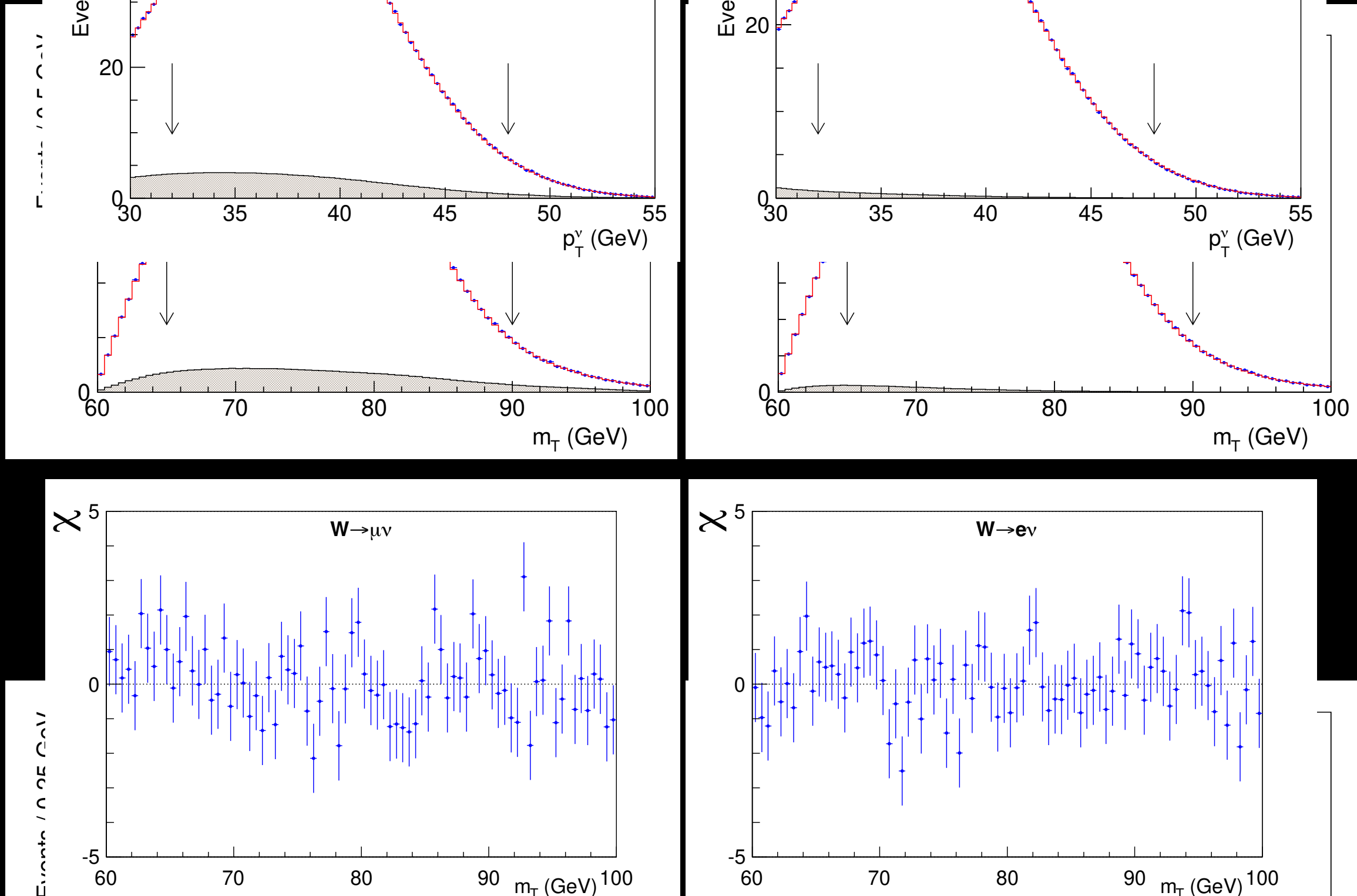
Photos resummation with ME corrections used to model final-state photon radiation

validated by studying the average radiation in EM towers around the charged lepton, and with the Z mass measurement

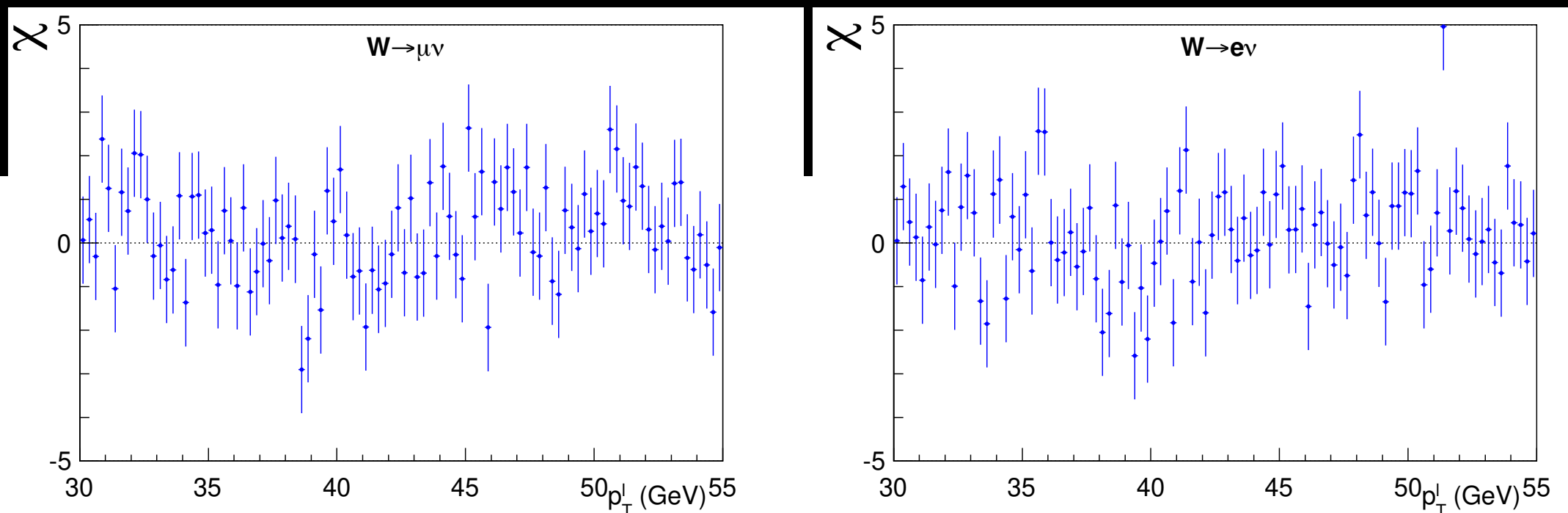
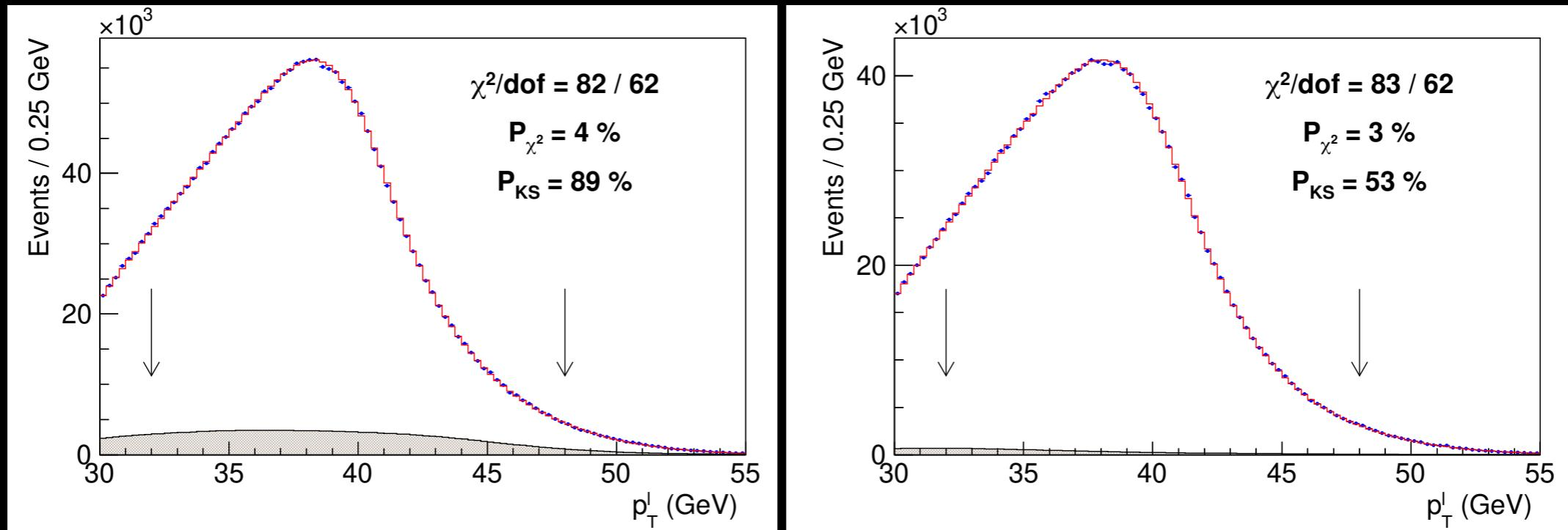


W boson mass measurement

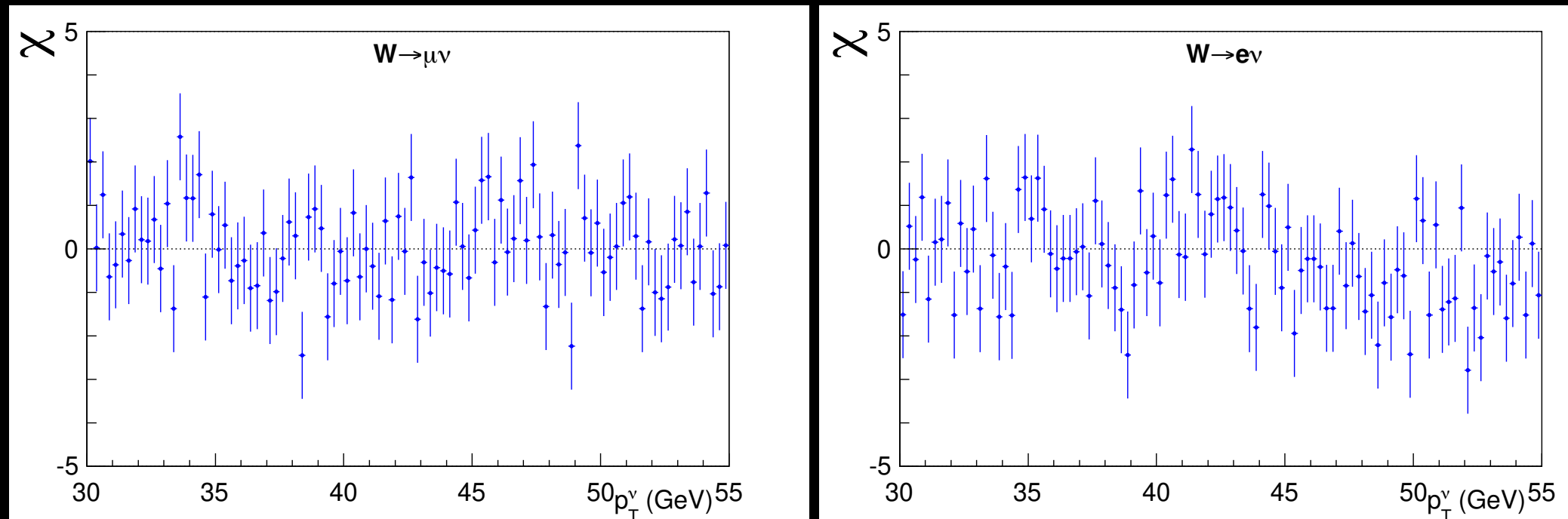
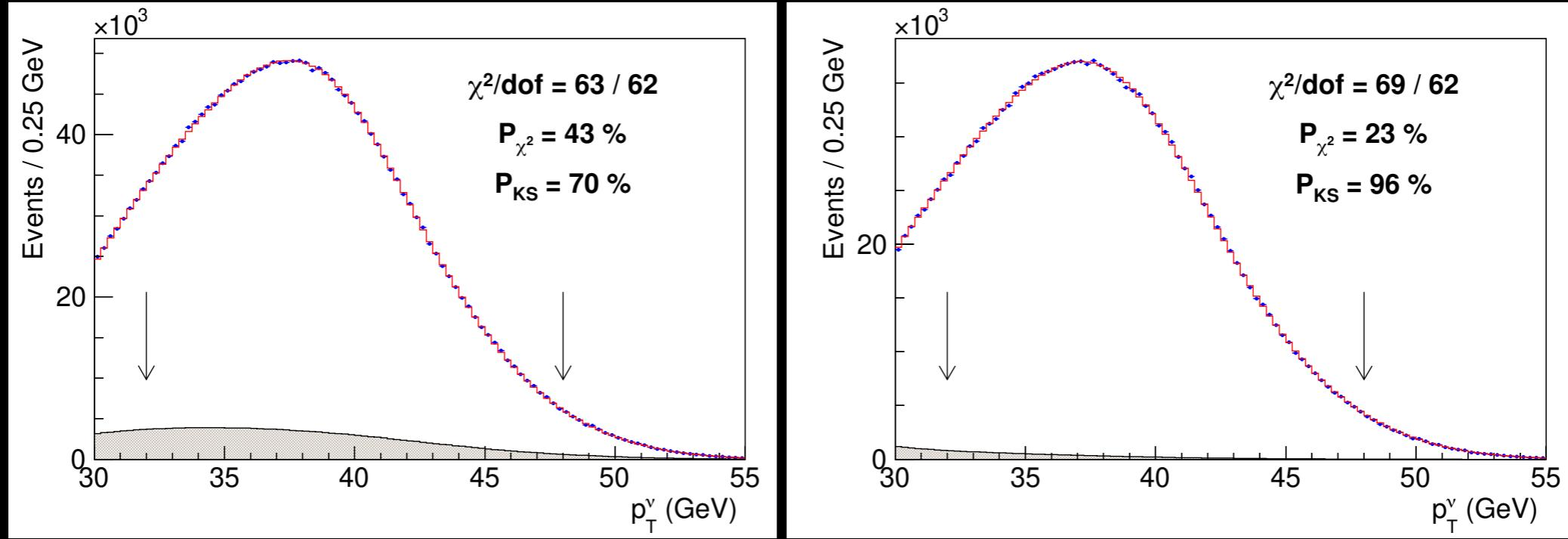
Result blinded by [-50,50] MeV offset until all previous steps complete



Mass measurement with p_T^ℓ distribution



Mass measurement with p_T^ν distribution



W boson mass measurement

Combination	m_T fit		p_T^ℓ fit		p_T^ν fit		Value (MeV)	χ^2/dof	Probability (%)
	Electrons	Muons	Electrons	Muons	Electrons	Muons			
m_T	✓	✓					$80\,439.0 \pm 9.8$	1.2 / 1	28
p_T^ℓ			✓	✓			$80\,421.2 \pm 11.9$	0.9 / 1	36
p_T^ν					✓	✓	$80\,427.7 \pm 13.8$	0.0 / 1	91
m_T & p_T^ℓ	✓	✓	✓	✓			$80\,435.4 \pm 9.5$	4.8 / 3	19
m_T & p_T^ν	✓	✓			✓	✓	$80\,437.9 \pm 9.7$	2.2 / 3	53
p_T^ℓ & p_T^ν			✓	✓	✓	✓	$80\,424.1 \pm 10.1$	1.1 / 3	78
Electrons	✓		✓		✓		$80\,424.6 \pm 13.2$	3.3 / 2	19
Muons		✓		✓		✓	$80\,437.9 \pm 11.0$	3.6 / 2	17
All	✓	✓	✓	✓	✓	✓	$80\,433.5 \pm 9.4$	7.4 / 5	20

Fit difference	Muon channel	Electron channel
$M_W(\ell^+) - M_W(\ell^-)$	$-7.8 \pm 18.5_{\text{stat}} \pm 12.7_{\text{COT}}$	$14.7 \pm 21.3_{\text{stat}} \pm 7.7_{\text{stat}}^{\text{E/P}} (0.4 \pm 21.3_{\text{stat}})$
$M_W(\phi_\ell > 0) - M_W(\phi_\ell < 0)$	$24.4 \pm 18.5_{\text{stat}}$	$9.9 \pm 21.3_{\text{stat}} \pm 7.5_{\text{stat}}^{\text{E/P}} (-0.8 \pm 21.3_{\text{stat}})$
$M_Z(\text{run} > 271100) - M_Z(\text{run} < 271100)$	$5.2 \pm 12.2_{\text{stat}}$	$63.2 \pm 29.9_{\text{stat}} \pm 8.2_{\text{stat}}^{\text{E/P}} (-16.0 \pm 29.9_{\text{stat}})$

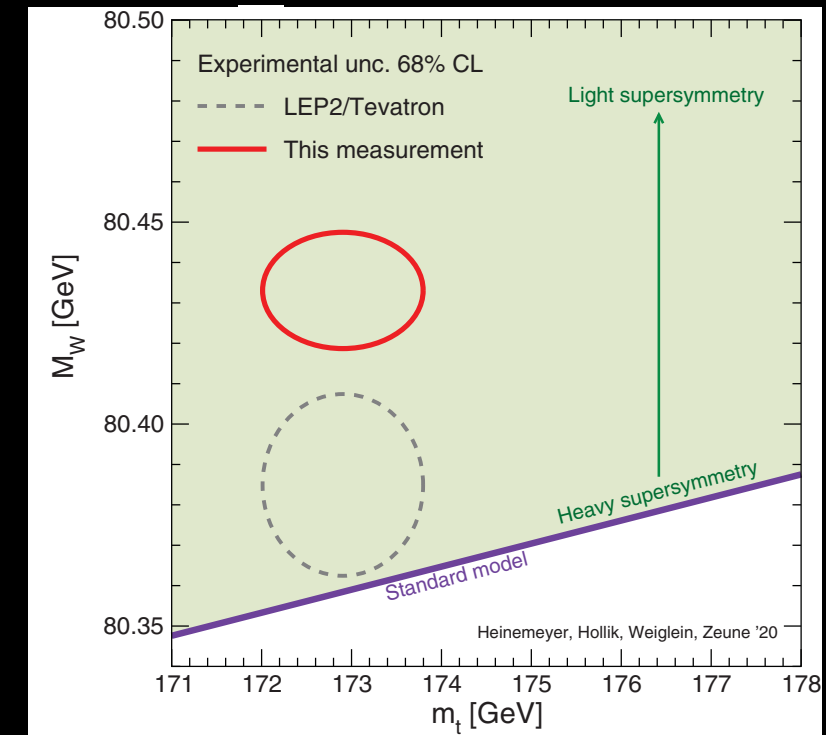
Summary

The W boson mass is a sensitive quantity to high-scale physics

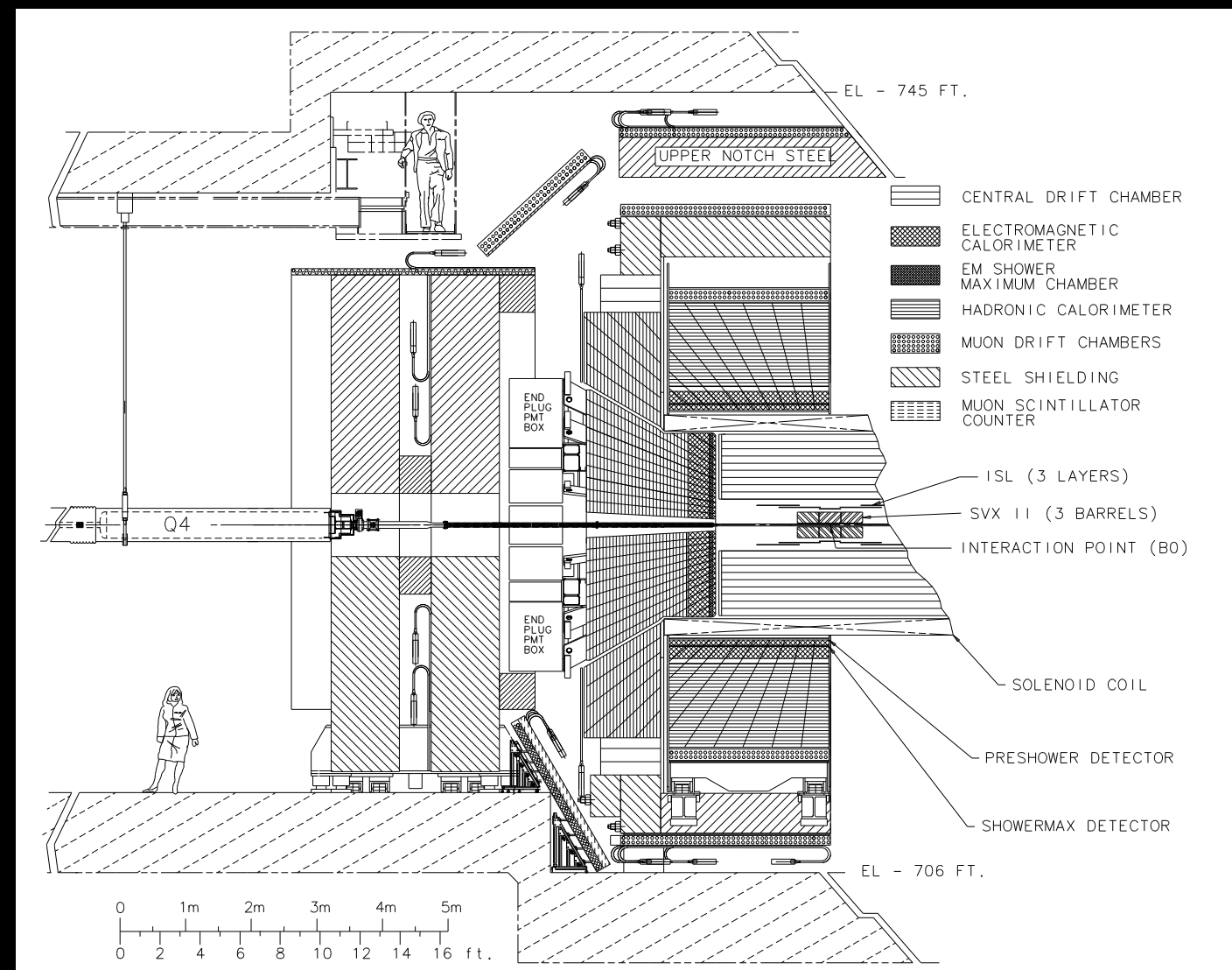
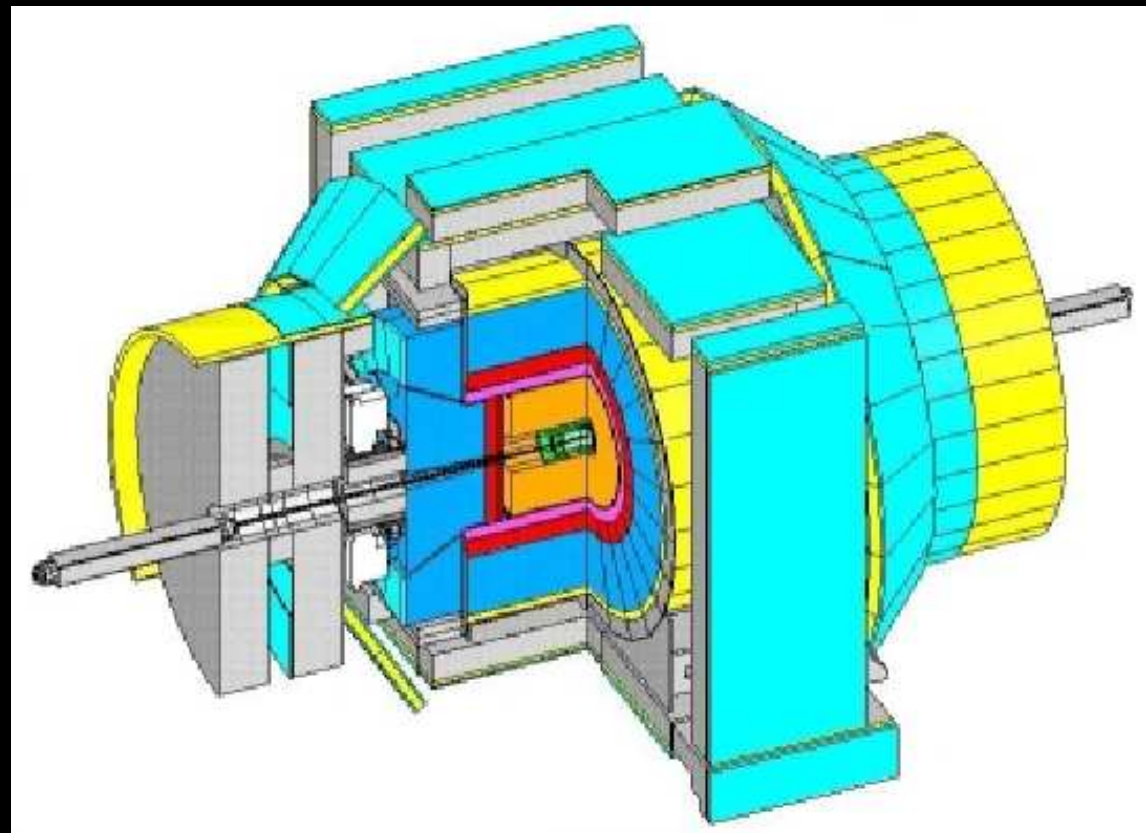
A measurement of m_W with <10 MeV precision has been achieved with the complete CDF data set
The result of >20 years of experience with the CDF II detector

Measured mass deviates from the SM by ~0.1% with high significance

Distribution	W boson mass (MeV)	χ^2/dof
$m_T(e, v)$	$80,429.1 \pm 10.3_{\text{stat}} \pm 8.5_{\text{syst}}$	39/48
$p_T^\ell(e)$	$80,411.4 \pm 10.7_{\text{stat}} \pm 11.8_{\text{syst}}$	83/62
$p_T^v(e)$	$80,426.3 \pm 14.5_{\text{stat}} \pm 11.7_{\text{syst}}$	69/62
$m_T(\mu, v)$	$80,446.1 \pm 9.2_{\text{stat}} \pm 7.3_{\text{syst}}$	50/48
$p_T^\ell(\mu)$	$80,428.2 \pm 9.6_{\text{stat}} \pm 10.3_{\text{syst}}$	82/62
$p_T^v(\mu)$	$80,428.9 \pm 13.1_{\text{stat}} \pm 10.9_{\text{syst}}$	63/62
Combination	$80,433.5 \pm 6.4_{\text{stat}} \pm 6.9_{\text{syst}}$	7.4/5



Backup



Uncertainties

Source	Uncertainty (MeV)
Lepton energy scale	3.0
Lepton energy resolution	1.2
Recoil energy scale	1.2
Recoil energy resolution	1.8
Lepton efficiency	0.4
Lepton removal	1.2
Backgrounds	3.3
p_T^Z model	1.8
p_T^W/p_T^Z model	1.3
Parton distributions	3.9
QED radiation	2.7
W boson statistics	6.4
Total	9.4

Source of systematic uncertainty	m_T fit			p_T^ℓ fit			p_T^ν fit		
	Electrons	Muons	Common	Electrons	Muons	Common	Electrons	Muons	Common
Lepton energy scale	5.8	2.1	1.8	5.8	2.1	1.8	5.8	2.1	1.8
Lepton energy resolution	0.9	0.3	-0.3	0.9	0.3	-0.3	0.9	0.3	-0.3
Recoil energy scale	1.8	1.8	1.8	3.5	3.5	3.5	0.7	0.7	0.7
Recoil energy resolution	1.8	1.8	1.8	3.6	3.6	3.6	5.2	5.2	5.2
Lepton $u_{ }$ efficiency	0.5	0.5	0	1.3	1.0	0	2.6	2.1	0
Lepton removal	1.0	1.7	0	0	0	0	2.0	3.4	0
Backgrounds	2.6	3.9	0	6.6	6.4	0	6.4	6.8	0
p_T^Z model	0.7	0.7	0.7	2.3	2.3	2.3	0.9	0.9	0.9
p_T^W/p_T^Z model	0.8	0.8	0.8	2.3	2.3	2.3	0.9	0.9	0.9
Parton distributions	3.9	3.9	3.9	3.9	3.9	3.9	3.9	3.9	3.9
QED radiation	2.7	2.7	2.7	2.7	2.7	2.7	2.7	2.7	2.7
Statistical	10.3	9.2	0	10.7	9.6	0	14.5	13.1	0
Total	13.5	11.8	5.8	16.0	14.1	7.9	18.8	17.1	7.4

Background fractions

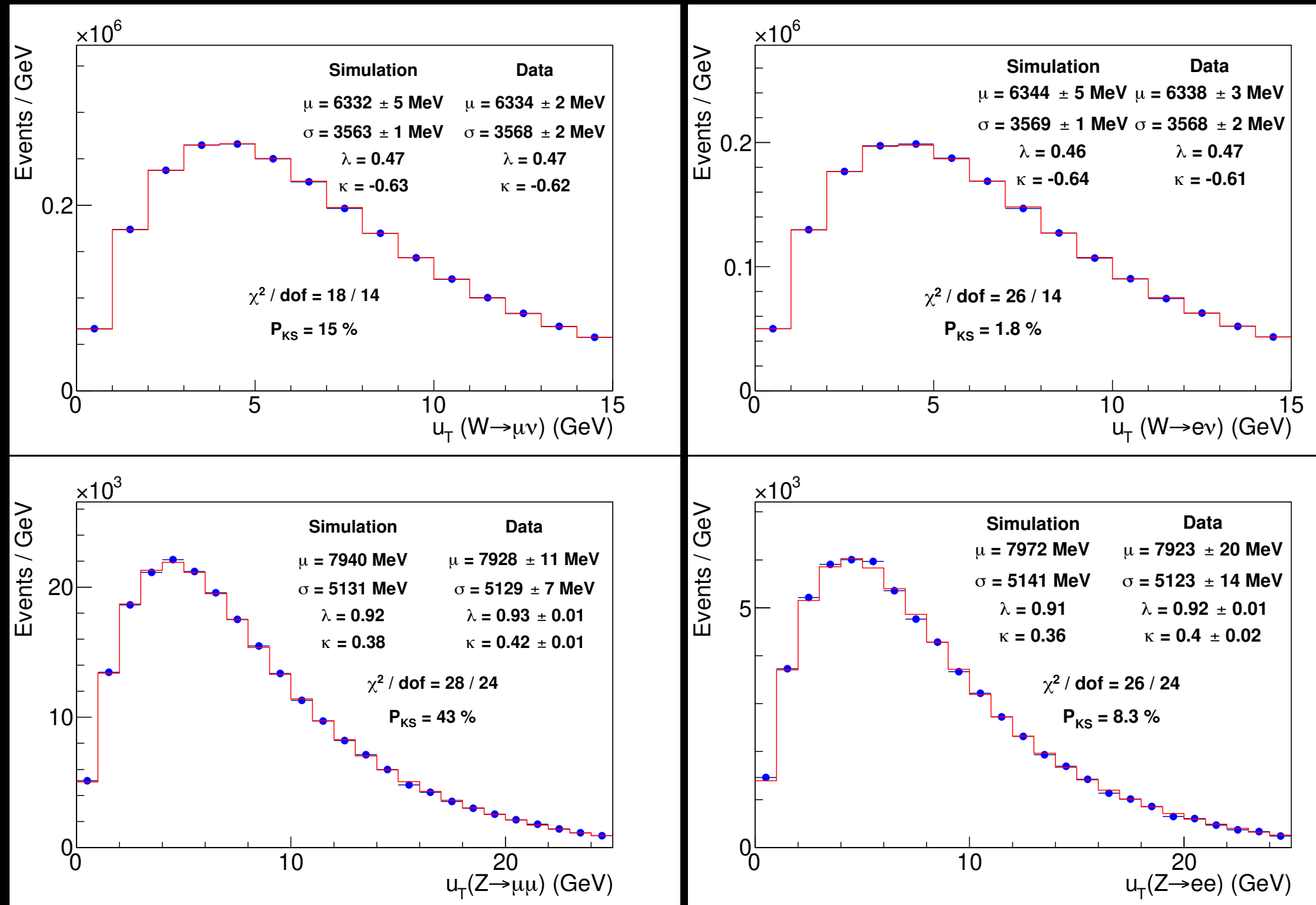
Source	Fraction (%)	δM_W (MeV)		
		m_T fit	p_T^μ fit	p_T^ν fit
$Z/\gamma^* \rightarrow \mu\mu$	7.37 ± 0.10	1.6 (0.7)	3.6 (0.3)	0.1 (1.5)
$W \rightarrow \tau\nu$	0.880 ± 0.004	0.1 (0.0)	0.1 (0.0)	0.1 (0.0)
Hadronic jets	0.01 ± 0.04	0.1 (0.8)	-0.6 (0.8)	2.4 (0.5)
Decays in flight	0.20 ± 0.14	1.3 (3.1)	1.3 (5.0)	-5.2 (3.2)
Cosmic rays	0.01 ± 0.01	0.3 (0.0)	0.5 (0.0)	0.3 (0.3)
Total	8.47 ± 0.18	2.1 (3.3)	3.9 (5.1)	5.7 (3.6)

Source	Fraction (%)	δM_W (MeV)		
		m_T fit	p_T^e fit	p_T^ν fit
$Z/\gamma^* \rightarrow ee$	0.134 ± 0.003	0.2 (0.3)	0.3 (0.0)	0.0 (0.6)
$W \rightarrow \tau\nu$	0.94 ± 0.01	0.6 (0.0)	0.6 (0.0)	0.6 (0.0)
Hadronic jets	0.34 ± 0.08	2.2 (1.2)	0.9 (6.5)	6.2 (-1.1)
Total	1.41 ± 0.08	2.3 (1.2)	1.1 (6.5)	6.2 (1.3)

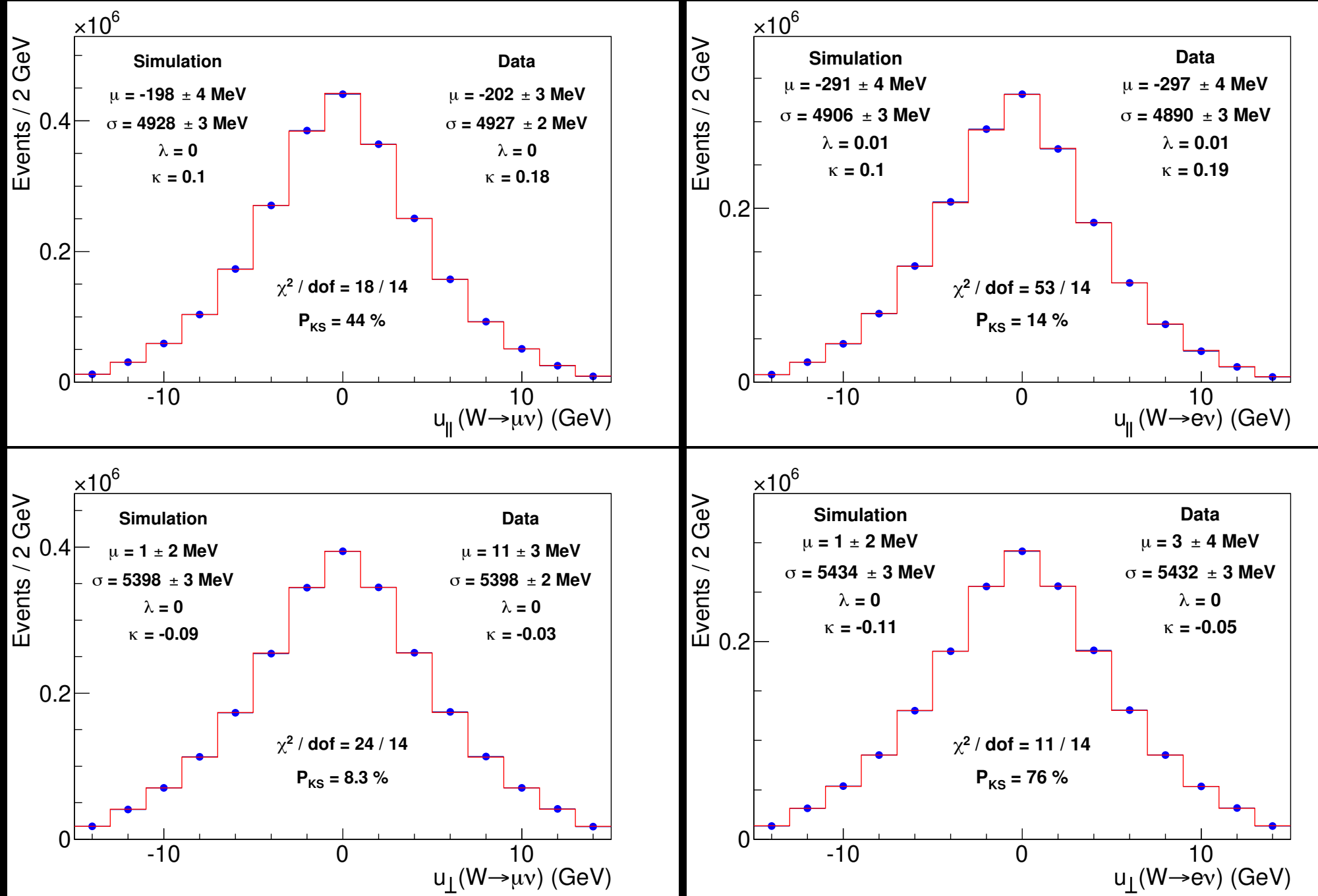
Initial state LO & NLO

W⁺ initial	Type	Pythia LO	Madgraph LO	Madgraph NLO
u dbar	v-v	81.7%	82.0%	82.7%
dbar u	s-s	8.9%	9.0%	8.8%
u sbar	v-s	1.6%	1.9%	1.8%
sbar u	s-s	0.3%	0.3%	0.3%
c sbar	s-s	2.9%	2.9%	-
sbar c	s-s	2.9%	2.9%	-
c dbar	s-v	0.7%	0.7%	-
dbar c	s-s	0.2%	0.2%	-
u g	v-g		-	3.7%
g dbar	g-v		-	1.8%
g u	g-s		-	0.4%
dbar g	s-g		-	0.5%
g sbar	g-s		-	0.02%
sbar g	s-g		-	0.02%

Recoil in W & Z events



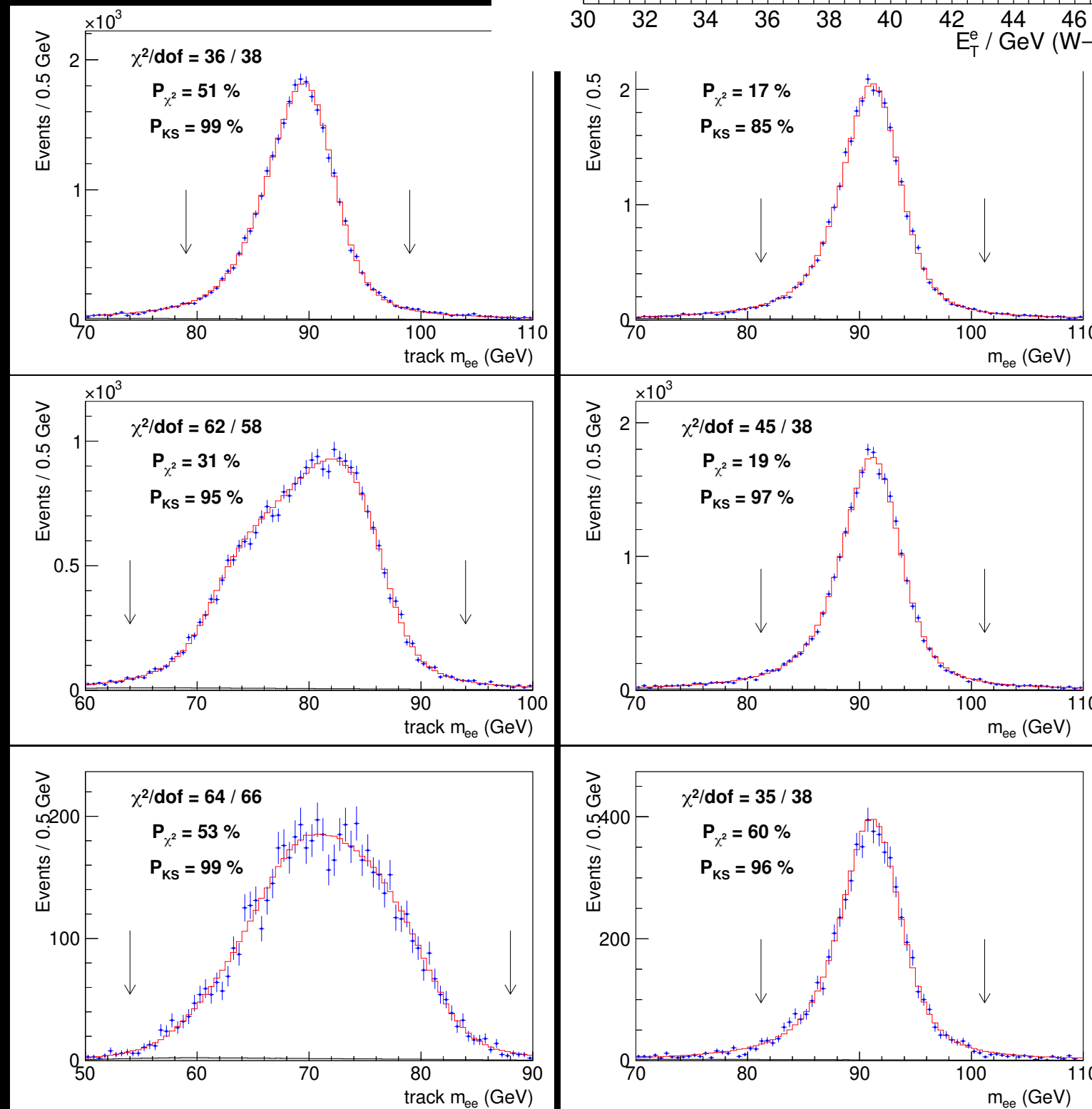
Recoil projections in W events



Recoil model parameters

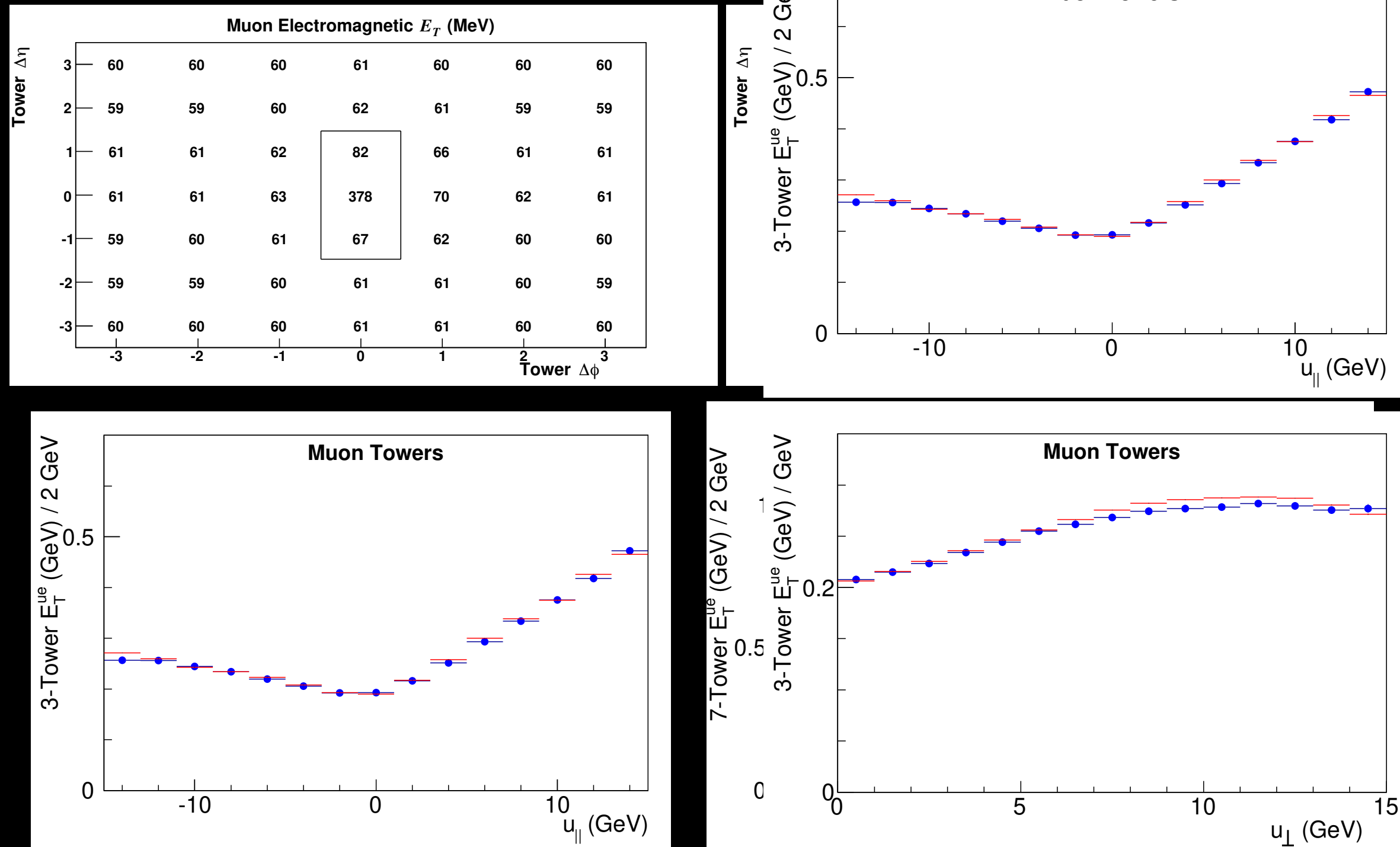
Parameter	Description	Source	m_T	p_T^ℓ	p_T^ν
a	average response	Fig. S23	-1.6	-2.9	-0.2
b	response non-linearity	Fig. S23	-0.8	-2.0	0.7
Response			1.8	3.5	0.7
N_V	spectator interactions	Fig. S24	0.5	-3.2	3.6
s_{had}	sampling resolution	Fig. S24	0.3	0.3	0.8
$f_{\pi^0}^4$	EM fluctuations at low u_T	Fig. S25	-0.3	-0.2	-1.0
$f_{\pi^0}^{15}$	EM fluctuations at high u_T	Fig. S25	-0.3	-0.3	-0.2
α	angular resolution at low u_T	Fig. S26	1.4	0.1	2.5
β	angular resolution at intermediate u_T	Fig. S26	0.2	0.1	0.7
γ	angular resolution at high u_T	Fig. S26	0.3	0.3	0.7
f_2^a	average dijet component	Fig. S27	0.1	-1.1	0.8
f_2^s	variation of dijet component with u_T	Fig. S27	-0.1	-0.2	-0.1
k_ξ	average dijet resolution	Fig. S28	-0.1	0.1	-0.3
δ_ξ	fluctuations in dijet resolution	Fig. S28	-0.2	0.2	-1.1
A_ξ	higher-order term in dijet resolution	Fig. S28	0.1	-1.0	0.7
μ_ξ	—"—	Fig. S28	-0.5	-0.4	-0.9
ϵ_ξ	—"—	Fig. S28	0.1	-0.2	0.4
S_ξ^+	—"—	Fig. S28	0.5	-0.4	1.4
S_ξ^-	—"—	Fig. S28	-0.3	-0.2	-0.5
q_ξ	—"—	Fig. S28	-0.2	0.0	0.2
Resolution			1.8	3.6	5.2

Z mass fits using tracker or calorimeter



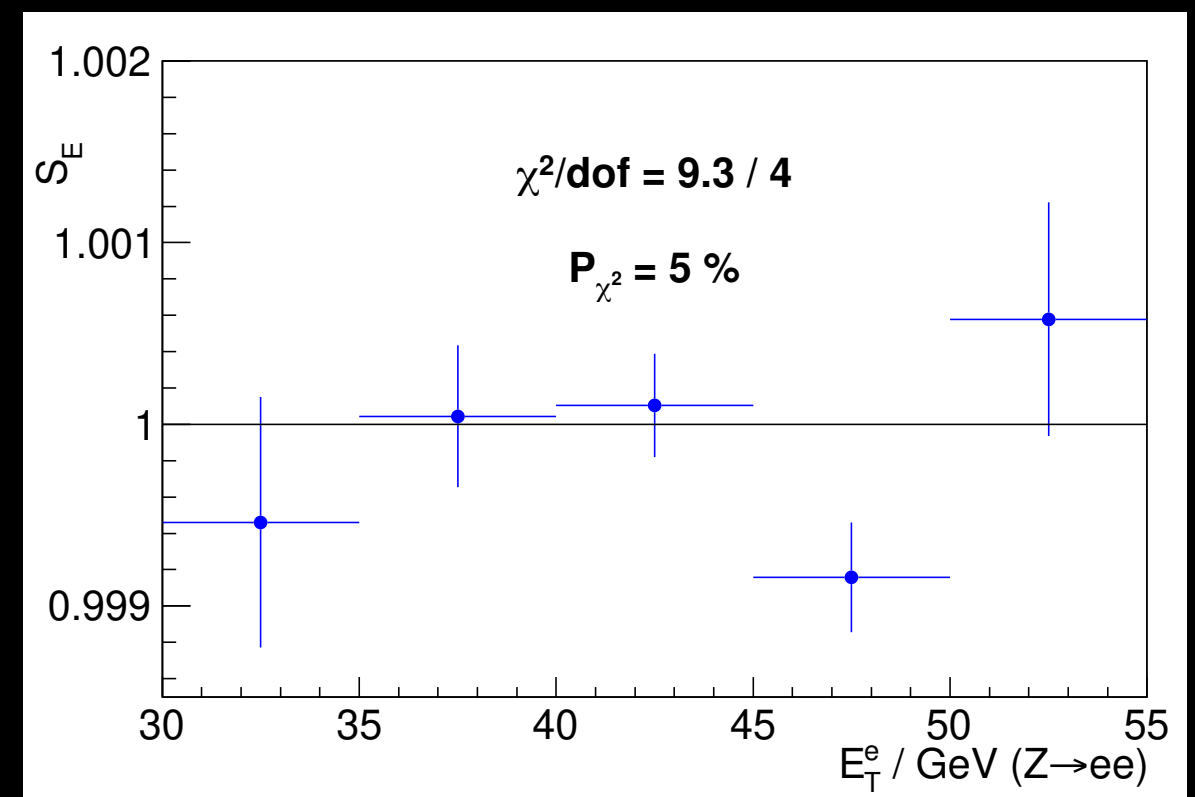
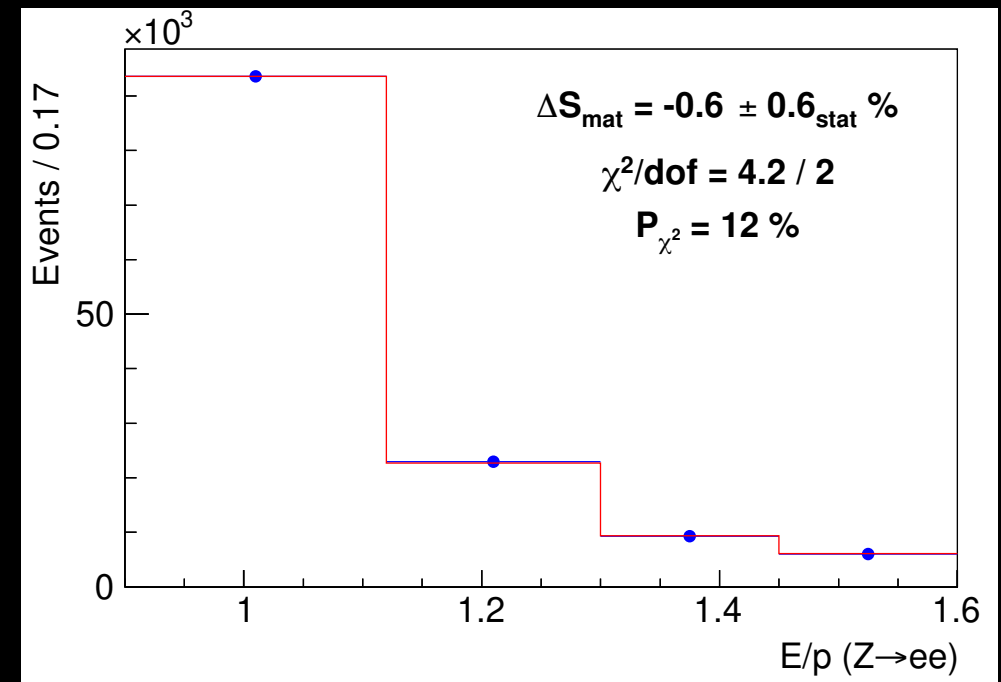
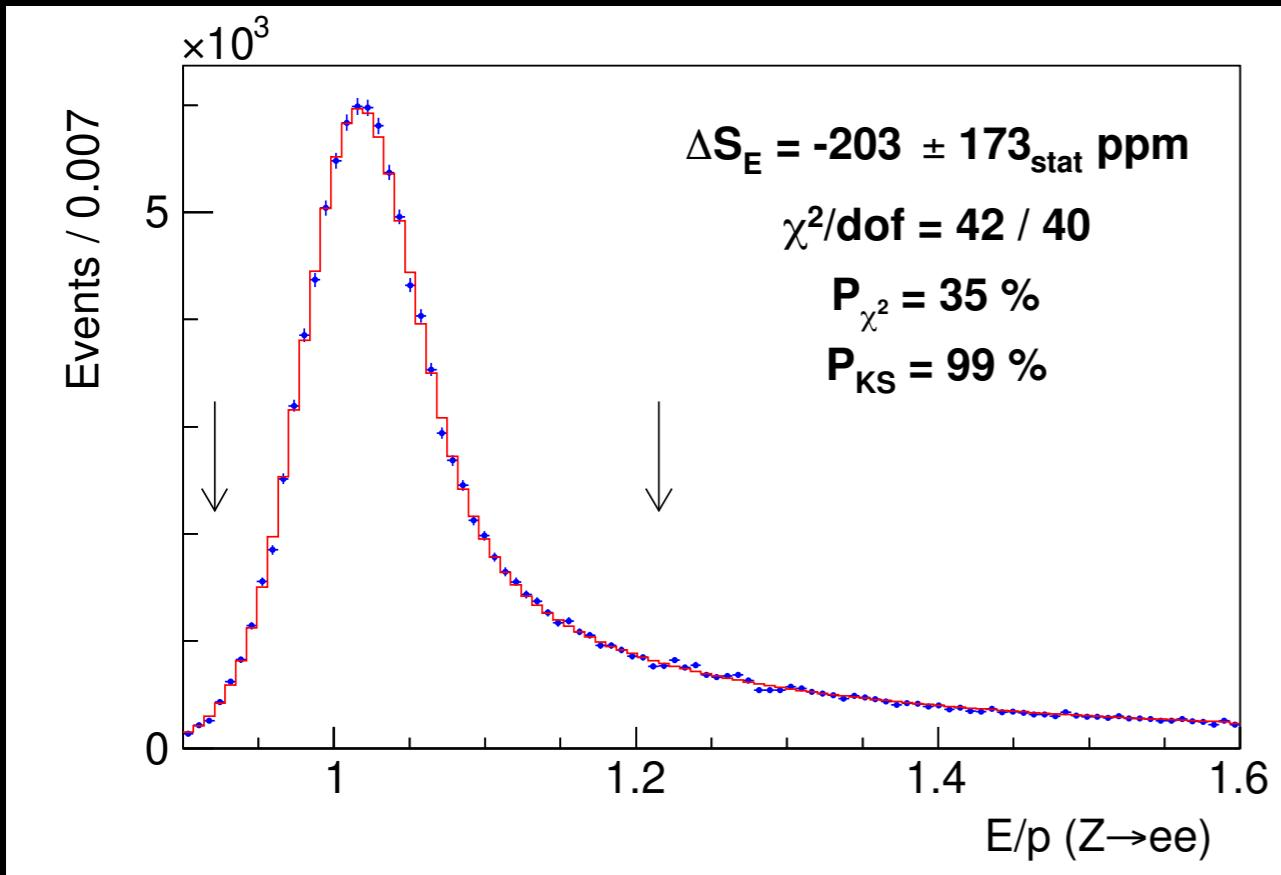
Electrons	Calorimeter	Track
$E/p < 1.1$ only	$91\ 190.9 \pm 19.7$	$91\ 215.2 \pm 22.4$
$E/p > 1.1$ and $E/p < 1.1$	$91\ 201.1 \pm 21.5$	$91\ 259.9 \pm 39.0$
$E/p > 1.1$ only	$91\ 184.5 \pm 46.4$	$91\ 167.7 \pm 109.9$

Recoil reconstruction in muon channel

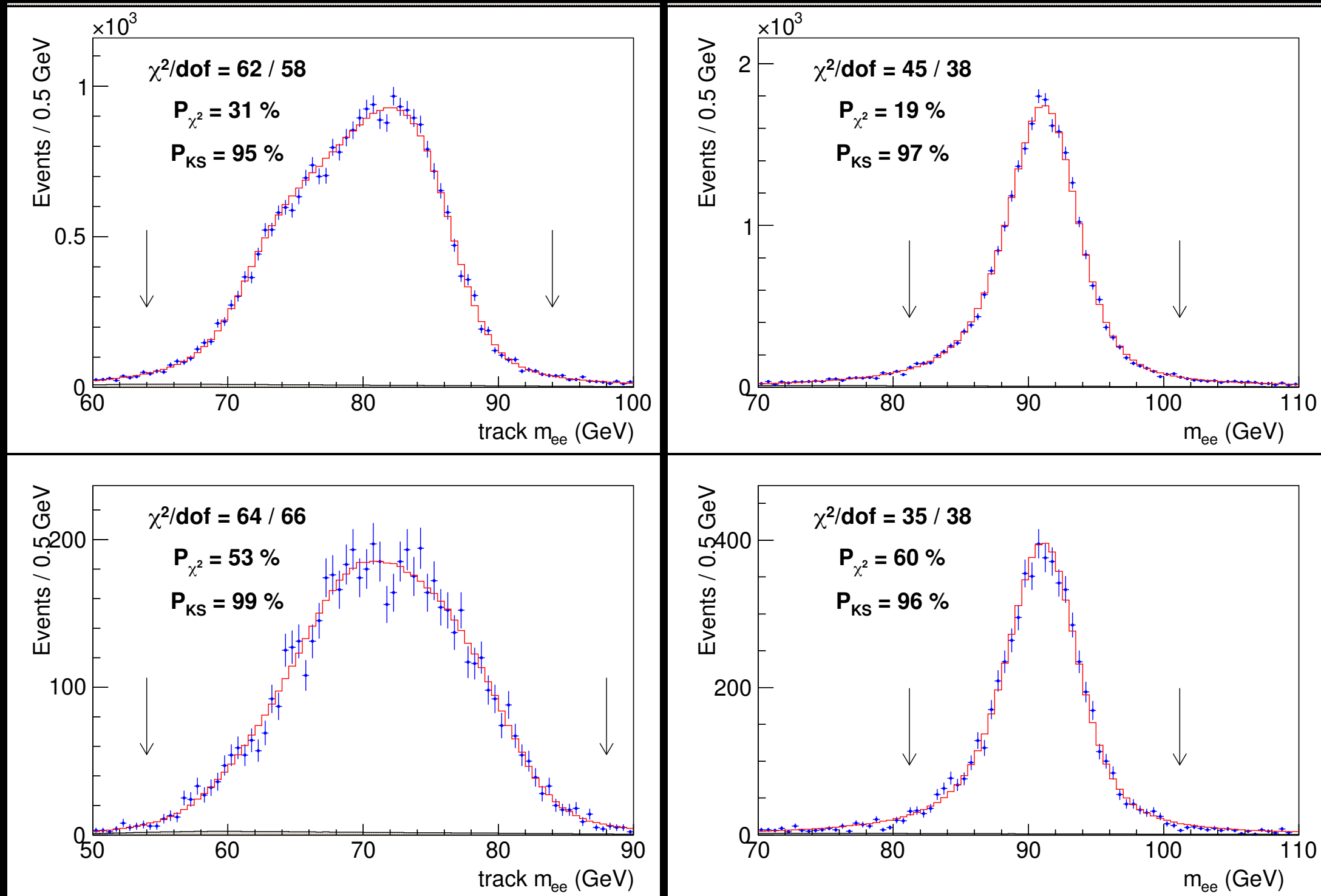


Electron momentum calibration

Gauge field potential



Electron momentum calibration



Muon momentum calibration

Source	J/ψ (ppm)	Υ (ppm)	Correlation (%)
QED	1	1	100
Magnetic field non-uniformity	13	13	100
Ionizing material correction	11	8	100
Resolution model	10	1	100
Background model	7	6	0
COT alignment correction	4	8	0
Trigger efficiency	18	9	100
Fit range	2	1	100
$\Delta p/p$ step size	2	2	0
World-average mass value	4	27	0
Total systematic	29	34	16 ppm
Statistical NBC (BC)	2	13(10)	0
Total	29	36	16 ppm

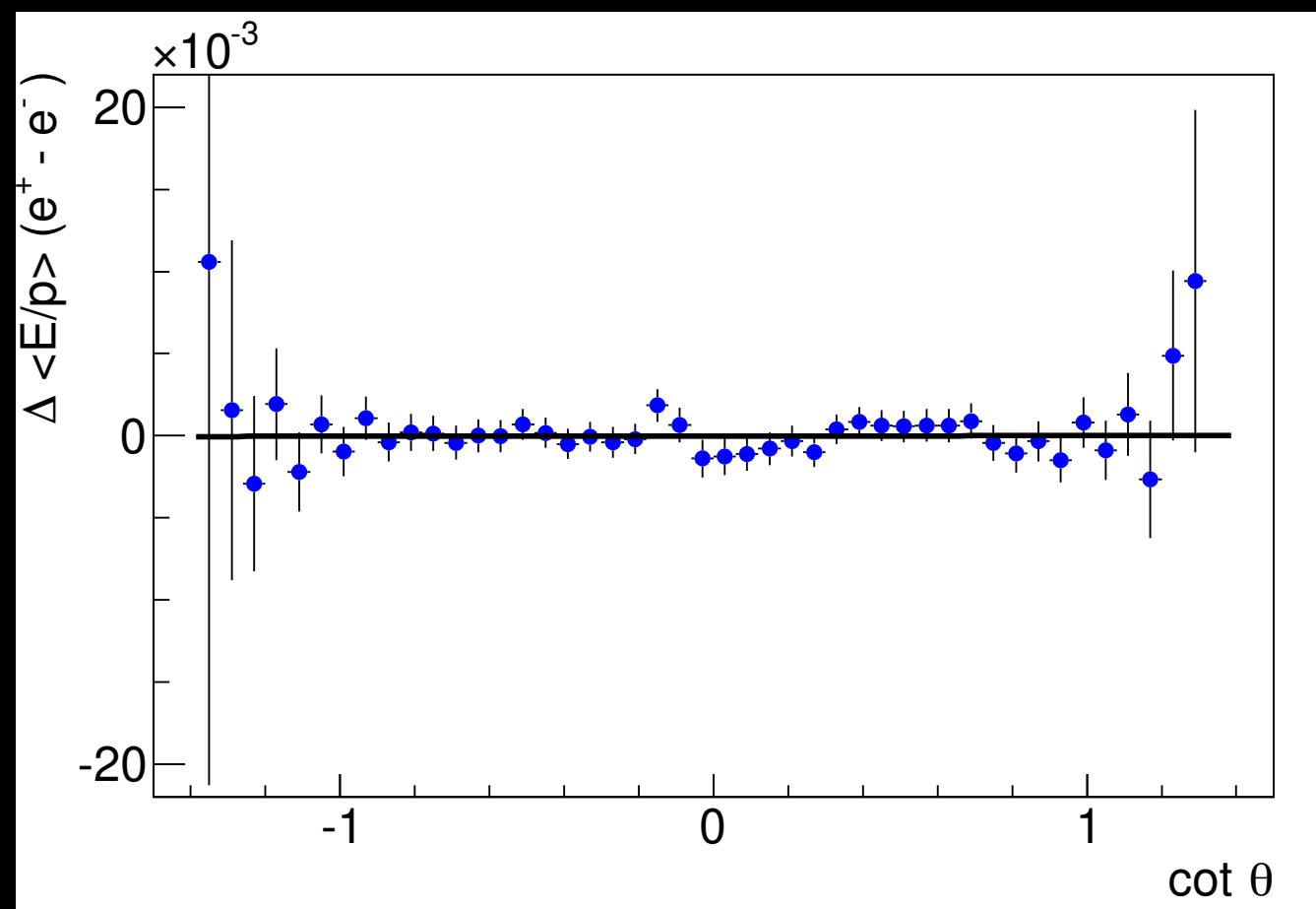
Track momentum calibration

Residual tracker misalignments studied using difference in E/p between electrons and positrons

Correction as a function of polar angle applied to measured tracks from W and Z decays

Linear dependence on cot theta would cause a bias in the m_W mass fit

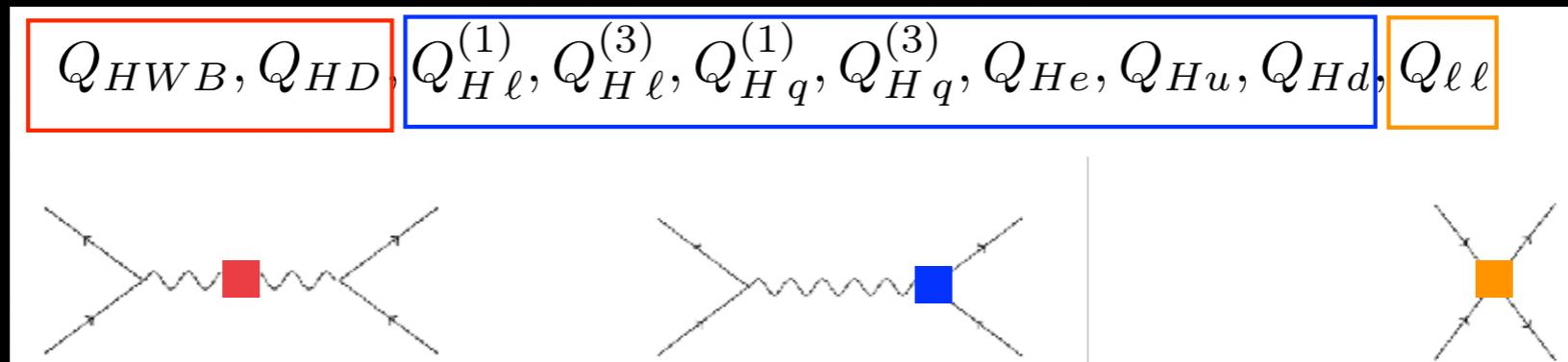
No linear correction required, statistical precision from E/p constrains the bias to <0.8 MeV



Measurement updates

Method or technique	impact
Detailed treatment of parton distribution functions	+3.5 MeV
Resolved beam-constraining bias in CDF reconstruction	+10 MeV
Improved COT alignment and drift model [65]	uniformity
Improved modeling of calorimeter tower resolution	uniformity
Temporal uniformity calibration of CEM towers	uniformity
Lepton removal procedure corrected for luminosity	uniformity
Higher-order calculation of QED radiation in J/ψ and Υ decays	accuracy
Modeling kurtosis of hadronic recoil energy resolution	accuracy
Improved modeling of hadronic recoil angular resolution	accuracy
Modeling dijet contribution to recoil resolution	accuracy
Explicit luminosity matching of pileup	accuracy
Modeling kurtosis of pileup resolution	accuracy
Theory model of p_T^W/p_T^Z spectrum ratio	accuracy
Constraint from p_T^W data spectrum	robustness
Cross-check of p_T^Z tuning	robustness

Electroweak observables at dimension 6



Parameter	Input Value
\hat{m}_Z	91.1875 ± 0.0021
\hat{G}_F	$1.1663787(6) \times 10^{-5}$
$\hat{\alpha}_{ew}$	$1/137.035999074(94)$

$$\frac{\delta m_W^2}{\hat{m}_W^2} = \hat{\Delta} \left[4C_{HWB} + \frac{c_{\hat{\theta}}}{s_{\hat{\theta}}} C_{HD} + 4 \frac{s_{\hat{\theta}}}{c_{\hat{\theta}}} C_{H\ell}^{(3)} - 2 \frac{s_{\hat{\theta}}}{c_{\hat{\theta}}} C_{\ell\ell} \right]$$

Observable	Experimental Value	Ref.	SM Theoretical Value	Ref.
$\hat{m}_Z[\text{GeV}]$	91.1875 ± 0.0021	[19]	—	—
$\hat{m}_W[\text{GeV}]$	80.385 ± 0.015	[49]	80.365 ± 0.004	[50]
$\Gamma_Z[\text{GeV}]$	2.4952 ± 0.0023	[19]	2.4942 ± 0.0005	[48]
R_ℓ^0	20.767 ± 0.025	[19]	20.751 ± 0.005	[48]
R_c^0	0.1721 ± 0.0030	[19]	0.17223 ± 0.00005	[48]
R_b^0	0.21629 ± 0.00066	[19]	0.21580 ± 0.00015	[48]
$\sigma_h^0 [\text{nb}]$	41.540 ± 0.037	[19]	41.488 ± 0.006	[48]
A_{FB}^ℓ	0.0171 ± 0.0010	[19]	0.01616 ± 0.00008	[32]
A_{FB}^c	0.0707 ± 0.0035	[19]	0.0735 ± 0.0002	[32]
A_{FB}^b	0.0992 ± 0.0016	[19]	0.1029 ± 0.0003	[32]

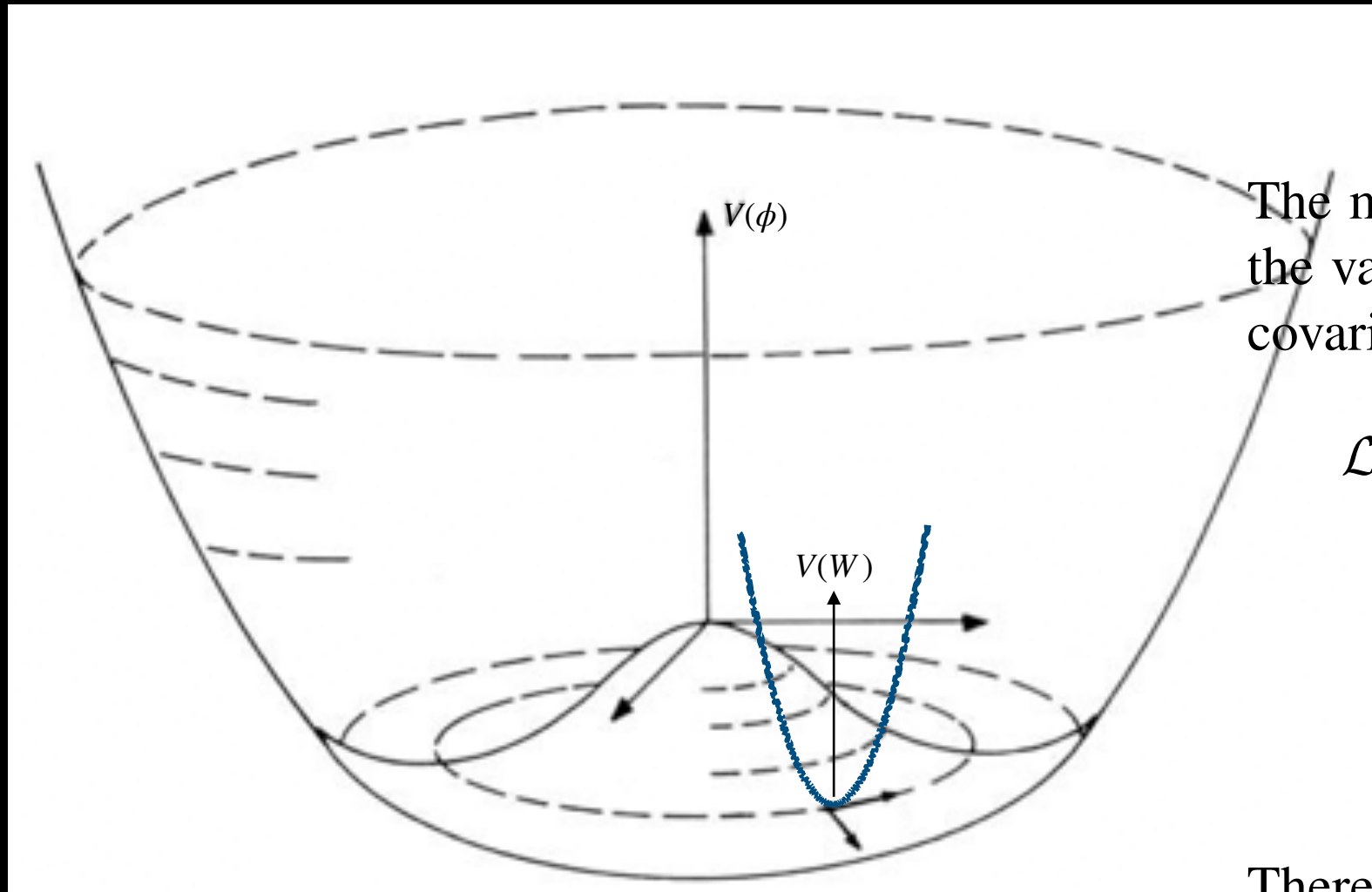
W boson mass fit results

Distribution	W -boson mass (MeV)	χ^2/dof
$m_T(e, \nu)$	$80\ 429.1 \pm 10.3_{\text{stat}} \pm 8.5_{\text{syst}}$	39/48
$p_T^\ell(e)$	$80\ 411.4 \pm 10.7_{\text{stat}} \pm 11.8_{\text{syst}}$	83/62
$p_T^\nu(e)$	$80\ 426.3 \pm 14.5_{\text{stat}} \pm 11.7_{\text{syst}}$	69/62
$m_T(\mu, \nu)$	$80\ 446.1 \pm 9.2_{\text{stat}} \pm 7.3_{\text{syst}}$	50/48
$p_T^\ell(\mu)$	$80\ 428.2 \pm 9.6_{\text{stat}} \pm 10.3_{\text{syst}}$	82/62
$p_T^\nu(\mu)$	$80\ 428.9 \pm 13.1_{\text{stat}} \pm 10.9_{\text{syst}}$	63/62
combination	$80\ 433.5 \pm 6.4_{\text{stat}} \pm 6.9_{\text{syst}}$	7.4/5

Distribution	M_W (MeV)	$\chi^2/\text{d.o.f.}$
$W \rightarrow e\nu$		
m_T	80408 ± 19	52/48
p_T^ℓ	80393 ± 21	60/62
p_T^ν	80431 ± 25	71/62
$W \rightarrow \mu\nu$		
m_T	80379 ± 16	57/48
p_T^ℓ	80348 ± 18	58/62
p_T^ν	80406 ± 22	82/62

Boson masses

Higgs field potential



$$m_H = v\sqrt{2\lambda} = 125 \text{ GeV}$$

$$\lambda \approx 0.1$$

Gauge field potential

$$V = -\frac{g^2 v^2}{8}[(W_\mu^+)^2 + (W_\mu^-)^2] - \frac{v^2(g^2 + g'^2)}{8}Z^\mu Z_\mu$$

$$m_W = \frac{v}{2}g$$

$$m_Z = \frac{v}{2}\sqrt{g^2 + g'^2}$$

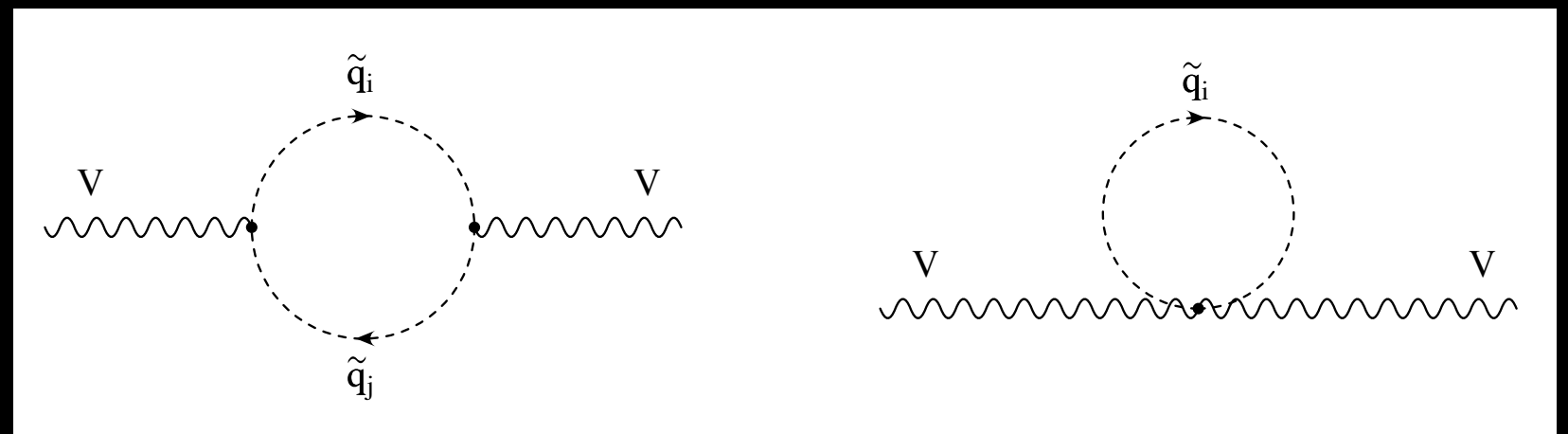
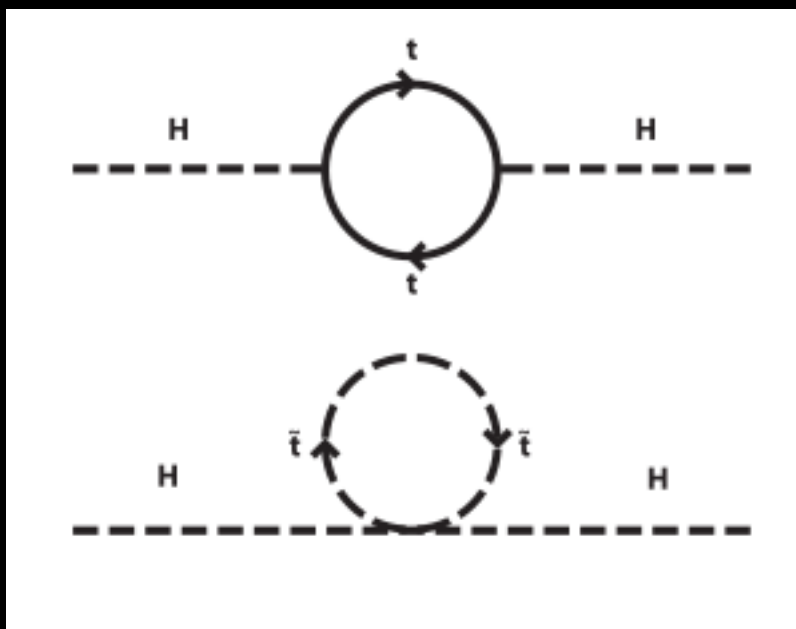
$$v = 246 \text{ GeV} \text{ and } g = 0.64:$$

$$m_W = 78.7 \text{ GeV}$$

W boson mass

The W boson mass is the most sensitive observable to sources of ‘naturalness’

Classic example: **Supersymmetry**



Mass splittings in supersymmetric isospin doublets: different mass shifts for W & Z bosons

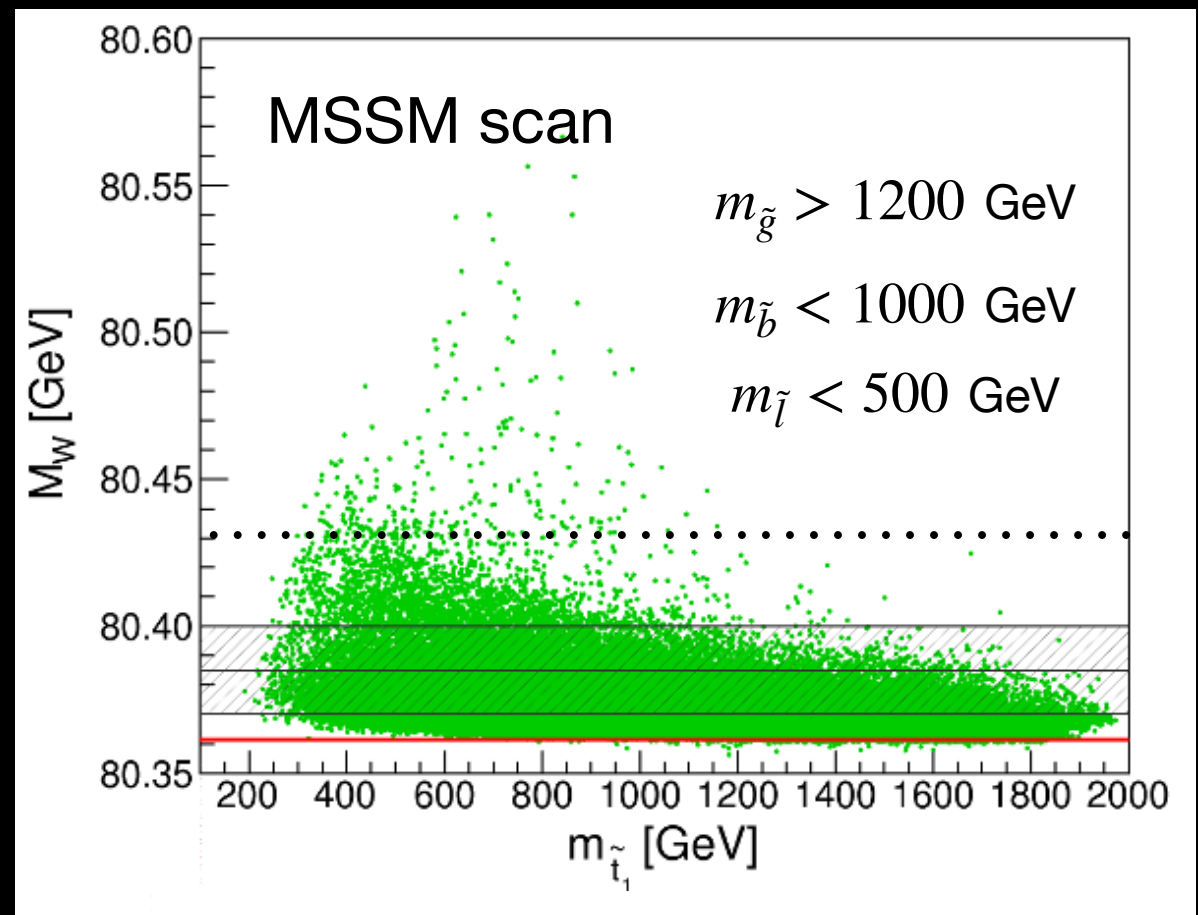
W boson mass

Difference in corrections to W and Z propagators encapsulated by ρ parameter

$$\Delta\rho = \frac{\Sigma^Z(0)}{M_Z^2} - \frac{\Sigma^W(0)}{M_W^2}$$

$$\Delta\rho_0^{\text{SUSY}} = \frac{3 G_\mu}{8 \sqrt{2} \pi^2} \left[-\sin^2 \theta_{\tilde{t}} \cos^2 \theta_{\tilde{t}} F_0(m_{\tilde{t}_1}^2, m_{\tilde{t}_2}^2) - \sin^2 \theta_{\tilde{b}} \cos^2 \theta_{\tilde{b}} F_0(m_{\tilde{b}_1}^2, m_{\tilde{b}_2}^2) \right. \\ + \cos^2 \theta_{\tilde{t}} \cos^2 \theta_{\tilde{b}} F_0(m_{\tilde{t}_1}^2, m_{\tilde{b}_1}^2) + \cos^2 \theta_{\tilde{t}} \sin^2 \theta_{\tilde{b}} F_0(m_{\tilde{t}_1}^2, m_{\tilde{b}_2}^2) \\ \left. + \sin^2 \theta_{\tilde{t}} \cos^2 \theta_{\tilde{b}} F_0(m_{\tilde{t}_2}^2, m_{\tilde{b}_1}^2) + \sin^2 \theta_{\tilde{t}} \sin^2 \theta_{\tilde{b}} F_0(m_{\tilde{t}_2}^2, m_{\tilde{b}_2}^2) \right].$$

$$\delta M_W \approx \frac{M_W}{2} \frac{c_W^2}{c_W^2 - s_W^2} \Delta\rho$$



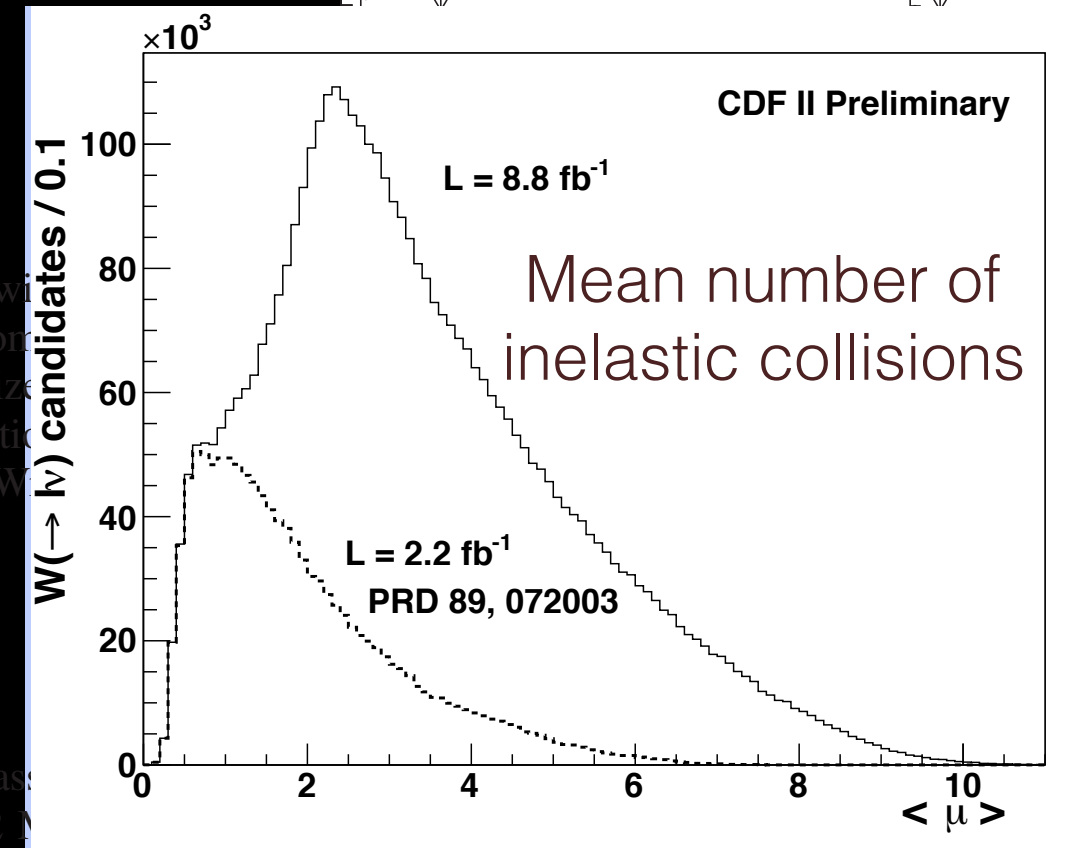
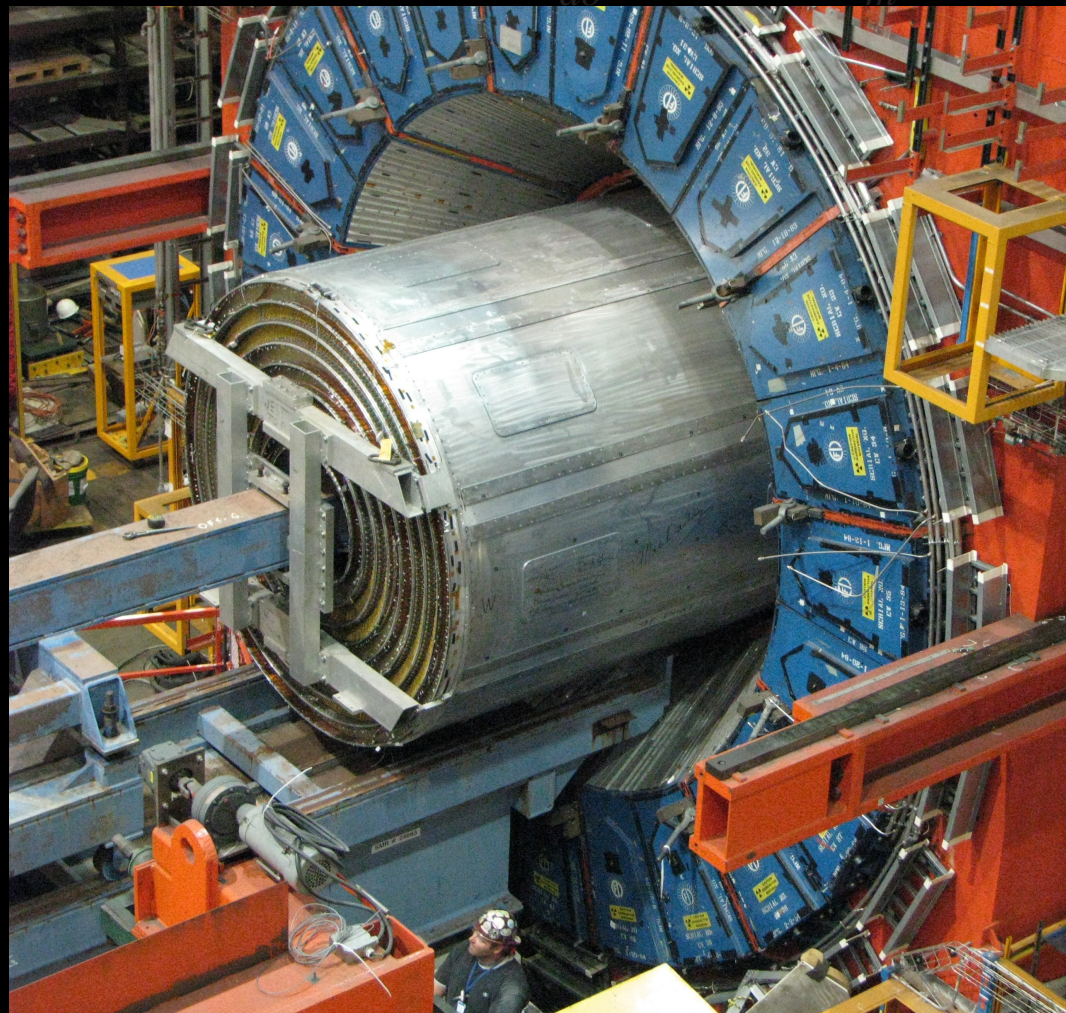
Heinemeyer, Hollik, Weiglein
Phys Rep 425, 265 (2006)

Heinemeyer, Hollik, Weiglein, Zeune
JHEP 12 (2013) 084

CDF II measurement of the W boson mass

4x the integrated luminosity of the previous measurement

Higher $\langle \mu \rangle$: peaks at 3



CDF II detector consists of

- silicon vertex detector
- large drift chamber
- coarse calorimeter towers
- outer muon chambers

Detector simulation

Developed custom simulation for analysis

Acceptance map for muon detectors

Parameterized GEANT4 model of electromagnetic calorimeter showers

Kotwal & CH, NIMA 729, 25 (2013)

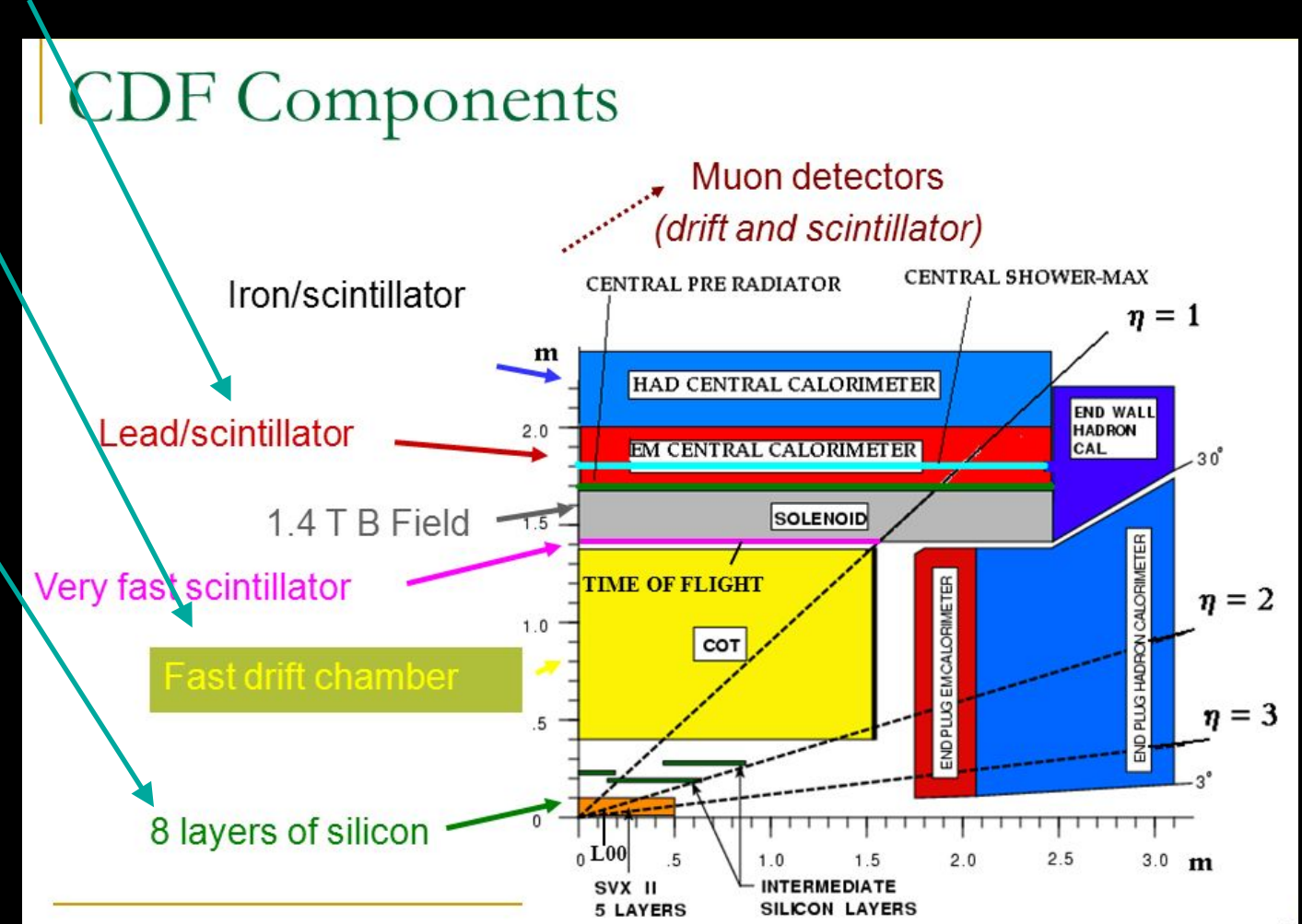
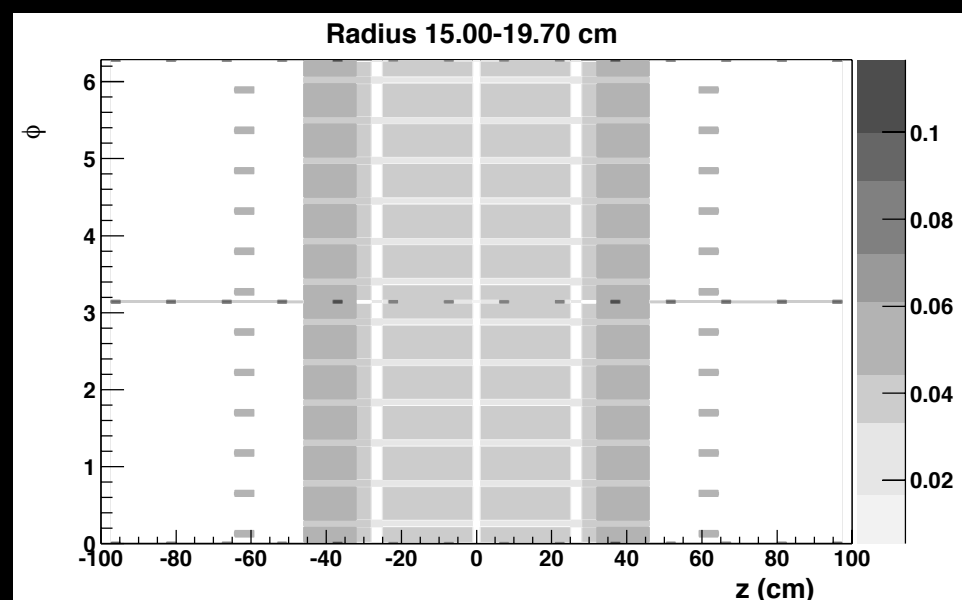
Includes shower losses due to finite calorimeter thickness

Hit-level model of central outer tracker

Layer-by-layer resolution functions and efficiencies

Material map of inner silicon detector

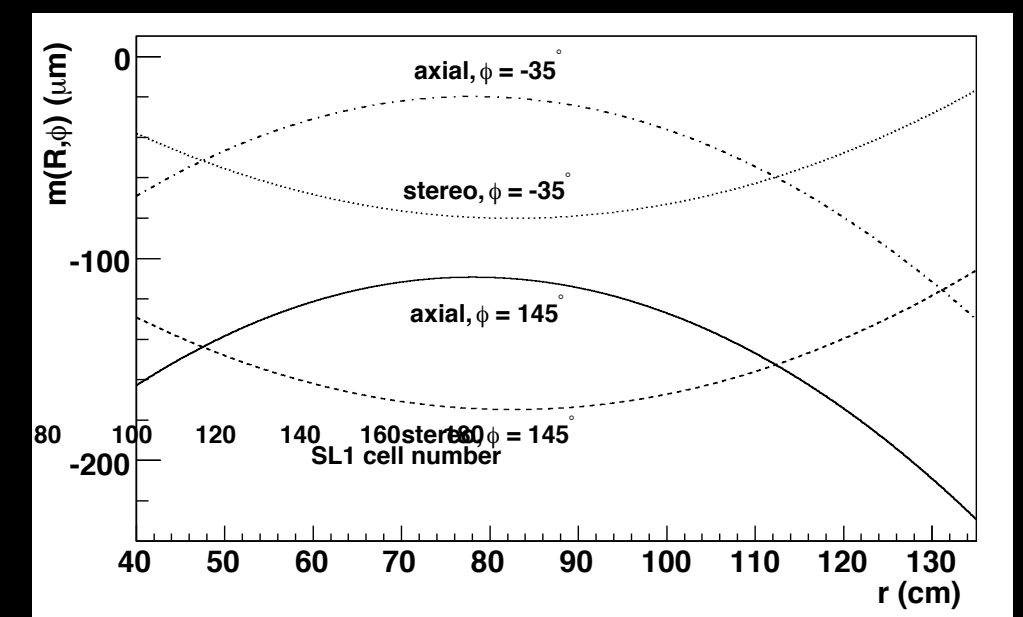
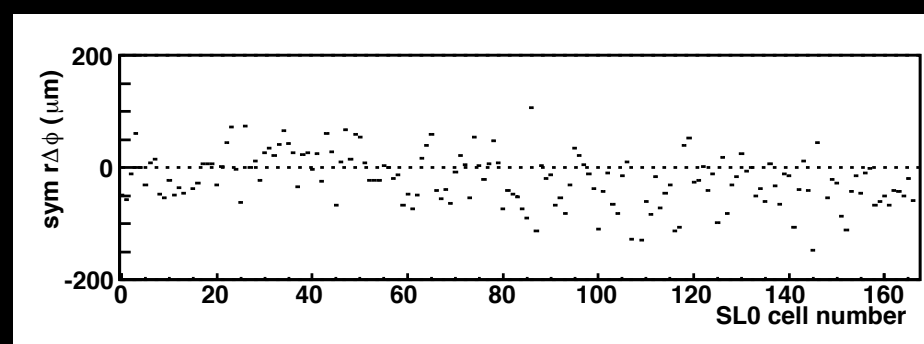
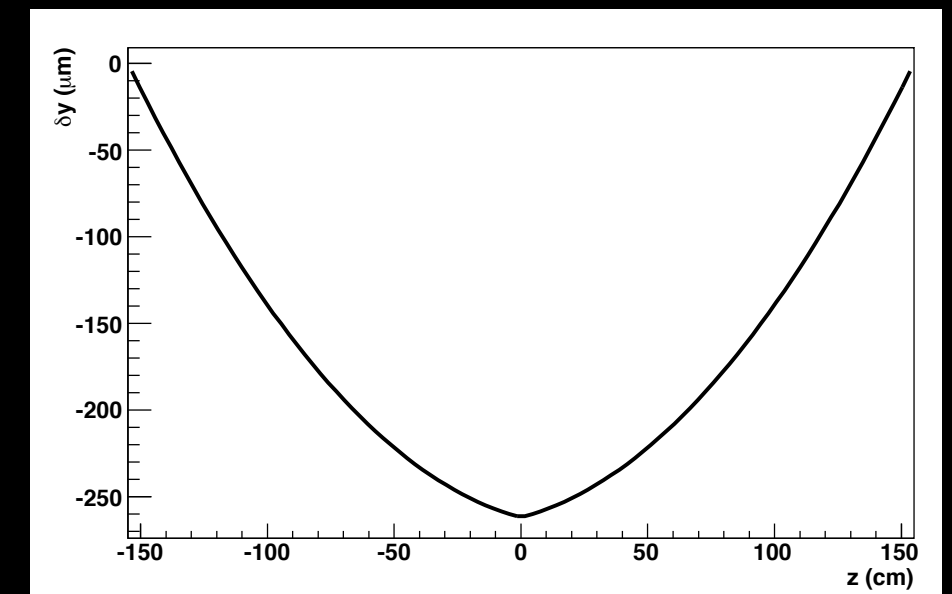
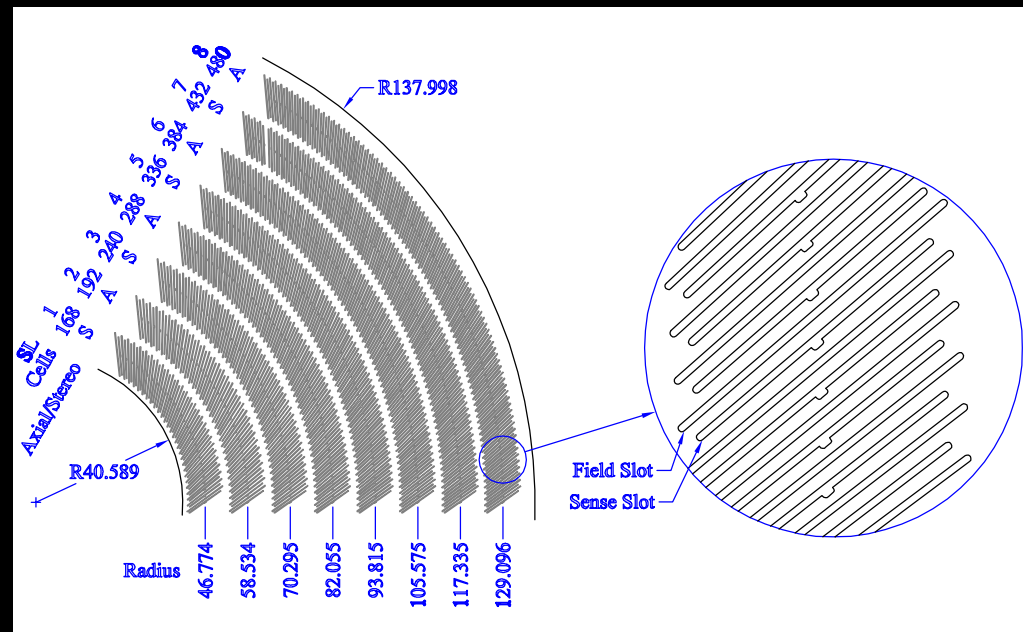
Includes radiation lengths and Bethe-Bloch terms



Muon momentum calibration

First step is to align the drift chamber (the “central outer tracker” or COT)

Two parameters for the electrostatic deflection of the wire within the chamber constrained using difference between fit parameters of incoming and outgoing cosmic-ray tracks



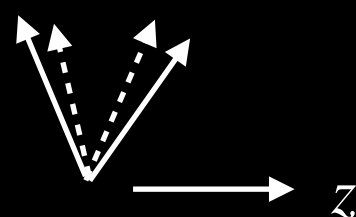
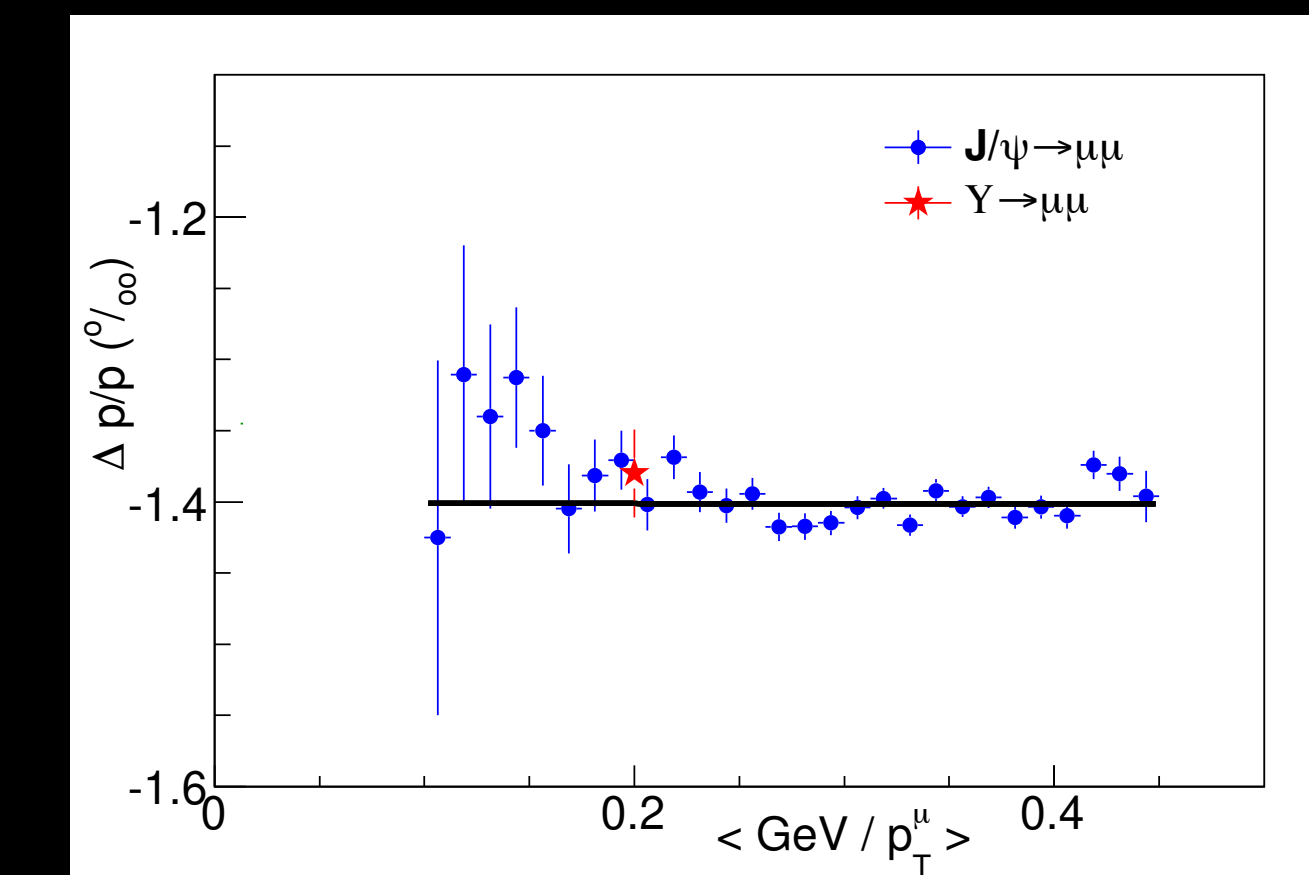
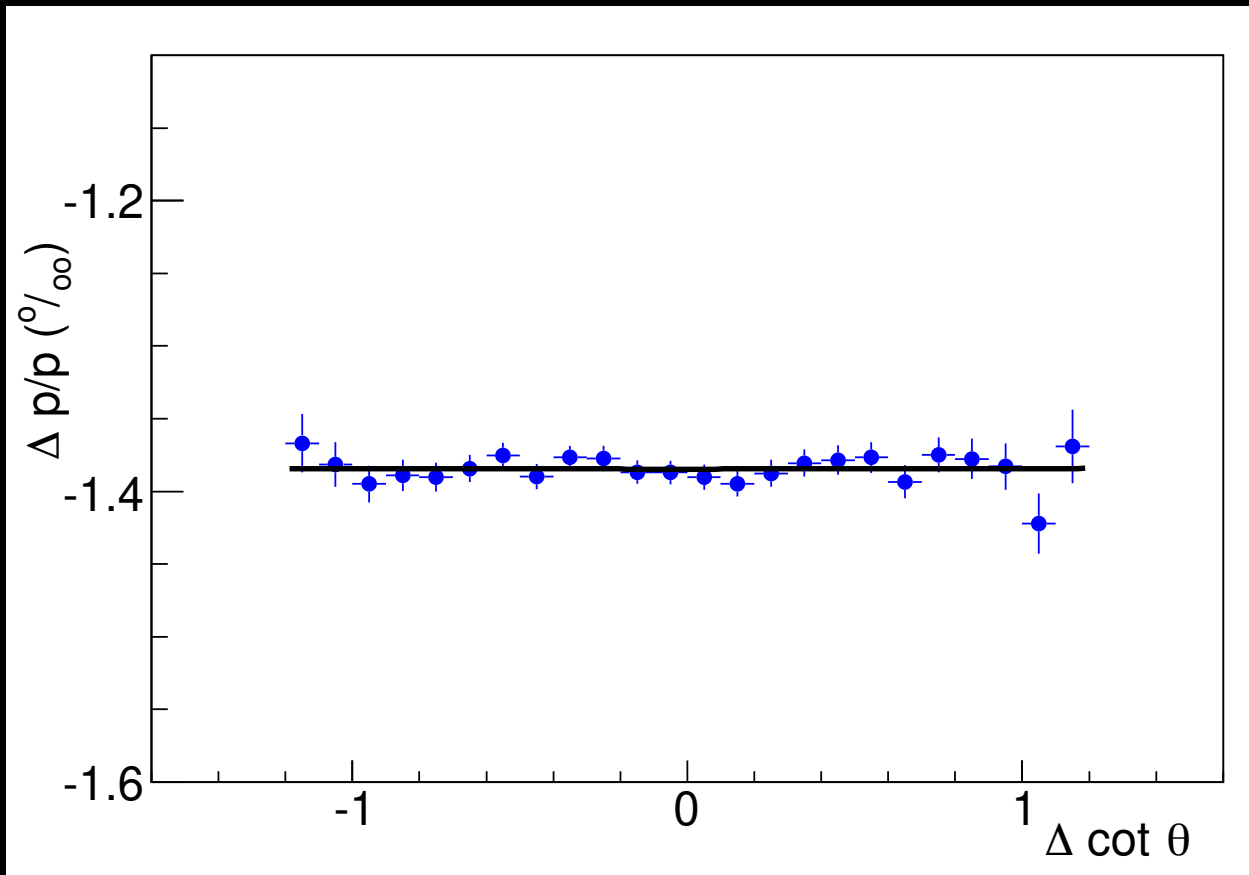
Muon momentum calibration

Second step is to calibrate the momentum scale using J/ψ decays to muons

Simulation corrections:

Correct the length scale of the tracker with mass measurement as a function of $\Delta \cot \theta$

Correct the amount of upstream material with mass measurement as a function of p_T^{-1}



Electron momentum calibration

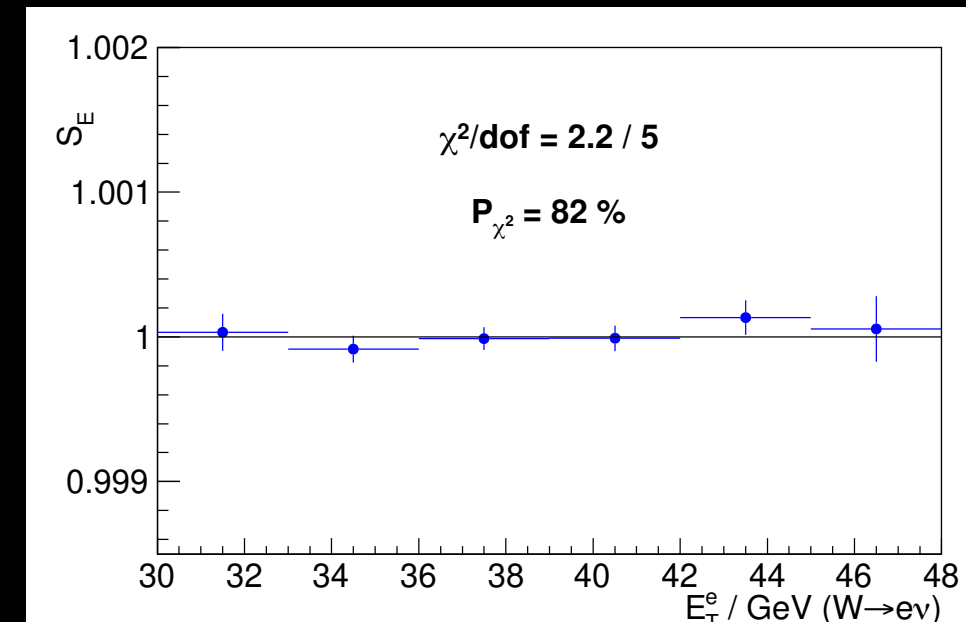
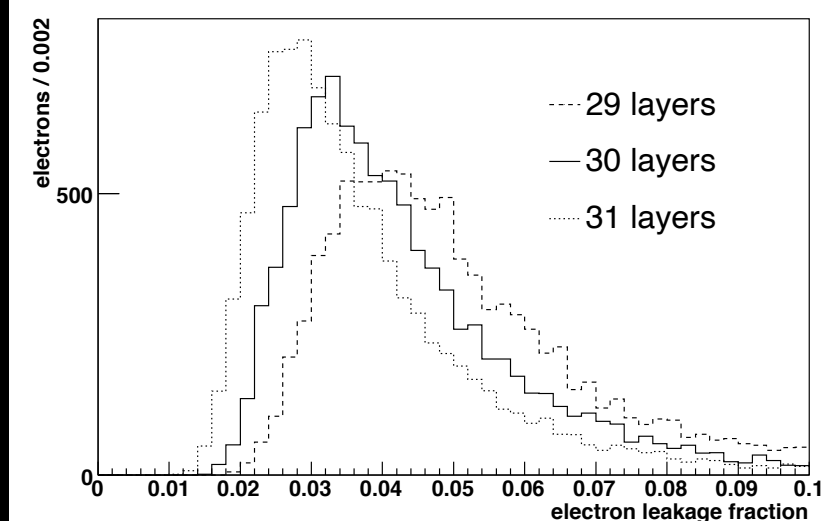
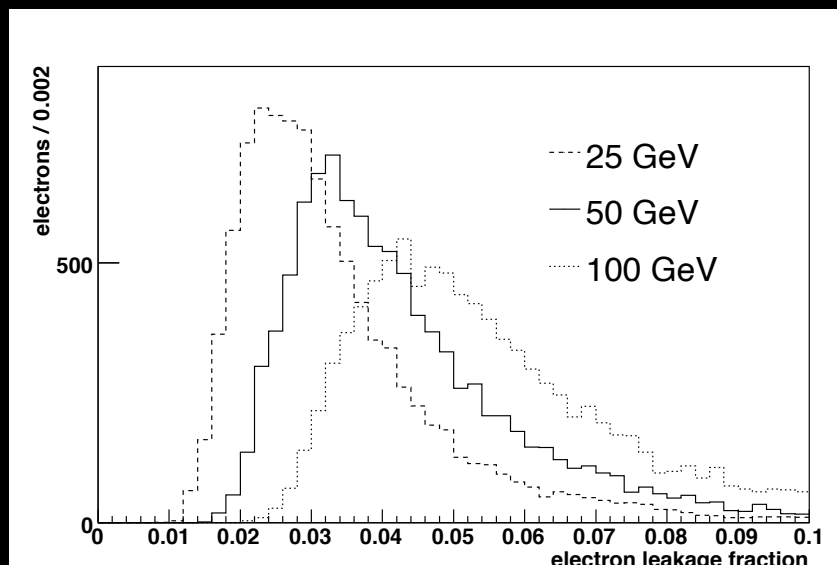
First step is to transfer the track calibration to the calorimeter (E/p) using W & Z decays

Parameterize calorimeter shower deposition and leakage based on GEANT4

Determine small calorimeter thickness corrections using region of low E/p in data

Fit calorimeter scale as a function of E_T to correct for any remaining energy dependence

Tower	Thickness (x_0)	Number of lead sheets
0	17.9	30
1	18.2	30
2	18.2	29
3	17.8	27
4	18.0	26
5	17.7	24
6	18.1	23
7	17.7	21
8	18.0	20



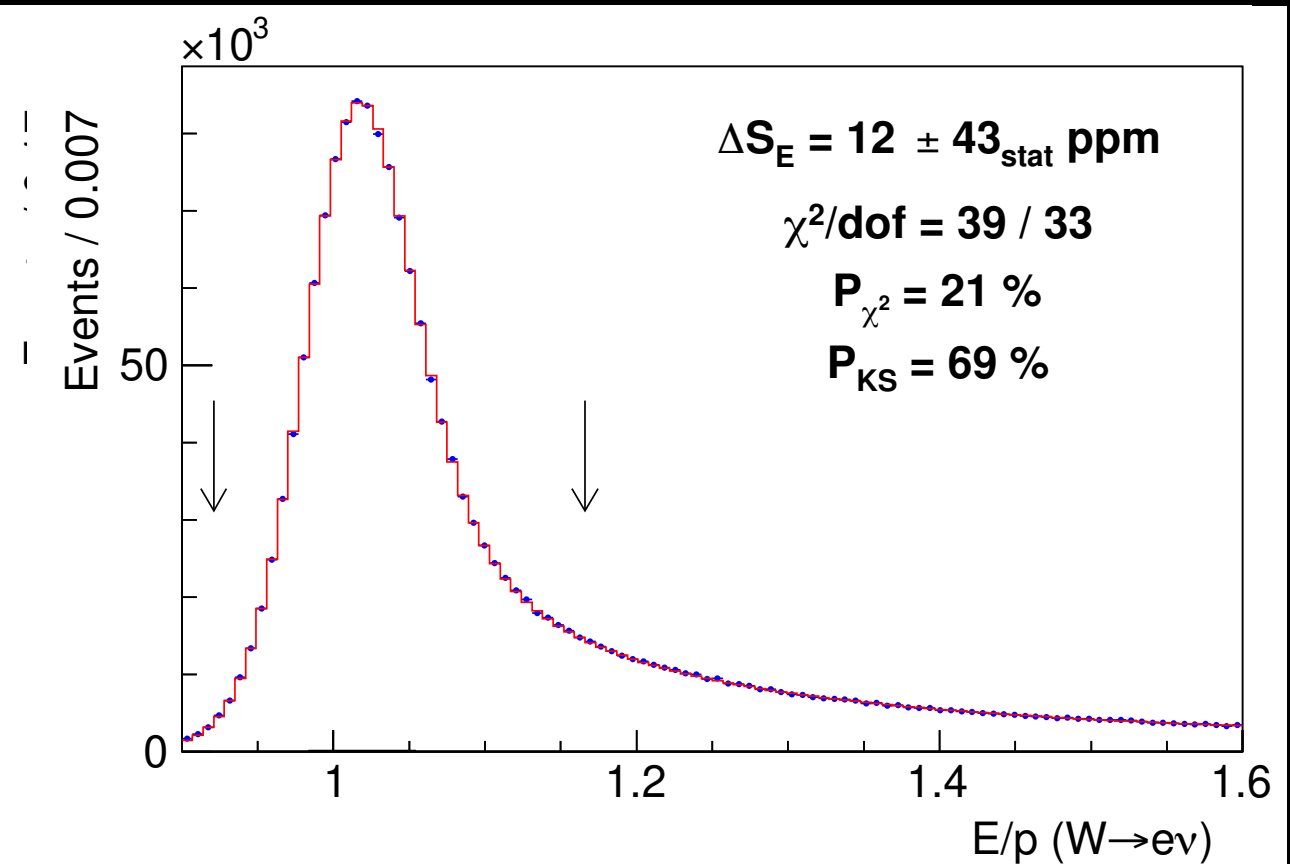
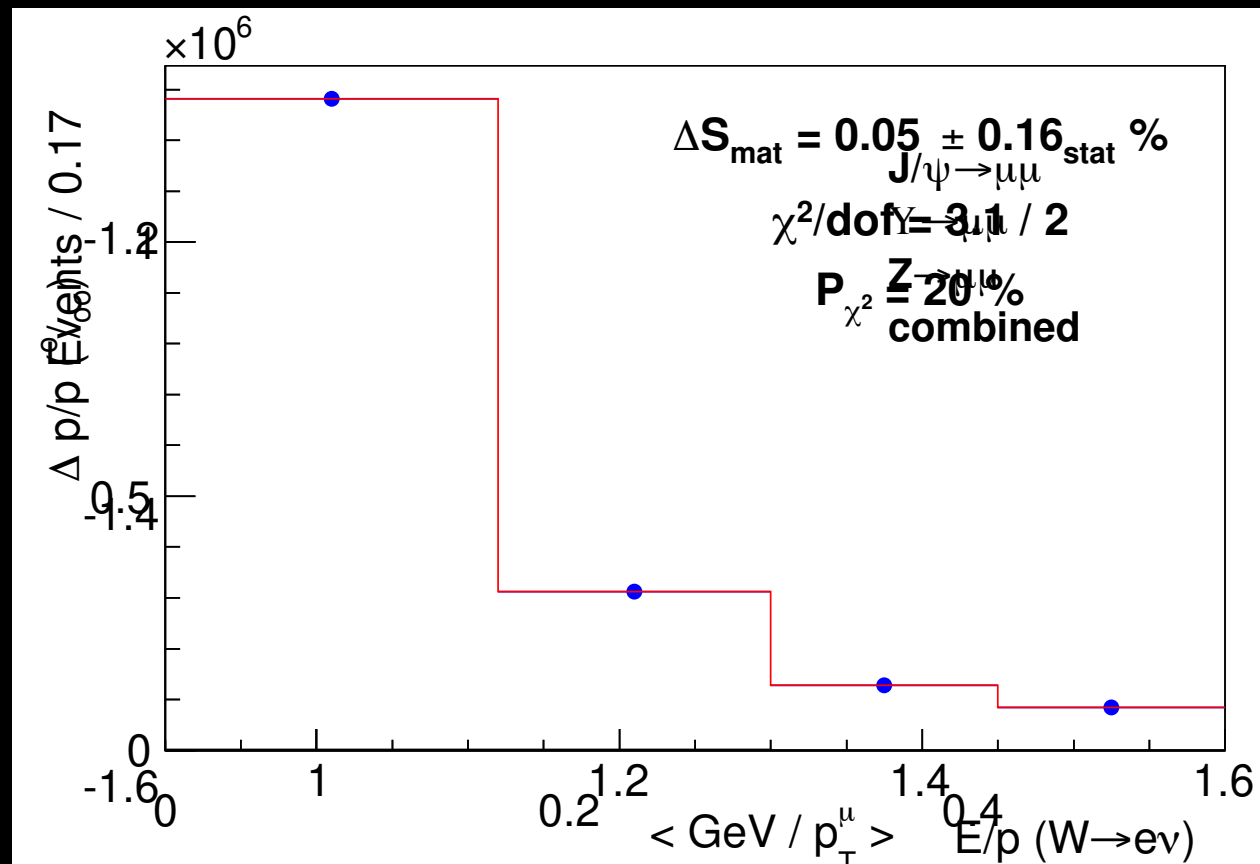
Electron momentum calibration

First step is to transfer the track calibration to the calorimeter (E/p) using W & Z decays

Model bremsstrahlung and pair production upstream of the drift chamber

Tune energy loss due to material upstream of the tracker (high E/p)

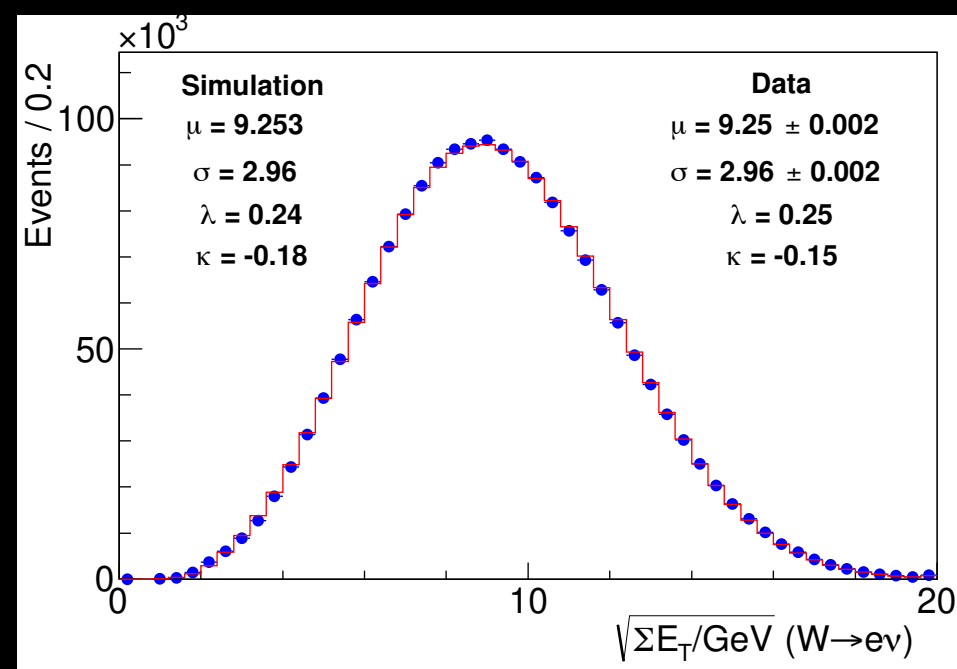
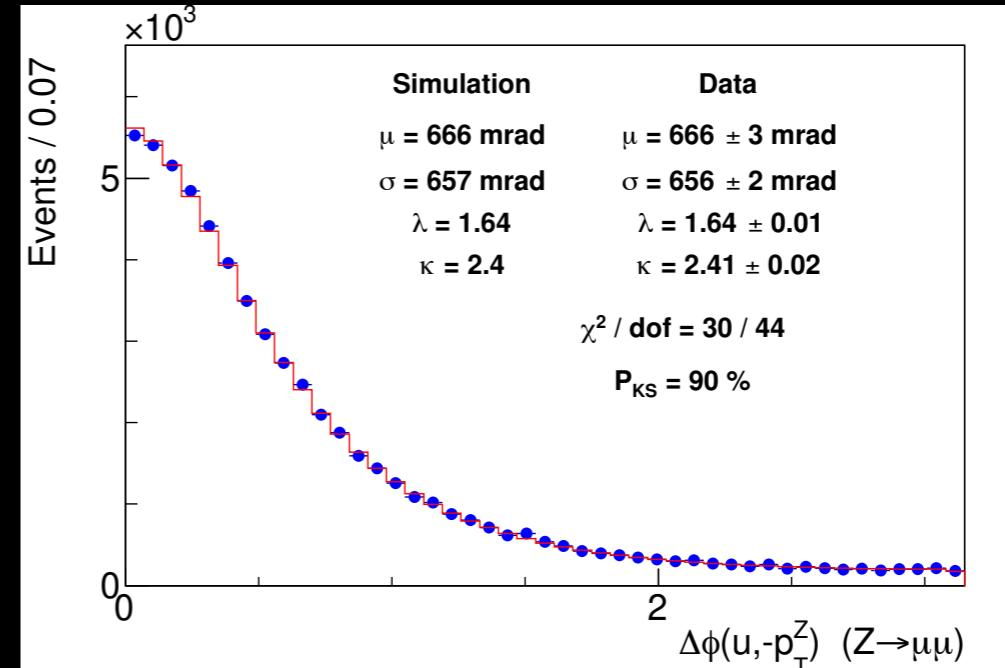
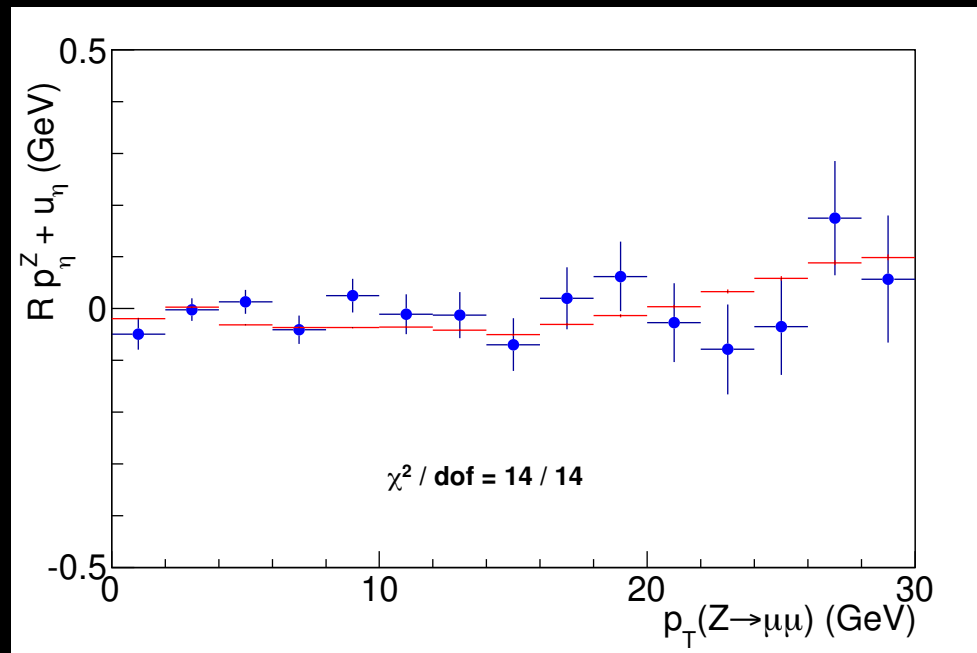
Sampling resolution given by $\sigma_E/E = \sqrt{\frac{12.6\%}{E_T} + \kappa^2}$ with $\kappa = 0.7 - 1.1\%$ increasing with tower η



Recoil momentum calibration

Fourth step is the calibration of the recoil resolution

Includes jet-like energy and angular resolution, additional dijet fraction term, and pileup



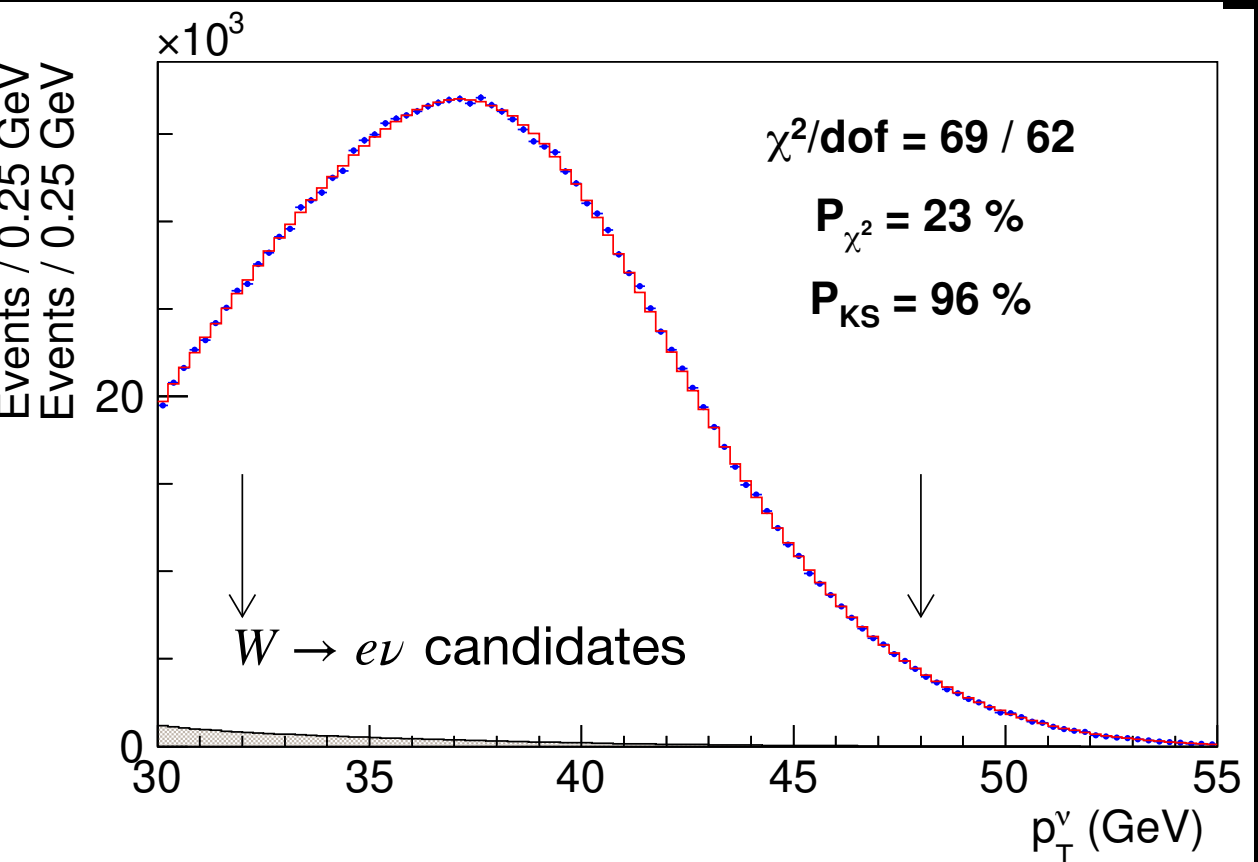
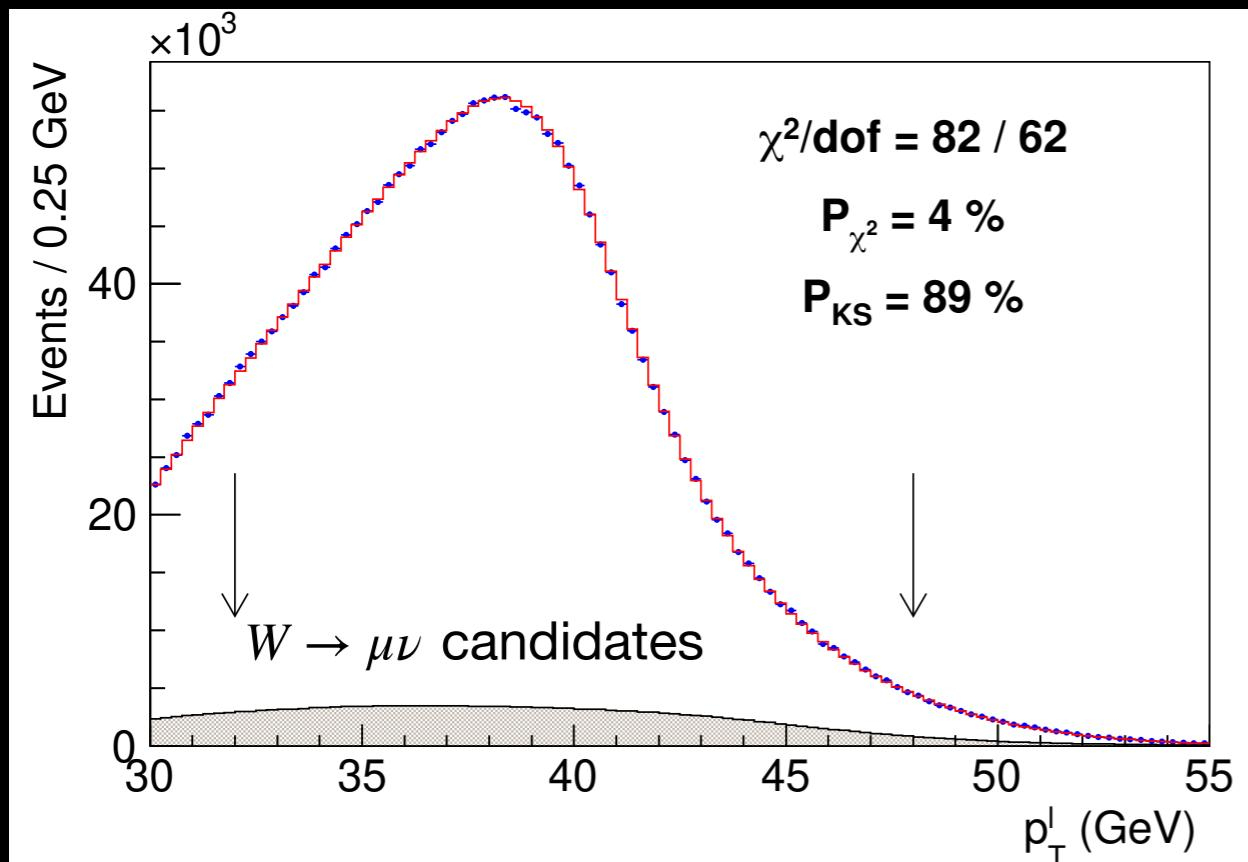
Backgrounds

**Electroweak backgrounds modelled with fast simulation tuned with data and full simulation
Cross-checked with full simulation tuned to data**

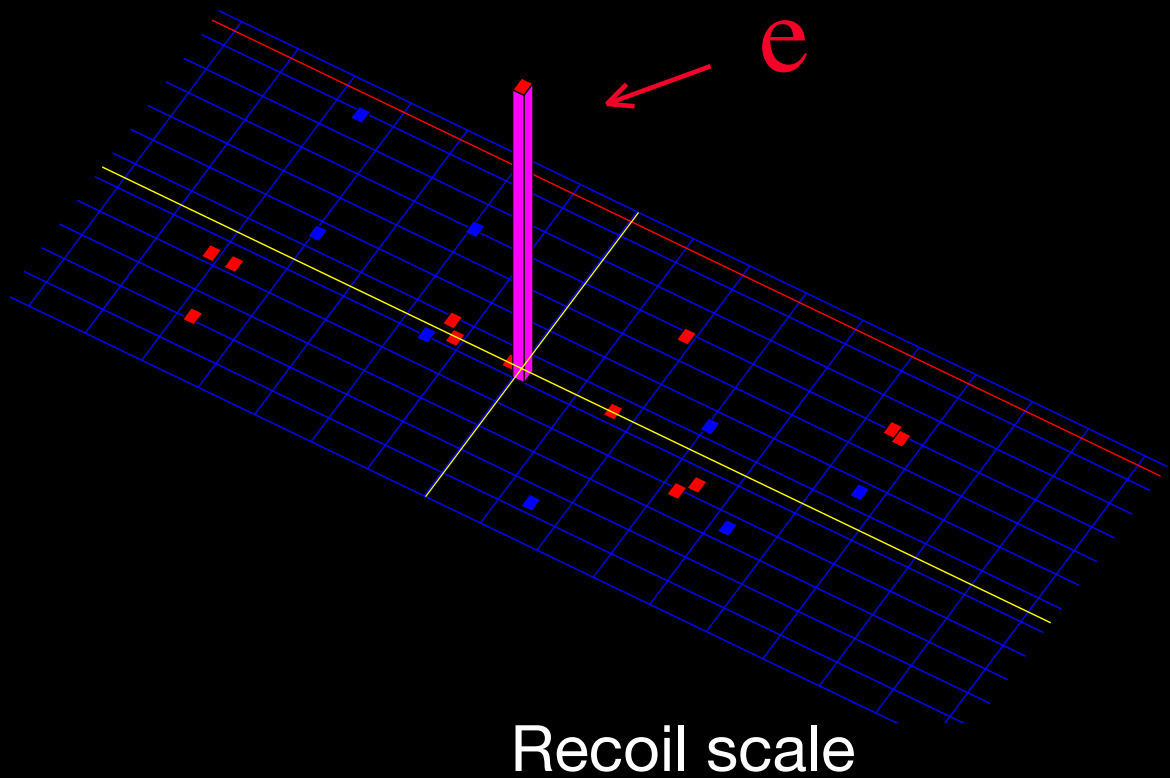
Largest background is $Z \rightarrow \mu\mu$ with one unreconstructed muon: **7.4% of data sample**

$W \rightarrow \tau\nu$ background is $\sim 1\%$ in each channel: largest background in electron sample

Background from hadrons misreconstructed as leptons estimated using data: 0.2-0.3%

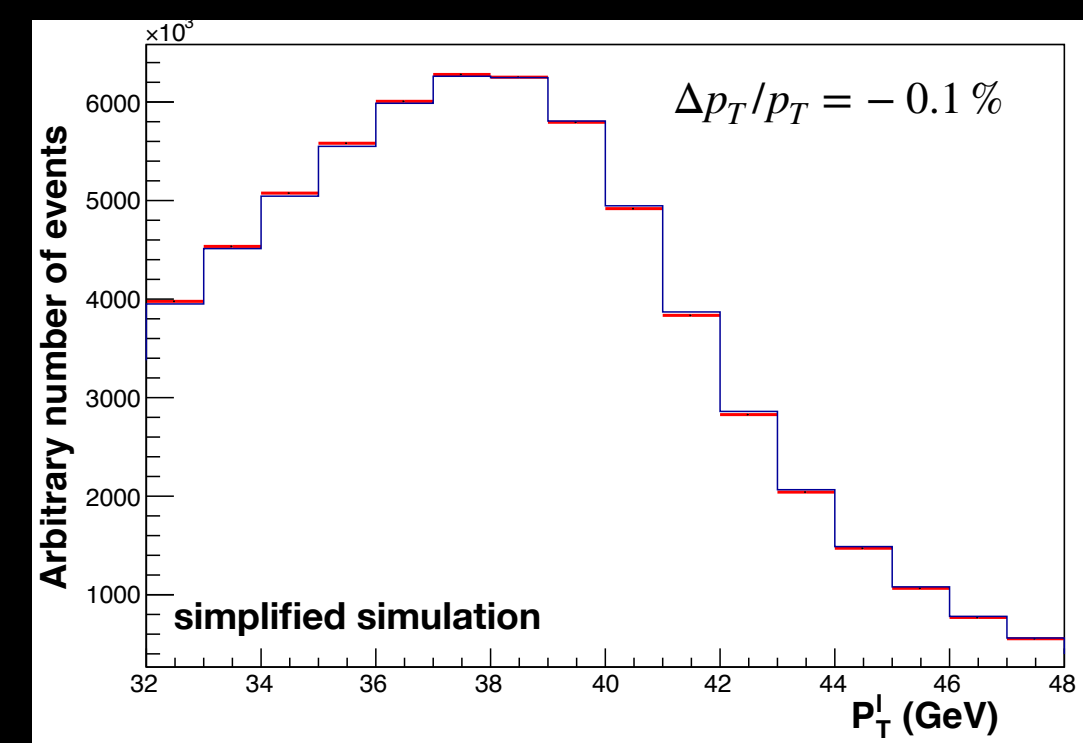
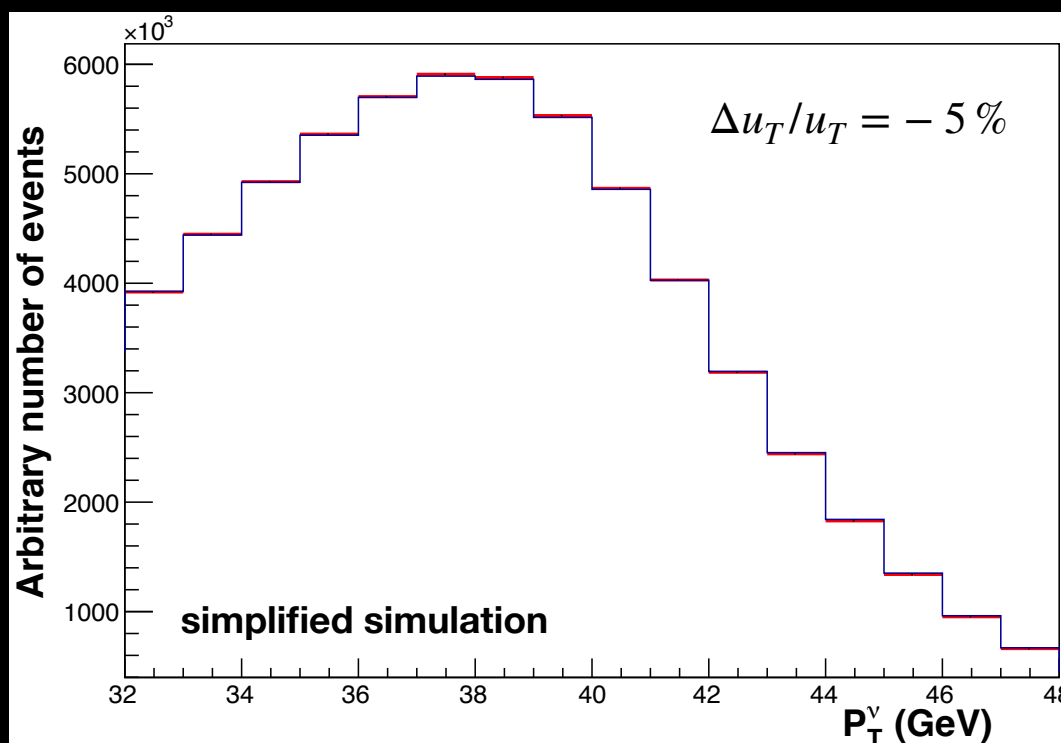
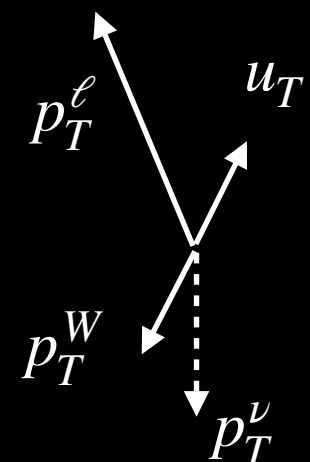


Calibrations



Measurement requires precise calibrations
and momentum scale and resolution

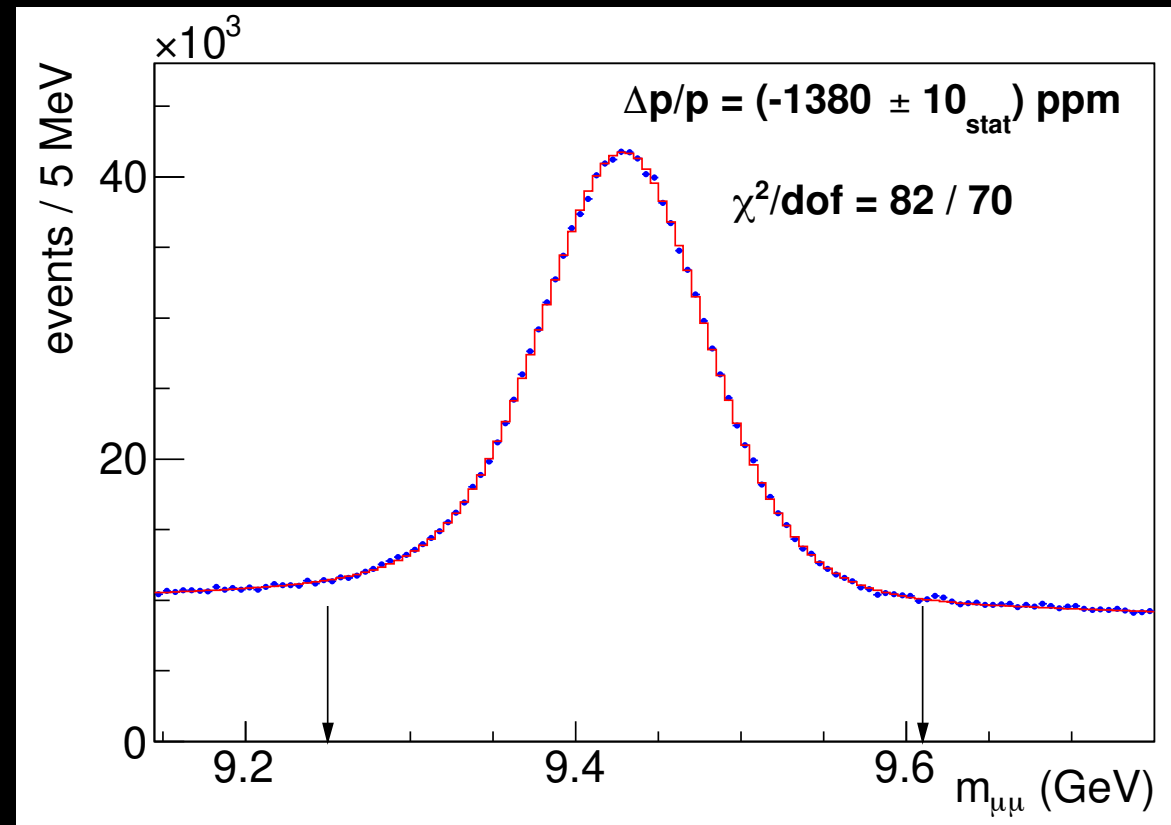
$$\vec{p}_T = -(\vec{p}_T^l + \vec{u}_T)$$



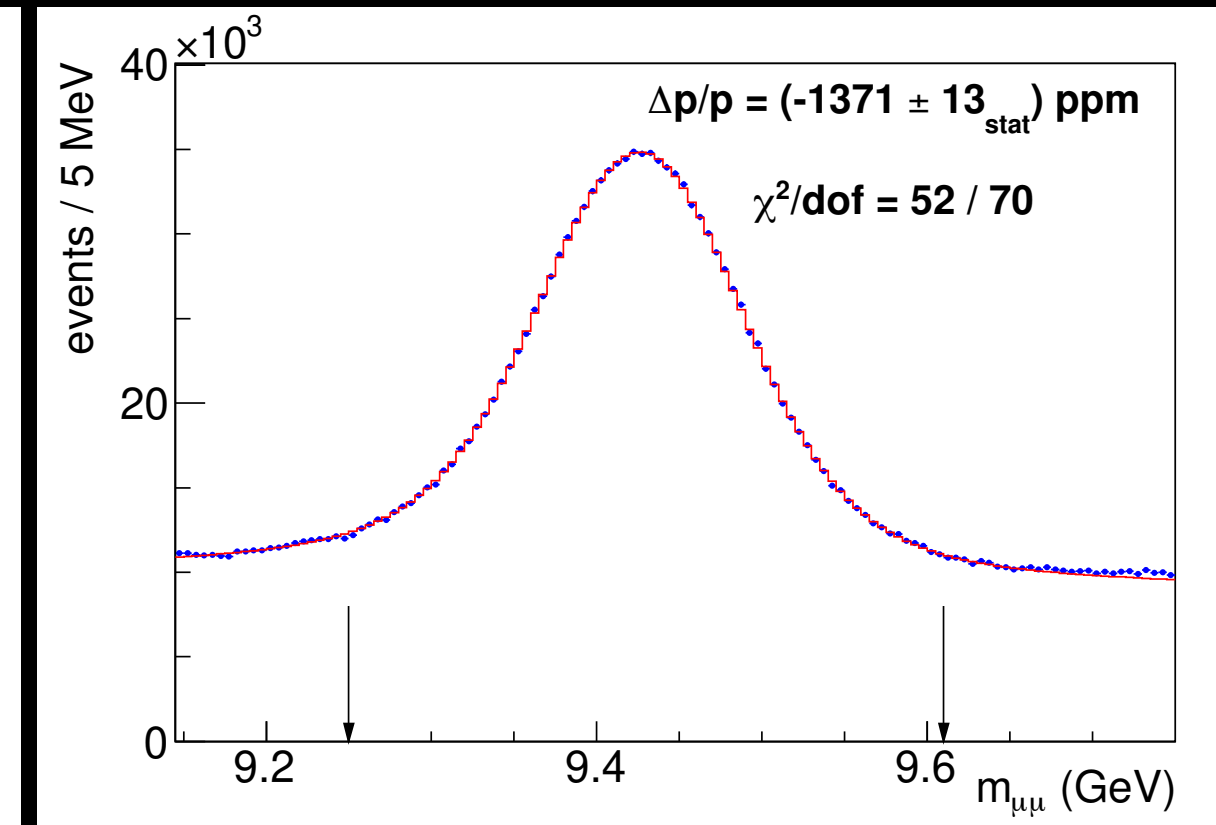
Muon momentum calibration

Third step is to calibrate the scale using γ decays to muons

Compare fit results with and without constraining the track to the collision point



with constraint



without constraint